Thèse

présentée à

Sorbonne Université

Ecole Doctorale N° 391 (SMAER)
Sciences mécaniques, acoustique, électronique & robotique

Institut des Systèmes Intelligents et de Robotique (ISIR)

par

Flavien Lebrun

pour obtenir le diplôme de
Doctorat de Sorbonne Université

STUDY OF VISUO-HAPTIC ILLUSIONS IN VIRTUAL REALITY

Understanding and Predicting the Detection of Hand Redirection

---

Soutenue le 14 Décembre 2022

Pr.	Géry CASIEZ	Professeur à l'Université de Lille	Rapporteur
Pr.	Ferran ARGELAGUET	Chargé de recherche à Inria Rennes	Rapporteur
Pr.	Jörg MÜLLER	Professor at the University of Bayreuth	Examinateur
Dr.	Agnes ROBY-BRAMI	Directrice de recherche INSERM	Examinatrice et Présidente du Jury
Dr.	Gilles BAILLY	Directeur de recherche CNRS	Directeur de thèse
Dr.	Sinan HALIYO	Maître de conférence à Sorbonne Université	Co-encadrant de thèse

First printing, 2021 August 21*st*

Remerciement

Merci d'abord à Gilles et Sinan mes encadrants. Merci Sinan de m'avoir donné ma chance dans la recherche et pour ta bonne humeur (tonitruante). Merci aussi pour nos discussions scientifiques et ton soutien tout au long de cette thèse. Merci Gilles pour ton suivi continu et pour ton investissement. J'ai eu de la chance d'avoir un directeur de thèse si investit. J'ai beaucoup appris avec toi sur le métier de chercheur et sur la conduite de recherche scientifique. Ta grande exigence m'a poussé à me dépasser.

Je remercie également tous les membres de l'ISIR, les personnes de l'équipe administrative, notamment Sylvie et Awatef, mais aussi les membres de l'équipe MSI. Je ne vais pas citer tout le monde pour n'oublier personne et je vous remercierai de toute manière de vive voix quand on se reverra ce qui arrivera bien sûr.

Je remercie mes amis (ceux hors de l'ISIR) qui m'ont moins vu pendant cette thèse mais qui ont toujours été là pour me soutenir. Mention spéciale pour les voironnais Mathilde, Titi, Amau et Tib : les anciens. J'ai été très touché de tous vous voir à la soutenance !

Merci à mes parents pour leur accompagnement depuis toujours vous nous avez toujours aidé et poussé dans mes études et j'ai l'impression que ça a payé. Merci à mes soeurs toutes géniales et presque toutes docteur aussi. Je remercie enfin mes grands parents pour leur présence tout au long du chemin.

Merci enfin à ma chérie qui a le plus souffert dans les périodes difficiles de cette thèse. Merci surtout d'avoir eu quelqu'un avec qui partager les réussites et les moments de joie qui seront les seuls instants, j'en suis sûr, dont on se rappellera !

Abstract

Current Virtual Reality (VR) devices, especially VR headsets, allow for realistic visual stimulation and immersion in virtual environments. This immersion can be improved by stimulating other senses, especially haptic modalities, i.e., the touch and proprioception. However, artificially mimicking real haptic stimuli is challenging. A promising and easy-to-deploy alternative is the use of visuo-haptic illusions. These illusions introduce a subtle shift between visual representations and haptic stimuli. When this shift is well controlled, the perception from the visual modality tricks the brain and modifies the haptic perception of the physical event. However, when this shift is too large, users detect the illusion, which negatively impacts presence in the virtual scene.

In this thesis, I revisit visio-haptic illusions by taking as a case study the illusion called "hand redirection". This illusion moves apart the virtual hand of the user from their real one. For example, it allows the users to believe that they are interacting with physical objects at different locations, while in reality they are interacting with a single physical object at the same location.

Our approach consists in considering measures, factors, and methods to study visuo-haptic illusions. First, we seek to clarify how to measure the effectiveness of an illusion because the concept of "illusion detection" is often vague, subjective, and ill-defined. However, defining precisely the detection threshold is necessary for designers to exploit these illusions in their scenarios. To this end, we describe how the main visuo-haptic illusions work in VR and define the different interpretations attached to the generic term of illusion detection. We then present common methods in Human-Computer Interaction (HCI) for measuring the detection threshold of these illusions in VR. We conclude that while these methods are useful, they do not predict users' ability to detect other illusions.

Next, we investigate factors related to visuo-haptic illusions. While previous studies mainly focus on the impact of a single factor – amplitude of the shift – on illusion detection, we propose to consider three classes of factors: task-related, system-related, and user-related factors. For task-related factors, we investigate the relationship between the amplitude of the shift, the hand trajectory, and the illusion detection. Regarding the system-related factors, we introduce the factor "redirection function", i.e., the function that controls the shift between the virtual and real hands. We then evaluate the influence of this factor on the illusion detection. Regarding the user-related factor, we hypothesize that users' visual and proprioceptive sensory

sensibilities can predict illusion detection. We present an experimental protocol and an analysis method to measure these sensibilities.

Finally, we consider both empirical and theoretical methods for studying visuo-haptic illusions. We present the results of three experimental laboratory studies. We also present an empirical model that relates users' natural tendency to perform curved trajectories to their ability to detect illusions. Finally, we present the first theoretical elements towards the development of a computational model based on the theory of sensory integration and motor control, which will allow the prediction of the illusion detection threshold, but also contribute to the design of other illusions.

Résumé

Grâce aux dispositifs actuels de réalité virtuelle (RV), notamment les casques de RV, les utilisateurs disposent d'un affichage visuel réaliste. Une des options pour améliorer l'immersion en RV est de stimuler d'autres modalités sensorielles, en particulier les modalités haptiques, c'est-à-dire le sens du toucher et de la perception du corps dans l'espace (*proprioception*). Cependant, stimuler artificiellement ces modalités de manière réaliste avec les interfaces actuelles est un défi. Une alternative prometteuse et facile à déployer est l'utilisation d'illusions visio-haptiques. Ces illusions introduisent un décalage subtil entre les représentations visuelles et les stimuli haptiques. Lorsque ce décalage est bien contrôlé, la perception provenant de la modalité visuelle trompe le cerveau et modifie la perception haptique de l'événement physique. Cependant, lorsque ce décalage est trop important, les utilisateurs détectent l'illusion, ce qui impacte négativement la présence dans la scène virtuelle.

Dans cette thèse, je revisite les illusions visio-haptiques en prenant comme cas d'étude l'illusion appelée "redirection de la main". Cette illusion écarte la main virtuelle de la main réelle de l'utilisateur. Elle permet par exemple de laisser croire à l'utilisateur qu'il interagit avec des objets physiques aux emplacements différents, alors qu'il interagit en réalité avec un seul objet physique au même endroit.

Notre approche consiste à considérer les mesures, les facteurs, et les méthodes pour étudier les illusions visio-haptiques. Tout d'abord, nous cherchons à clarifier comment mesurer l'efficacité d'une illusion car le concept de "détection d'illusion" est souvent vague, subjectif et mal défini. Or, définir précisement le seuil de détection est nécessaire aux designers pour exploiter des illusions dans leur scénarios. Pour cela, nous décrivons comment les principales illusions visio-haptiques fonctionnent en RV et définissons les différentes interprétations attachées au terme générique de détection d'illusion. Nous présentons ensuite des méthodes courantes en Interaction Homme-Machine (IHM) pour mesurer le seuil de détection de ces illusions en RV. Nous concluons que bien que ces méthodes soient utiles, elles ne permettent pas de prédire la capacité des utilisateurs à détecter d'autres illusions.

Ensuite, nous étudions les facteurs liés aux illusions visio-haptiques. Alors que les études précédentes se concentrent principalement sur l'impact d'un seul facteur - l'amplitude du décalage - sur la détection de l'illusion, nous proposons de considérer trois classes de facteurs : les facteurs liés à la tâche, au système et à l'utilisateur. En ce qui concerne les facteurs liés à la tâche, nous étudions le lien entre l'amplitude

du décalage, la trajectoire des mains et la détection de l'illusion. En ce qui concerne les facteurs liés au système, nous introduisons le facteur "fonction de redirection", c'est-à-dire la fonction qui contrôle le décalage entre les mains virtuelles et les mains réelles. Nous évaluons ensuite l'influence de ce facteur sur la détection des illusions. En ce qui concerne le facteur utilisateur, nous faisons l'hypothèse que les sensibilités sensorielles visuelles et proprioceptives des utilisateurs peuvent prédire la détection d'une illusion. Nous présentons un protocole expérimental et une méthode d'analyse pour mesurer ces sensibilités.

Enfin, nous considérons à la fois des méthodes empiriques et théoriques pour étudier les illusions visio-haptiques. Nous présentons les résultats de trois études expérimentales en laboratoire. Nous présentons également un modèle empirique qui fait le lien entre la tendance naturelle des utilisateurs à réaliser des trajectoires courbées et leur capacité à détecter les illusions. Enfin, nous présentons les premiers éléments théoriques vers l'élaboration d'un modèle computationel s'appuyant sur la théorie de l'intégration sensorielle et du contrôle moteur, qui permettra de prédire le seuil de détection, mais aussi contribuera à la conception d'autres illusions.

Contents

Abstract **v**

Résumé **vii**

1 Introduction **1**
1.1 Approach and Originality 2
1.2 Research Questions 3
1.3 Scope : Hand Redirection 4
1.4 Research domains 5
1.5 Contributions 6
1.6 Overview of the Thesis 6

2 Illusion in Virtual Reality: Manipulating Visual Feedback to Influence Global Perception **9**
2.1 Famous Illusion not based on a manipulation of the C/D ratio . . . 10
2.1.1 Audio-Visual Illusion 10
2.1.2 Rubber hand illusion 11
2.1.3 Visuo-Tactile Illusion 13
2.2 Control to Display ratio based illusion 15
2.2.1 What is Control to Display ratio ? 15
2.2.2 Visuo-Vestibular Illusion 16
2.2.3 Visuo-Haptic Illusion with proportional gain 20
2.2.4 Visuo-Haptic Illusion with non-proportional gains 23
2.3 Conclusion 26

3 Definition and Measures of Illusion Detection **27**
3.1 Criteria of Evaluation 28
3.1.1 Immersion and Presence 28
3.1.2 Embodiment 31
3.2 Impact of Illusions on Presence 34
3.2.1 Model of Illusions in VR 35
3.2.2 Detection of the illusion 37
3.3 Evaluation of Illusion Detection 39

3.3.1 Measures of Presence and Embodiment 39
3.3.2 Detection of C/D ratio based illusion 42
3.4 Conclusion 46

4 Study of Task Factors: Impact of Hand trajectory on Illusion Detection 49
4.1 Motivations and Approach 50
4.1.1 Scope of the Model 52
4.1.2 Intermediate Research Questions 52
4.1.3 Problem Formulation 52
4.2 Data Collection 55
4.2.1 Participants 55
4.2.2 Apparatus 55
4.2.3 Experimental Design 56
4.3 Analysis 1: Trajectory and Amplitude of Redirection 57
4.3.1 Empirical Results 57
4.3.2 Refining and Evaluating the Model 59
4.3.3 Model Comparison 59
4.3.4 Discussion 61
4.4 Analysis 2: Detection threshold 61
4.4.1 Amplitude of Redirection and Detection Threshold 61
4.4.2 Hand Trajectory and Detection Threshold 62
4.4.3 Further Explanations 62
4.4.4 User-Dependent Detection Threshold 64
4.5 Discussion 65
4.5.1 Main findings 65
4.5.2 Implications for design 66
4.5.3 Limitations 66
4.6 Conclusion 67

5 Study of System Factors: What is the design Space of Hand Redirection Illusion 69
5.1 Motivation 70
5.1.1 Usual Implementation of Hand Redirection 71
5.2 Generalization of the Hand Redirection Function 72
5.3 User Study 74
5.3.1 Participants and Apparatus 74
5.3.2 Experimental Design 75
5.4 Analysis 77
5.5 Results 77
5.5.1 Outliers 77
5.5.2 Target effect 78
5.5.3 Redirection Function effect on Detection 78
5.5.4 Interval of Non-Detection 79
5.5.5 Point of Subjective Equality 80
5.5.6 Participant Analysis 80
5.6 Hand Trajectory analysis 81
5.7 Discussion 82
5.8 Implications for Design 84
5.9 Conclusion 84

6 Study of Users Factors **85**
6.1 Why Users Sensory Sensibilities Are Relevant for studying Illusion Detection? . . . 86
6.1.1 Models about the Sense of Agency . . . 87
6.1.2 Models about the Sense of Ownership . . . 88
6.2 Measures of Sensory Sensibilities . . . 89
6.3 Methodology . . . 91
6.4 Data Collection . . . 91
6.4.1 Participants and Apparatus . . . 92
6.4.2 Task and Conditions . . . 92
6.4.3 Procedure . . . 93
6.4.4 Design . . . 94
6.4.5 Measures . . . 94
6.5 Analysis . . . 94
6.5.1 Mathematical Formalization of Sensory Sensibility . . . 94
6.5.2 Bimodal Data Analysis . . . 95
6.5.3 Frame of Reference . . . 98
6.6 Results . . . 98
6.6.1 Bimodal Data . . . 98
6.6.2 Unimodal Data . . . 99
6.6.3 Individual Level . . . 102
6.7 Limitations . . . 103
6.8 Conclusion . . . 103

7 Conclusion and Perspectives **105**
7.1 Contributions to Our Research Questions . . . 106
7.1.1 RQ1: How to Define and Measure the Detection of Illusion? 106
7.1.2 RQ2: What **Task Factors** to Consider and How they Influence Illusion Detection? . . . 107
7.1.3 RQ3: How **System** Factors or Properties Influence Illusion Detection? . . . 108
7.1.4 RQ4: How do **users'** sensory-motor abilities influence their capacity to detect the illusion? . . . 109
7.1.5 RQ5: How to study visuo-haptic illusion? . . . 109
7.1.6 RQ6: Can we exploit results from cognitive science to elaborate HCI models of visuo-haptic illusion? . . . 110
7.2 Common Perspectives to our 6 Research Questions . . . 110
7.2.1 Predictive Model of Hand Trajectory . . . 110
7.2.2 Computational Approach to Break in Agency . . . 112
7.2.3 Link between Users abilities . . . 112
7.3 Conclusion . . . 112

A Bibliography **113**

1

Introduction

Virtual reality (VR) systems have become widely available in recent years. The driving reason is the commercialization of low-cost VR devices, such as head-mounted displays (HMD), providing realistic visual information. With these devices, users can experience a strong feeling of *presence* in a virtual environment (**VE**), i.e., the intimate conviction of being in another environment and that what is happening in this environment is real [Slater, 2009]. However, to further increase this feeling of presence, improving the realism of visual information is not efficient compared to adding information for other modalities [Dinh et al., 1999]. Today, it is possible to create realistic auditory information. However, it is more challenging to provide information that will stimulate all the haptic modalities, i.e., the sense of touch and kinesthesia (the non-visual perception of our body in space).

One approach to providing haptic feedback in VR is to use of mechanical interfaces such as haptic gloves, exoskeletons, or robotic arms [Perret and Vander Poorten, 2018]. Those interfaces can provide large kinesthetic feedback. However, these are limited in the diversity of haptic information they can create, for

example force feedback devices such as the *Phantom* [Massie et al., 1994] or the *Virtuose* [Haption, 2019] cannot provide tactile or temperature information. Moreover, they are technologically and conceptually complex. A second approach, called *passive haptics* [Achibet et al., 2015], consists in using physical objects to act as real counterparts to virtual objects in the VR scene. It enables a realistic haptic interaction, but the variety of virtual scenes is limited by the position and the types of real elements present in the real world.

A third approach that we promote in this thesis leverages on the rendering of visual information to trick the brain and create *visuo-haptic illusions*. These illusions rely on the introduction of a shift between the visual and haptic information coming from the same physical event (see Figure 1.2). To solve the mismatch between visual and haptic information, the brain often favors perception coming from the visual modality [Pavani et al., 2000, Burns et al., 2006]. Thus, the visual information can "manipulate" the multi-modal perception of physical events and compensate for the lack of realism of the haptic information. Visuo-haptic illusions can reduce the limitations of mechanical haptic interfaces [Abtahi and Follmer, 2018, Gonzalez et al., 2020], reduce the number of physical objects needed for passive haptic [Azmandian et al., 2016] or help give physicality to virtual objects without haptic information [Lécuyer, 2009, Ujitoko and Ban, 2021].

A key parameter of visuo-haptic illusion is the amplitude. It corresponds to the gap between the visual and haptic information. This amplitude can be too important for the brain to solve the sensory mismatch. Users then "detect" the illusion, which leads to a decrease in presence. In practice, VR designers need to know when users are likely to detect illusions to maintain a high level of immersion. In this thesis, our main research question is thus: **Why and how do users detect visuo-haptic illusions in VR ?**.

1.1 Approach and Originality

Our approach to address this research question is summarized in Figure 1.1. It consists of considering the measures, the factors, and the methods to study visuo-haptic illusions. Firstly, the term: "illusion detection" remains vague and needs to be clarified. We aim to define understandably how to **measure** the effectiveness of an illusion. Secondly, previous studies mainly focus on the impact of one factor – the amplitude of shift – on the detection of the illusion. In contrast, we propose to consider **three classes of factors**: the factors related to the *Task*, the *System* and the *User*. Finally, the common methods to study the detection of illusions are empirical. We propose to use not only empirical methods but also **theoretical**

methods by elaborating computational models. The originality of our approach is thus to identify and study the different aspects related to the problem of the detection of visuo-haptic illusions. Doing so, we derive six research questions that we address in this thesis.

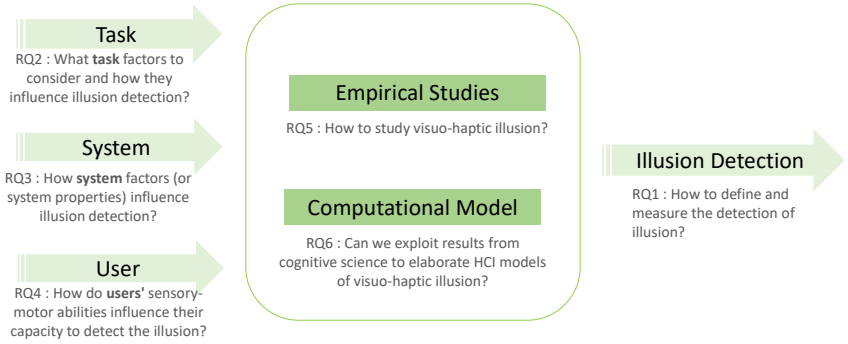

Figure 1.1: Summary of our approach and our 6 research questions.

1.2 Research Questions

RQ1 *How to define and measure the **illusion detection**?* We leverage on the literature from the field of HCI, VR as well as cognitive science and neurosciences to understand which criteria and protocols to consider when evaluating visuo-haptic illusions and how the detection of the illusion is related to concepts such as presence or embodiment.

RQ2 *What **task** factors* to consider and how they influence illusion detection? The amplitude of illusion, constrained by the scenario/application, is generally the only task factor taken into account. While being an important factor, it remains unclear how it precisely influences the illusion detection. Moreover, other task factors can also impact the detection of illusion and should be considered.

RQ3 *How **system** factors or properties influence illusion detection?* What are the different properties that a designer can consider to create an illusion for given a task and a user. In other words, we study the design space of visuo-haptic illusions and how it influences illusion detection. The system can be separated between software and hardware. We focus, in this thesis, on the software because it is more easily modified, even though future research on the impact of hardware should be conducted.

RQ4 *How do **users'** sensory-motor abilities influence their capacity to detect the illusion?* We observe that the ability to detect illusions depend not only on the task and the system but also the user. We hypothesize that visual and

proprioceptive sensibilities of users can explain and predict these differences.

RQ5 *How to study visuo-haptic illusion?* Common empirical studies about visuo-haptic illusions only measure the ability of users to detect the illusion. We argue that analysing additional *behavioral* markers such as users' movement trajectories can help to better understand when and why users detect the illusion.

RQ6 *Can we exploit results from cognitive science to elaborate HCI models of visuo-haptic illusion?* We aim to explain and predict illusion detection with a *cognitive* computational model. We investigate how multi-sensory integration and motor control theories can link user sensory sensibilities with the probability of detecting illusion.

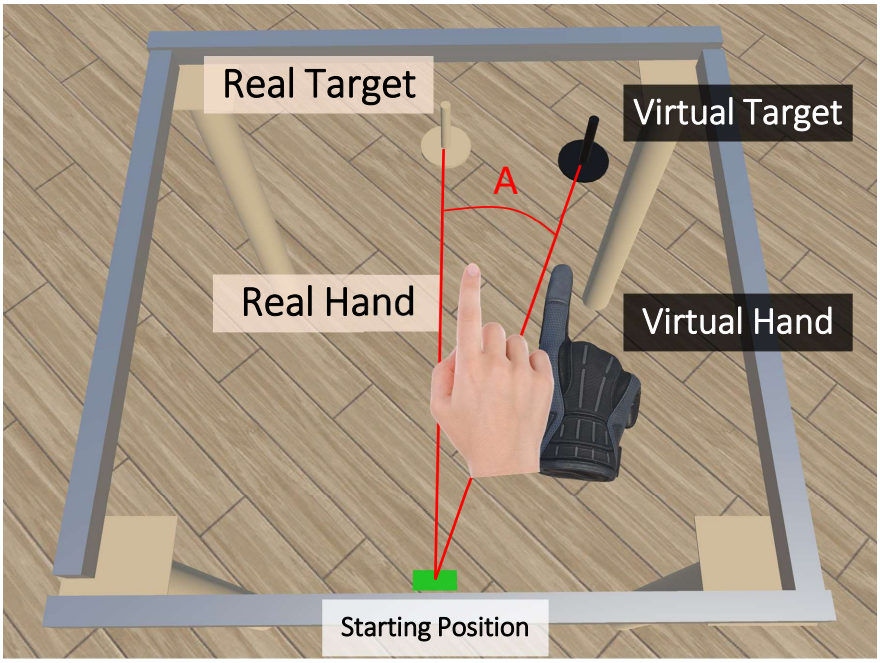

Figure 1.2: Illustration of Hand redirection. The real hand and the virtual hand are in the same position at the beginning of the movement on the starting position. The amplitude of redirection A can be represented as the angle between the real target, the starting position, and the virtual target. During the movement, the two hands will be shifted gradually. The shift will be equal to the distance between the two targets at the end of the movement. It ensures that the two hands will reach their respective targets.

1.3 Scope : Hand Redirection

The scope of this thesis is limited to one specific visuo-haptic illusion: **Hand Redirection** [Kohli et al., 2012, Azmandian et al., 2016]. This illusion is illustrated in Figure 1.2: The setup is the following: A virtual target is at a different location than its corresponding physical target. However, the real and virtual hands are initially at the same location. Note that the real hand and the real target are invisible to the user (they are only represented here to depict the illusion). The objective of this illusion is to ensure that when the virtual hand reaches the virtual target, the real

hand reaches the real target. To achieve this visuo-haptic illusion, the virtual hand is gradually separated from the real hand during the movement. Users unconsciously redirect their hands' path to reach for the target.

We focus on this illusion for two main reasons: First, this illusion is easy to implement and has been shown to work in several applications [Kohli et al., 2012, Azmandian et al., 2016, Cheng et al., 2017]. Second, it involves both the visual and proprioceptive modalities and users' movements, and thus is suitable for a sensory-motor approach. Therefore, we use this illusion in two data collection experiments. In the rest of this thesis, we talk about the "amplitude of redirection" to speak about the "amplitude of illusion" of hand redirection.

1.4 Research domains

In this thesis, we built on four research domains: HCI, Virtual Reality, psychology, and cognitive sciences.

One objective of the HCI and VR communities is to improve user experiences by providing more natural and efficient ways to interact with a virtual environment. Visuo-haptic illusions is one class of solutions to leverage haptic feedback in VR and thus user experience. As such, we consider the interaction techniques proposed in these communities to implement visuo-haptic illusions [Azmandian et al., 2016, Razzaque, 2005, Abtahi and Follmer, 2018]. We also adapt their experimental protocols to study the detection of the illusions [Steinicke et al., 2009, Zenner and Krüger, 2019]. Finally, we propose novel computational models and tools to design and evaluate these techniques.

We also build on the literature in psychology and cognitive sciences. Some visuo-haptic illusions, e.g. the famous Rubber Hand Illusion, have been studied [Botvinick and Cohen, 1998] in these fields to understand concepts relevant to our work, such as the embodiment of a virtual body [Kilteni et al., 2012]. In addition, this literature also studies the cognitive mechanisms that explain presence in VR as well as the apparition of illusions [Gonzalez-Franco and Lanier, 2017]. Finally, we build on the multi-sensory integration theory [Colonius and Diederich, 2020] from cognitive sciences to propose computational models that could help explain and predict the detection of illusions.

1.5 Contributions

In this thesis, we provide theoretical, methodological, artifact, and empirical contributions:

Theoretical: We provide a better understanding of the term illusion detection. We present different criteria to consider when implementing visuo-haptic illusions. We also present mechanisms that lead to the apparition of an illusion and show how these mechanisms can impact the VR experience. Moreover, we propose a model based on Bézier curves to predict users' hand trajectories under redirection according to the amplitude of illusion. With the help of this model, we highlight the link between the curvature of hand trajectories and the illusion detection.

Methodological: We adopt an experimental protocol to measure users' visual and proprioceptive sensory sensibilities in VR. We then propose a novel method (based on a Bayesian Inference approach) to analyse the collected data.

Artifact: We explore the design space of hand redirection illusion by considering different redirection functions, i.e., the function that controls the shift between the virtual hand from the real one. We show that the detection of the illusion does not seem to be influenced by the redirection function.

Empirical: We conducted three data collection experiments. In the first two, we measure participants' hand redirection detection thresholds and log their hand trajectories. In the last one, we measure participants' visual and proprioceptive sensory sensibilities for the left and right hand localization. We highlight the greater contribution of proprioception in VR compared to the real world for the hand's position.

1.6 Overview of the Thesis

CHAPTER 2 We present a review of interaction techniques for visuo-haptic illusions in Virtual Reality. We first describe classic illusions based on the manipulation of visual feedback. We then explain how manipulation of the Control to Display ratio has been used as a vector of illusion.

CHAPTER 3 We address RQ1 (*How to define and measure the detection of illusion?*). We first present the criteria to consider when evaluating illusions. We then detail the mechanisms explaining the apparition of illusions in VR and highlight how the failure of these mechanisms impacts the previously presented criteria, leading to the **illusion detection**. Finally, we review existing methods to collect and

analyze empirical data about visuo-haptic illusions.

CHAPTER 4 We address questions RQ2 (*What task factors to consider and how they influence illusion detection?*) and RQ5 (*How to study visuo-haptic illusion?*). We propose an empirical model that links the influence of the most common **task** factor – the amplitude of redirection – to hand trajectories (RQ2). We conduct a data collection experiment to log participants' hand trajectories to calibrate our model. Based on this model, we investigate the relation between hand trajectory and the detection of illusion (RQ5).

CHAPTER 5 We address RQ3 (*How system factors (or system properties) influence illusion detection?*) by exploring the design space of hand redirection illusion. In particular, we investigate one **system** property, the redirection function, i.e., the function that controls the shift between the virtual avatar and the real body's movements. We then evaluate the influence of the these redirection functions on illusion detection.

CHAPTER 6 We address RQ4 (*How do users' sensory-motor abilities influence their capacity to detect the illusion?*) and RQ6 (Can we exploit results from cognitive science to elaborate HCI models of visuo-haptic illusion?). We first present a method adapted from the literature to measure **users**' visual and proprioceptive sensibilities (RQ4). We then present a model from the cognitive science literature that can help predict users' probability of detecting illusions based on their sensory sensibilities (RQ6).

CHAPTER 7 This chapter concludes this thesis. We summarize our contributions and discuss the research questions we did not cover yet. We also present the perspectives opened by this work.

2

Illusion in Virtual Reality: Manipulating Visual Feedback to Influence Global Perception

Current VR devices, especially VR headsets, allow realistic visual stimulation and immersion in a virtual environment. One way to improve this immersion is to stimulate other sensory modalities. It has indeed been shown that increasing the number of stimulated sensory modalities benefits the realism of a virtual environment and the presence in this environment [Melo et al., 2020].

For several stimuli to be associated with the same event, they must be spatially and temporally close. For example, a sound is not associated with a light flash if the flash is seen after hearing the sound and in a different direction. Thus for the design of multisensory VR experiences, the classical approach is to look for a perfect spatio-temporal alignment when providing different stimuli. However, a volunteer dissociation introduced between the stimuli can, on the opposite, enriches the VR

experience. This dissociation is at the origin of illusions, where the perception coming from a modality tricks the brain and changes its multi-modal perception of the physical event. We will see, in particular, that it is possible to influence perceptions of tactile and proprioceptive stimuli.

In this chapter, we detail the main illusions based on perceptual dissociation. These illusions mostly come from the field of HCI. We describe what modality they involve, how visual stimuli are disturbed, and the expected consequences of this disruption. This chapter is divided in two sections: illusions not based on Control to Display ratio (C/D ratio) , e.g., the rubber hand illusion and illusions based on C/D ratio, e.g., redirected walking and hand redirection). In the next chapter, we present how illusions' effectiveness is evaluated.

C/D ratio: the ratio between the distance that a control or input device (e.g., a computer mouse) is moved by the operator and the consequent distance that the object it controls (e.g., the cursor) is moved on the display (e.g., the computer screen).

2.1 Famous Illusion not based on a manipulation of the C/D ratio

Humans have four traditional senses in addition to sight: smell, taste, hearing, and touch. There are some illusions where vision can influence an olfactory or gustatory perception. For example, the color of food can sometimes influence the taste of food, Spence et al. [2010]. Concerning the sense of smell, Morrot et al. [2001] have shown that a white wine colored in red smelled by participants is described only by terms defining red wines. We do not dwell further on these two modalities. Before discussing visuo-haptic illusions, let us linger on the reciprocal influence of sight and hearing.

2.1.1 Audio-Visual Illusion

Vision and audition are the principal modalities of attention stimulation. We more likely focus our attention on an event if the visual and auditory perceptions of this event are temporally and spatially aligned [Stein, 2004]. Moreover, our brain seeks to associate a sound with a visual stimulus that is spatially and temporally close. This principle, called "the unity assumption" [Welch, 1999, Vatakis and Spence, 2007], is the basis of several visual-auditory illusions that we detail.

The hearing influence, in particular, the temporality of the visual perceptions. If we see a repetitive flash combined with a repetitive sound, the flash's perceived frequency is that of the sound, even if the two signals do not have the same frequency [Shipley, 1964]. In the same way, if two sounds are presented in a time close to a single flash, two flashes can be perceived [Shams et al., 2002]. The vision, on its side, can influence the spatiality of the auditory perceptions. This phenomenon is illustrated in particular with the famous ventriloquist illusion, where one associates

the origin of a sound with a shifted visual stimulus [Bertelson et al., 2000]. Another famous illusion, the McGurk effect [McGurk and MacDonald, 1976], reflects a reciprocal influence between hearing and vision. The effect occurs when a voice sound does not correspond to the mouth movement observed simultaneously. In this case, we perceive a mixed sound corresponding to an in-between of auditory perception and lip-reading.

In VR, the influence of hearing on vision has been used to improve the effect of *self-motion*. We can experience this illusion in a train station. When we observe another train starting, the impression of moving while being motionless appears. The addition of a rotating sound to match a rotating image has been shown to enhance the effect of *self-motion* [Riecke et al., 2009]. However, except for this example, few applications to our knowledge exploit a shift between audio and visual stimuli to create illusions in VR. The auditory interfaces being of good quality, it is probably not necessary to create interaction techniques to overcome the limitations of audio stimuli in VR.

Most of the work on illusion involving vision in virtual reality involves the Haptic modality. We describe what encompasses this modality and introduce a famous and widely studied illusion in cognitive science and psychology: the Rubber Hand Illusion (RHI).

2.1.2 Rubber hand illusion

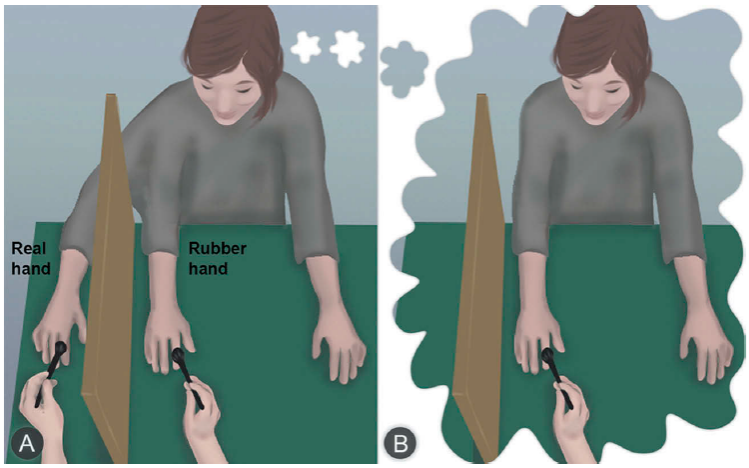

Figure 2.1: Illustration of the Rubber Hand Illusion: participants see a rubber hand in place of their hidden real hand. The rubber hand and the real hand are synchronously stroked with a brush. The spatiotemporal similarity between the seen brush stroke and feel brush stroke causes the appropriation of the rubber hand as a part of the body. The illustration is taken from [Seinfeld et al., 2021]

The Rubber Hand Illusion (RHI) [Botvinick and Cohen, 1998] is a visuo-haptic illusion that manipulates the Sense of Ownership (SoO), i.e., the feeling that we

Haptic, which comes from the Greek "I touch", is the discipline that explores the sense of touch and what we could call our two other senses: the vestibular system and proprioception. Unlike vision and hearing, whose perceptive organs are localized (eyes and ears), haptic sensory receptors are more globally distributed. They are mainly present in the superficial layer of the skin for tactile perceptions in the muscles, tendons, and joints for proprioceptive perceptions and in the inner ear for the vestibular system. Touch provides information on objects' shapes, textures, stiffness, and temperatures. Proprioception helps us to perceive our body in space and to feel forces. The vestibular system informs us about our body's linear acceleration and orientation in space.

have and own a body in which with we can manipulate our environment (a summary of the basic principle underlying the Sense of Ownership can be found in chapter 3). The objective of the RHI is to lead a user to believe that a rubber hand is his real hand. The appropriation of the rubber hand as a body part is achieved by simultaneously stroking the visible rubber hand and the user's invisible real hand with a brush (see Figure 2.1). Following the unity assumption, the brain will associate the visual and tactile stimuli. Consequently, the tactile stimuli are perceived as coming from the rubber hand. Thus the rubber hand becomes a part of the body. The RHI illusion creates a shift between the proprioceptive perception (real hand) and the visual perception (rubber hand) of the position of our body members.

The spatiotemporal congruence of tactile and visual stimuli causes the illusion but is not sufficient alone to induce a strong Sense of Ownership on the rubber hand. Tsakiris and Haggard [2005] show that the artificial hand must be consistent in orientation and appearance with the representation we have of our body, and Argelaguet et al. [2016] show that a realistic virtual hand causes a stronger Sense of Ownership.

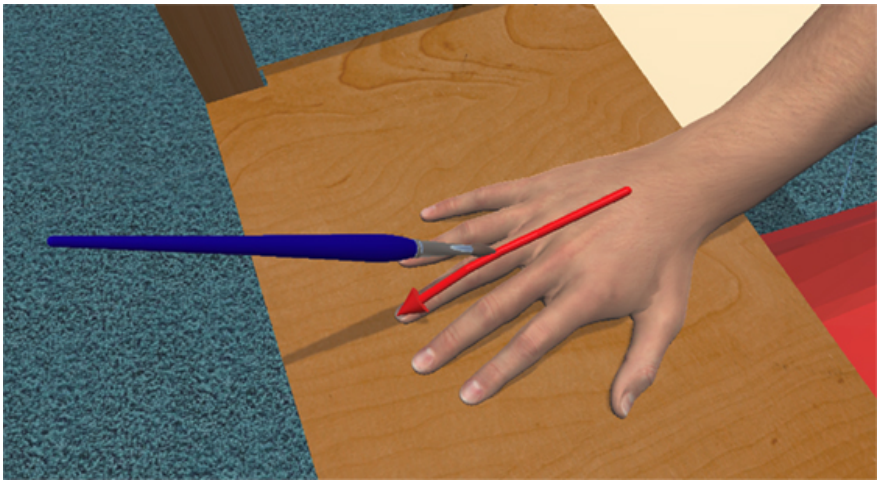

Figure 2.2: Illustration of the 6-fingered virtual hand proposed by Hoyet et al. [2016]. Participants gain ownership over this virtual hand through an adaptation of the RHI. The additional finger is visually stimulated (in the VE) by a brush, as seen in the image. A real finger is also stimulated by a brush (in the real world) in a spatiotemporal congruent way with the virtual stimulation. After a sufficiently long synchronous stimulation time, the users feel that they own this extra finger.

This appropriation of a virtual hand can be transposed into VR with a virtual avatar of the real hand [Slater et al., 2008]. It shows that users can accept an offset between the real and virtual hands. The illusion has also been adapted to the appropriation of a virtual leg [Kokkinara and Slater, 2014] and a full virtual avatar [Slater et al., 2010]. With the help of RHI, it is also possible to create consequent alterations to the virtual avatar while preserving the Sense of Ownership. Slater et al. [2010] show that men can feel ownership over a female virtual avatar. Users can also tolerate a larger virtual arm than its real counterpart [Kilteni et al., 2012]. It is

also possible to add an extra limb to our virtual avatar. Hoyet et al. [2016] studies the addition of a sixth finger to our virtual hand (see Figure 2.2). By a method similar to the RHI, they make the participants accept the possession and control of this additional finger.

A synchronous visuo-tactile stimulation is not the only way to elicit a feeling of ownership over an artificial body. Sanchez-Vives et al. [2010] have shown that a Sense of Ownership over an artificial limb can be elicited by synchronous visuo-proprioceptive stimulation. That is to say, match the movements of the real limb to the movements of the virtual limb. In VR, tracking the movements of a real body and recreating these movements with a realistic avatar induce a strong Sense of Ownership over the virtual avatar, even if a permanent shift is introduced between the position of the real body and the virtual avatar.

In this section, we introduced the RHI. We showed that it could be leveraged to manipulate the representation of users' avatars in VR while maintaining a Sense of Ownership over this avatar. In the next section, we show how visuo-tactile illusions help overcome several issues of physical interaction in VR.

2.1.3 Visuo-Tactile Illusion

Stimulating all the haptic modalities in VR is a complex problem, and the subject of many works [Bouzbib et al., 2021]. The use of visuo-haptic illusion, where the visual feedback is manipulated to influence global perceptions of a physical event, is a solution to avoid the addition of new costly and cumbersome interfaces. This approach is mostly called *pseudo-haptic* [Lécuyer, 2009, Ujitoko and Ban, 2021] although some works, exploiting a mismatch between real and virtual user movements, are not associated with this designation. We describe here the main works that exploit a shift between visual and tactile perceptions before developing in the next section a family of visuo-haptic illusions that exploit the manipulation of the C/D ratio.

Tactile perception Illusion

The manipulation of Visual feedback has been used in VR to modify the tactile perception of object characteristics. Work has focused on the flexibility of materials and their roughness.

Objects' Softness The manipulation of the visual representation of a real object in a virtual environment (for example a screen or VR scene) can change the global perception of the softness of this object. Tactile perceptions dominate proprioceptive

perceptions for evaluating the softness of an object [LaMotte, 2000]. That is why we can talk of visuo-tactile interaction for the perception of softness more than a visuo-proprioceptive interaction, even if both modalities intervene.

Sanz et al. [2013] introduced a technique using visual image distortion to elicit a tactile sensation of softness. Users can locally deform a virtual object at the mouse cursor position on a screen (see Figure 2.3). This image will be more or less deformed according to the time the mouse button is pressed. This is a pseudo-haptic sensation. The tactile information is not modified. Only the visual softness information is manipulated, causing the change in softness global perception. Ban et al. [2014] improved this technique in VR by considering the posture of the user's hand. When compressing a virtual object, if it is compressed differently than a real object, the visual hand posture is changed to match the compression. Another approach is to change the color of the user's virtual skin when applying pressure to a surface. Punpongsanon et al. [2015] show that among four techniques of coloring the user's finger, only one technique, changing the skin color, modifies the perception of the softness of a cushion. Similarly, Achibet et al. [2014] change the color of the user's hand when the user changes the gripping force of a virtual object. Thus we see that either the manipulation of the visual representation of the object or the user representation in the virtual world can help change the global perception of softness.

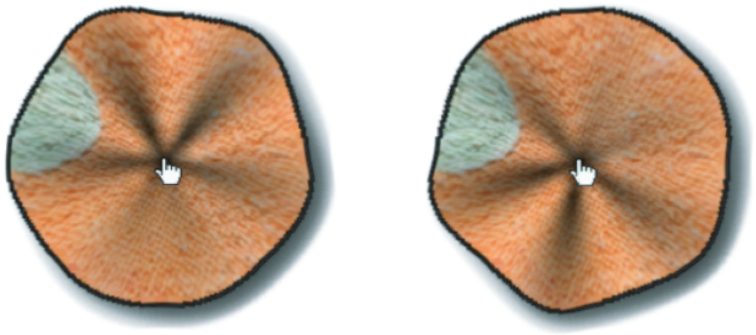

Figure 2.3: Examples of the visualization of the deformation of an image by the technique of Sanz et al. [2013]. By clicking on the image, users can deform it locally according to its elastic properties. The pressure exerted by the user is proportional to the time the mouse is pressed. Playing on the visual deformation for the same pressure influences the visuo-tactile perception of the object's flexibility. It is also possible to play on the deformation profiles of materials to create different sensations. Here we observe two different deformation profiles for the same pressure.

Objects' Macro Texture Visual manipulations are also introduced to influence the visuo-haptic perception of macro-texture. Lécuyer et al. [2008] change the mouse cursor size to simulate a hole or a bump. Users can correctly identify a bump (the cursor gets bigger) and a hole (the cursor gets smaller) when dynamically

manipulating the cursor.

2.2 Control to Display ratio based illusion

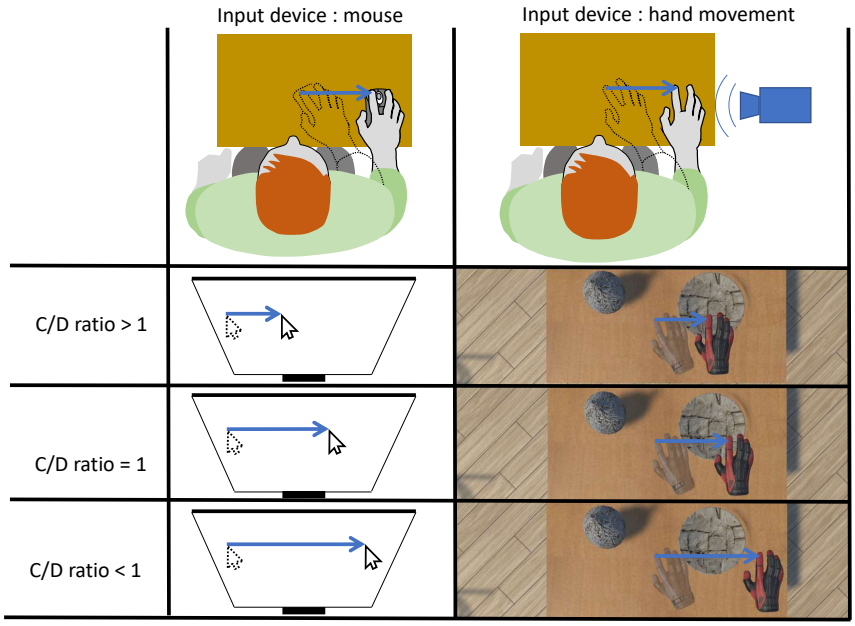

Figure 2.4: Illustration of the manipulation of the C/D ratio. Based on the chosen C/D ratio, the same movement of the input device results in a different movement of the user representation. Per line, we see the effect of a C/D ratio greater, equal, or smaller than 1. The movement of the user representation is respectively smaller equal, or greater than the movement of the input device. First Column: this manipulation of the C/D ratio is often used for the control of mouse movement [Casiez et al., 2008]. Second Column: the change in C/D ratio between users' real movements and the movements of their virtual avatar is the basis of many illusions in VR.

Although we have seen some examples of visuo-tactile manipulation by changing the representation of an object or the user in the virtual environment, a large part of visuo-haptic illusions is based on a manipulation of the C/D ratio. We develop these techniques in the next section.

2.2.1 What is Control to Display ratio ?

Control to Display ratio (C/D ratio) design the transfer function between the movement of the control device (for example, a computer mouse or real movements) and the consequent movement of the user representation in the virtual environment (for example a cursor or a virtual avatar; see Figure 2.4) [Casiez et al., 2008]. The C/D ratio can be 1:1, i.e., if the movement of the user representation is similar to the movement of the real hand. It can also differ from a 1:1 mapping, like most current transfer functions between mouse and cursor movements. For example, pointer acceleration is the default behavior on many operating systems [Casiez et al., 2008]. It dynamically manipulates the C/D ratio between the mouse and the cursor as a function of the mouse velocity: when the velocity of the control device is high, C/D ratio is low (less than 1) (see the last line of the Figure 2.4), and when

the control device moves slowly, the C/D ratio is high (above 1) (see the first line of the Figure 2.4). The term CD gain which represents the inverse of C/D ratio is often used as well.

Similarly, several illusions in VR take advantage of a C/D ratio that differs from a 1:1 mapping. We introduce these different illusions in the next section. We first detail visuo-vestibular illusions for which the input device is the user's head motion, and the user representation in VR is the user's visual field. In the following, we detail visuo-haptic illusions where the input device is the user's movements. We separate these illusions into two groups: 1) illusions where the direction of the display movements in VR is the same as the control movements and 2) illusions where this direction is different.

2.2.2 Visuo-Vestibular Illusion

The vestibular system is a sensory organ located in the inner ear. It works like an inertial measurement unit, informing us about our body's linear acceleration and orientation in space.

The mismatch between visual and vestibular perceptions is an important research topic in VR. Indeed, differences in orientation (when the system is badly calibrated, for example) or differences in acceleration (when the virtual avatar is in movement and the user is immobile in the real world) are the main causes of nausea and dizziness sometimes experienced in VR [Rebenitsch and Owen, 2016] (referred to as cyber-sickness). Therefore, when users turn their head or moves in the real world, the visual field movements (in VR) should match those real movements to minimize these effects.

However, we show in this section that it is possible to play on this correspondence and to introduce a different ratio between users' head movements and users' visual field. It means introducing a shift between visual and vestibular perception; that is why we discuss visuo-vestibular shifts in the rest of this section. We first develop interaction techniques based on a voluntarily exaggerated visuo-vestibular shift that the user is aware of. We then analyze interaction techniques where the shift remains imperceptible for the user to consider the cyber-sickness.

Perceptible manipulation

A visuo-vestibular shift is sometimes introduced by accepting that the user perceives it [Marshall et al., 2019]. The sensory dissociation is voluntarily exaggerated to blur the user's reference points or accentuate a sensation while neglecting realism.

One of the earliest uses of a visuo vestibular shift to create an illusion is the 1890s attraction: *Haunted Swing* [Wood, 1895]. In this illusion, the participants have the feeling that they are sitting in a swing that takes them almost upside down. In reality, they do not move; only the "walls" of the room turn. Today, in the attraction "Superman Ride of steel VR" [man], the passengers of a roller coaster wear a VR helmet and observe greater slopes and higher speed than the real attraction. The sensations are thus increased tenfold without changing the physical installation.

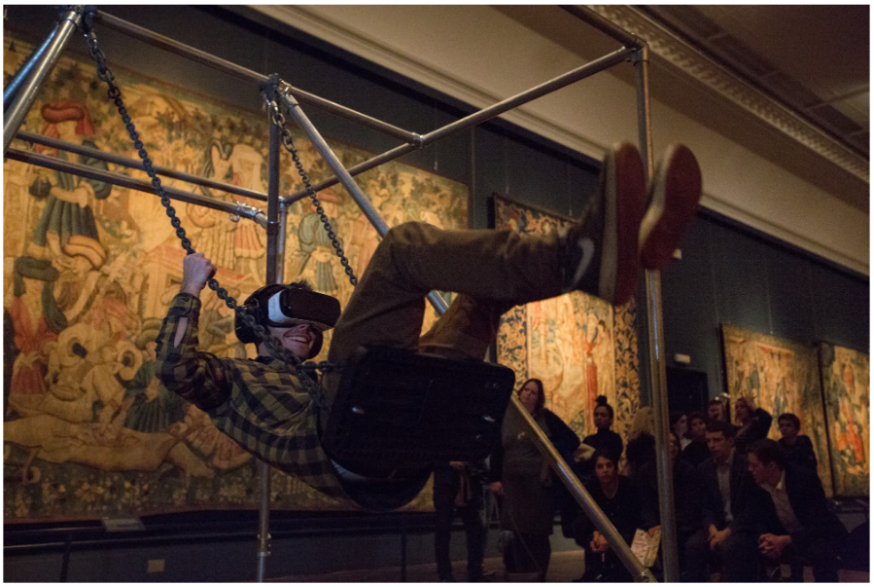

Figure 2.5: With *Oscilatte* [Tennent et al., 2017] the user has the illusion to realize faster swings and larger amplitudes. This visual-vestibular shift is detected but increases the sensations of the user.

In the same way with *Oscilatte* [Tennent et al., 2017] (see Figure 2.5) the amplitude of the movements of a real swing is amplified in VR. With [Tennent et al., 2019], the virtual environment is transformed so that the user has the impression of moving forward in a straight line instead of a swinging movement.

In the entertainment field again, Balance Ninja [Byrne et al., 2016] is a game where each player must have the other lose balance on a beam. The inner ear is disturbed by galvanic vestibular stimulation (GVS) to provoke the imbalance. It causes a sensation of tilting. The particularity of the game is that the more a player has the body leaning, the more the other player is stimulated, and thus the more likely he is unbalanced. Byrne et al. [2018] proposed a variation of this game by disturbing only the visual field with the help of VR helmets. When a player is leaning, the visual field of the other player is leaned in the same way. As a result, he sees himself leaning while his body is straight. This shift increases the loss of balance.

Galvanic vestibular stimulation is a technique to make the subject feel a variation of his balance. With the help of electrodes, electrical messages are transmitted to the vestibular zone of our inner ear to stimulate the vestibule and thus influence the subject's balance.

The techniques presented here, therefore, have the disadvantage of being able to cause cyber-sickness. In all the applications that we present hereafter, the shift between the stimuli is designed to be **imperceptible** by the user. These applications aim to enhance the realism of the user's experience in VR.

Imperceptible manipulation

walking in VR In VR, the virtual environment is potentially infinite, but the real counterpart is limited. To solve this problem, the user's real movements are often decreased compared to the virtual ones. For example, it is possible to use treadmills or teleportation, where users remain immobile in the real world while moving in the virtual world. This introduces a discrepancy between his visual and vestibular perceptions. Some techniques have been proposed to reduce this shift sensation [Cevette et al., 2012, Weech et al., 2018]. On the contrary, other approaches exploit a controlled shift to solve this displacement problem.

Adding noise to the vestibular perception encourages the brain to consider the noisy perception less reliable. It may thus choose to resolve the conflict between the perceptions by favoring the visual perception. Cevette et al. [2012] have shown that cyber-sickness can be reduced by using noisy GVS stimuli. Weech et al. [2018] showed that noisy vestibular stimuli by bone transmission could also reduce cyber-sickness by overcoming the negative effects that GVS can cause.

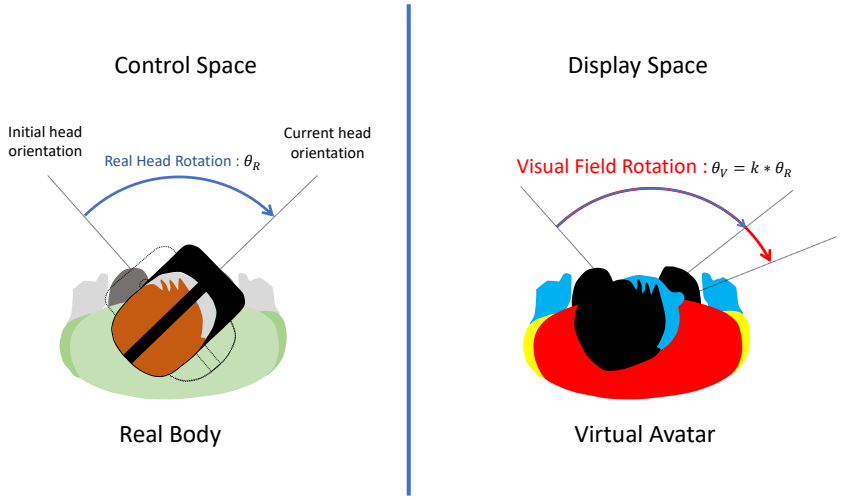

Figure 2.6: Illustration of a non-1:1 C/D ratio between head rotation in the real and the virtual world.

To avoid these intrusive devices, the ideal solution is to propose a natural mode of locomotion. Real-world walking as a mode of travel in VR improves user comfort, immersion [Usoh et al., 1999] and offers a better perception of space than walking in place or using a treadmill [Wilson et al., 2016]. However, a perfectly similar movement in VR and in the real world is still limited by the actual workspace. Therefore, it is necessary to control the trajectory of users to avoid physical obstacles and increase or decrease virtual movements compared to real movements. This approach is called *Redirected Walking*.

The manipulation of the C/D ratio between the movements of the visual field and the movements of the user provides a solution to these issues. Williams et al. [2006] add a constant gain between the horizontal head displacement and the visual field displacement in VR. With this mapping, it is possible to carry out a displacement larger in the VE than in the real world. Razzaque [2005] add a gain between the head's rotation and the visual field's rotation in VR (see Figure 2.6). It has also been proposed to dynamically introduce a continuous rotation of the visual field during the users' movements. By unconsciously correcting their trajectory to correspond to the rotation of the visual field, they have the impression of walking in a straight line. In contrast, their real displacements are curved (see Figure 2.7). In this case we speak about *Redirected Walking* Razzaque [2005]. For all these transformations, the shift introduced between the perceptions is accepted and, to a certain extent, not detected by the user because it is below a threshold amplitude, preventing cyber-sickness.

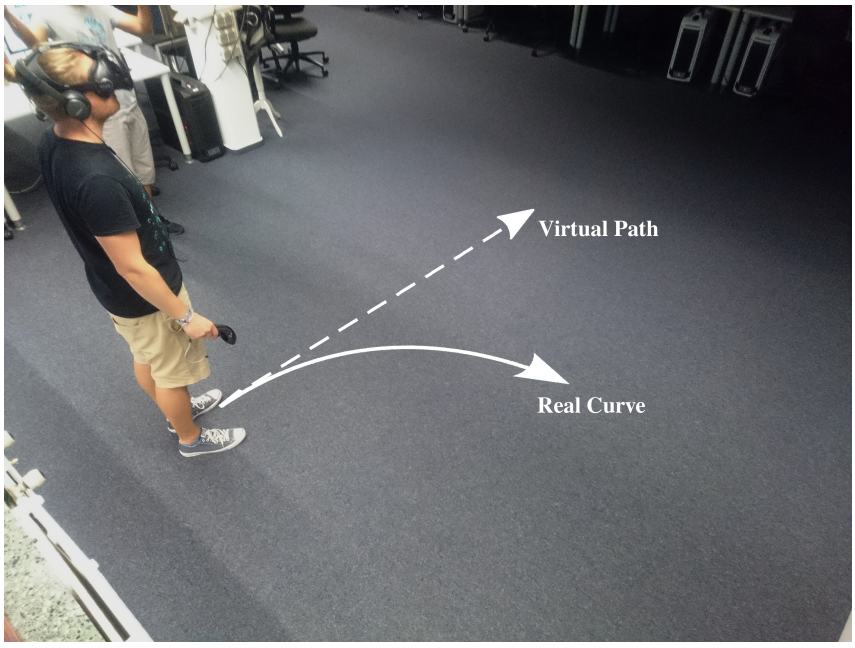

Figure 2.7: Illustration of the *Redirected Walking* interaction technique thanks to the progressive shift of the visual field compared to the orientation of the head, the user will correct this shift imperceptibly. He will thus follow a curved trajectory (solid line) while having the feeling to move in a straight line (dotted line).

Redirected Walking Several works have proposed methods for expanding the non-detectable visuo-vestibular offset. Matsumoto et al. [2017] give the illusion to the user of walking up or down on a real flat floor. They propose to decrease the C/D ratio of the distance traveled when going up in the virtual environment and increase this C/D ratio when going down in the virtual environment. It simulates the difference in energy expended going up or down a slope. It makes it possible to offer greater slopes without the user noticing. Sun et al. [2018] propose a technique of *Redirected Walking* based on saccadic suppressions. When our eyes are in motion, the nervous system blocks visual information processing, resulting in temporary blindness. Sun et al. [2018] take advantage of these periods of blindness to rotate the visual field and increase redirection.

Imperceptible Visuo-vestibular illusions have been used primarily to make natural walking accessible in VR. Among other techniques, Azmandian et al. [2016] leverage a non-1:1 C/D ratio between head rotation in the real and virtual world to manipulate the trajectory of the user's hands. Their goal is to improve the realism of haptic interactions in VR. Many interaction techniques based on manipulating the C/D ratio between users' limb movements and their virtual avatar movements have been proposed to achieve this goal. We describe them in the following section.

2.2.3 Visuo-Haptic Illusion with proportional gain

By manipulating the C/D ratio between users' limb and avatar movements, we introduce a shift between users' visual and proprioceptive perceptions. This shift is notably used in Pseudo-Haptic [Lécuyer, 2009, Ujitoko and Ban, 2021] to modify global perceptions of objects and environment properties. Here we list the main physical properties of the objects that can be manipulated with Pseudo-Haptic. We use these examples to detail the different ways of creating illusions based on a gain between real and virtual movements.

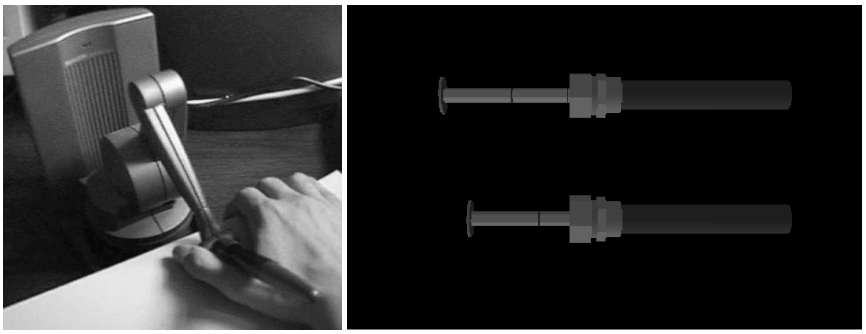

Figure 2.8: Experimental apparatus of Lécuyer et al. [2001]: on the left, the haptic device (PHANToM/sup TM/) that creates the haptic information of the spring, on the right, the visual representation of the spring.

Force Perceptions

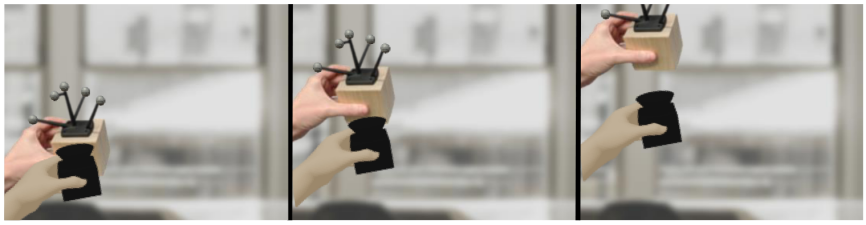

Figure 2.9: Illustration of the manipulation of the C/D ratio to modify the perception of the weight of an object used by [Samad et al., 2019] and by [Dominjon et al., 2005]. Observe that the C/D ratio in the three panels is less than 1 between the virtual and real hand displacement. Our brain compares the energy spent to move the object to the perceived displacement. It then calculates the object's weight thanks to the ratio of displacement to energy expended. Because the visual displacement is reduced, this ratio is higher, and therefore the user perceives the object as heavier than it is.

constant gain One of the first applications of visuo-proprioceptive shifts is to modify the perceived stiffness of objects. Lécuyer et al. [2001] compare a real stiffness simulated by a force feedback interface (PHANToM/sup TM/) and a virtual stiffness simulated by the image of a deforming spring (see Figure 2.8). They show that by introducing a **constant** gain between the displacements of the virtual spring and the real PHANToM, the user perceives a greater or lesser stiffness for the same haptic stiffness. Kumar et al. [2017] extend this technique by not providing haptic feedback to participants. They show that changing the deformation of a virtual spring for the same real mouse movement induces a different stiffness perception. Using a similar technique, it is also possible to simulate not a force (like stiffness) but a torque, i.e., an effort capable of having a mechanical system to rotate around a point (for example a torque of a motor is the rotational effort it is capable of exerting). Paljic et al. [2004] manipulates the perceived torque by introducing a gain between the angular deformations of a torsion spring and the rotation of its virtual counterpart. This rotation gain is similar to the one proposed by Razzaque [2005] between virtual and real head rotation (see paragraph 2.2.2) with the difference that here the control and display device are real and virtual torsion springs.

Adding a constant gain is also used to influence the perception of the mass of an object in VR. Dominjon et al. [2005] show that we perceive an object lighter than it is if we increase the virtual movement of this object when we manipulate it (see Figure 2.9). Samad et al. [2019] reproduce this technique in VR (see Figure 2.9) with a realistic hand avatar which reinforces the embodiment. They also propose a model for predicting perceived weight based on an energetic approach. The perceived weight is related to the energy needed to move it. The concept was also transposed to the rotational motion of an object for the perception of inertia by Yu and Bowman [2020]. A visual rotation larger than its actual rotation has us perceive inertia smaller than what it is.

Figure 2.10: Illustration of the transition of a cube between two media of different viscosity in VR in one of the applications of [Lécuyer et al., 2000]. When this surface change occurs, the cube slows down for the same effort applied to the space ball controlling its movements. The user perceives resistance which he interprets as a force exerted on his hand by the space-ball.

infinite gain Lécuyer et al. [2000] show that a user manipulating an immovable object (a space-ball) can feel different sensations of viscosity or friction. They do this by changing the speed of the object being handled as it changes environment (see Figure 2.10). The user experiences this difference in speed while the pressure applied has not changed. He translates this shift by a sensation of force exerted by the space-ball and, thus, a proprioceptive perception of friction. We note here a difference in the perception of forces of a spring. The user feels a proprioceptive perception when he has not made any movement (the space-ball is immobile). The gain is **infinite**. A visual stimulus thus creates proprioceptive perception.

Non-Constant Gain To stimulate static friction, it is possible to use the stick-slip phenomenon. This phenomenon illustrates the jerky motion between two solids sliding against each other. We observe the alternation of sliding and static phases where the friction momentarily prevents the displacements. Ujitoko et al. [2019] simulate the stick-slip phenomenon when users explore a surface with an input device, for example, a stylus (see Figure 2.11). They add a non-constant gain between the movements of the real and virtual styli. Thus the movements created by the stylus are sometimes blocked at a point (stick) and sometimes slightly accelerated (slip) to recover the correspondence between the movements of the real stylus and its virtual counterpart. During the stick phase, the user perceives static friction preventing the movement.

Temporal Manipulation

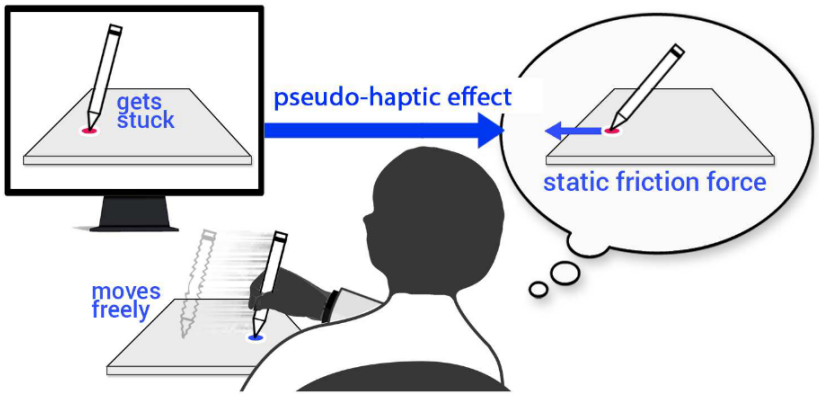

Figure 2.11: The exploitation of the stick and slip phenomenon allows us to feel the saccades in a sliding movement between two solids. The visual movement is blocked when the effort applied to the input tool (here a stylus) is too weak. When the applied effort becomes enough, the visual movement is accelerated to recover the colocalization with the real stylus. The user thus experiences a static friction perception induced by this non-constant gain between the real and visual movements.

We observe in the previous technique exploiting the stick and slip [Ujitoko et al., 2019] that this method introduces a delay between the virtual and real movements of

the user. This idea has been studied by Kasahara et al. [2017]. They propose to study the effect of adding a delay or an advance of the movements of a user's avatar in VR with respect to the movement of the real body. This temporal visuo proprioceptive shift influences our perception of our psychological state. For example, participants reported feeling more elegant but heavier and tired when adding a delay. In contrast, participants reported feeling lighter and more energetic when a lead was added.

The techniques developed in this section are variations of the C/D ratio manipulation. With these techniques, the virtual movements have the same direction as the real movements. Only the amplitude or the temporality of the movements change. In the next section, we present a family of techniques where the direction of movement is modified. Its objective is the manipulation of the user's movements.

2.2.4 Visuo-Haptic Illusion with non-proportional gains

As we already mentioned, with the C/D ratio manipulation presented in the previous section, the virtual avatar performs the same movement as the real body but at a different scale or a different temporality. In other words, the gain applied to the virtual movement is the same for the three axes (x, y, and z). The direction of the movement is the same in real and virtual (see Figure 2.4). For the techniques we present here, the movement of the virtual avatar, especially the hand, is gradually shifted from the movement of the real body. The gain is no longer the same for the three axes (x, y, and z). Through this shift, one can manipulate the movement or the perception of virtual objects. This family of techniques, called *Hand Redirection*, has been mainly used for the improvement of *Passive Haptics*.

Passive Haptics refers to the use of real objects to create haptic interaction while exploring virtual objects [Insko, 2001]. To allow a satisfactory interaction, two main criteria must be fulfilled [Nilsson et al., 2021]. The first criterion is conformity: all haptic properties like size, shape, texture, and stiffness must be sufficiently similar between the real and the virtual object. The second criterion is colocalization: the two objects must be perceived close enough spatially.

The increasing complexity of VR scenes makes it difficult to multiply real objects to match the number and diversity of virtual objects. One solution is to use one real object to serve as a real counterpart to several virtual objects. This real object will therefore be non-conform to most virtual objects and non-co-located. In the vast majority of cases, redirection is used to solve these conformity and colocalization problems. In the rest of this section, we define two different methods of redirection and show that they are used to overcome these problems.

Hand redirection by warping the Virtual Environment

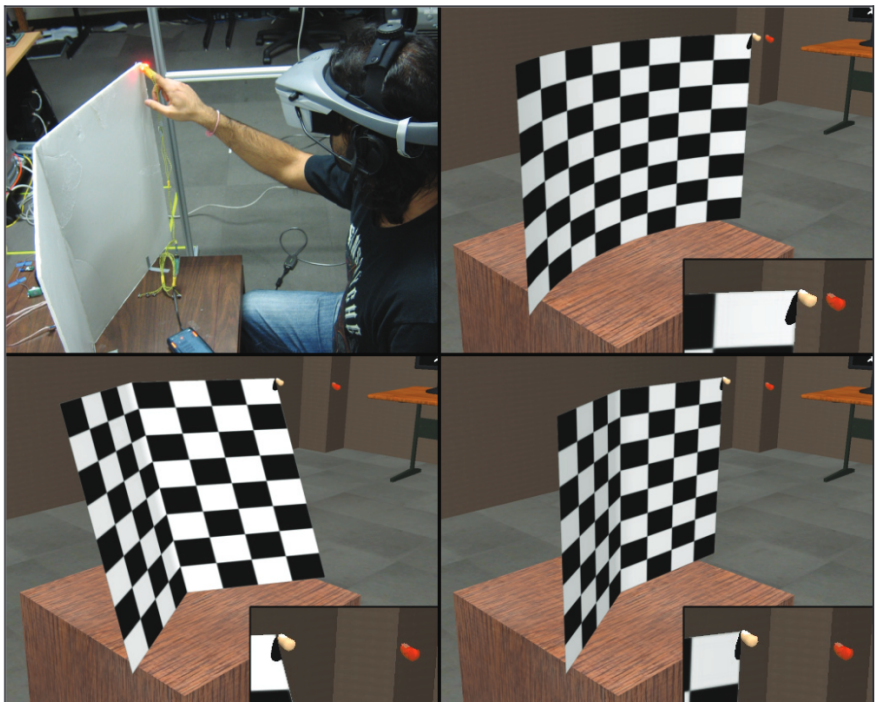

Figure 2.12: In this illustration Kohli et al. [2012] present to users a real target (top left) and 3 virtual targets (the other panels). The virtual space is warped to solve the mismatch between the real and virtual objects. This warp is realized by an adaptation of the *thin-plate spline* technique [Bookstein Fred, 1992]. First, the geometrical limits of the two objects and the points on their surface must be matched. Then the space is warped to fit with these matching. During the user's movement toward the object, the position of the virtual finger is calculated with the position of the real finger and the warping of the Virtual Environment. There is, therefore, a shift between the real and virtual hands. We see examples of these shifts in the figures representing the virtual environment. The real finger's position is represented in red. Thus, the user has the illusion of conformity and co-location of the virtual and real objects.

The first method uses a warping of the virtual space to improve the conformity between virtual and real objects. Kohli et al. [2012] propose a technique to match the same real object to several similar but differently oriented virtual objects. They manipulate the virtual environment to keep the user unaware of the difference in orientation between the real and virtual objects. It is necessary to match the physical and virtual object's boundaries. So the virtual space is deformed to ensure this correspondence (see Figure 2.12). Then given the position of the real hand, the position of the virtual hand is calculated according to this deformation. As a result, the C/D ratio between the movement of the real and virtual hand is not constant and non-linear. Ban et al. [2012] exploit a similar technique to associate several virtual shapes to the same real object. When the user explores the object, the deformation of the space makes the virtual hand follow a curved path to match the shape of the virtual object. The real hand explores a flat physical surface. In these two examples, all the virtual space is deformed to match the constraints of the real world.

Hand redirection by dissociating the movements of the real and virtual hands

The second method uses a progressive shift between the real and virtual body without distorting the rest of the virtual environment. These methods help, in particular, to

manipulate the hand movements of the user. Azmandian et al. [2016] propose a technique which they call *Body Warping* to solve the problem of colocalization of a real object with several virtual objects. This technique is based on a progressive shift of the virtual hand with respect to the real hand while moving toward a target. In this technique, the C/D gain is not the same for every direction (x,y,z). If we consider a shift restrain to (x,y) plane, as we can see in the Figure 2.13, the gain in the x-direction is different from the gain in the y-direction. Because of this shift, the virtual hand deviates from the optimal trajectory to reach the target. Users correct the deviation and shift their real hands in the opposite direction. The offset evolves until it reaches the distance between the virtual target and the physical target at the end of the movement. Users finally touch a physical and a virtual target that is not co-located.

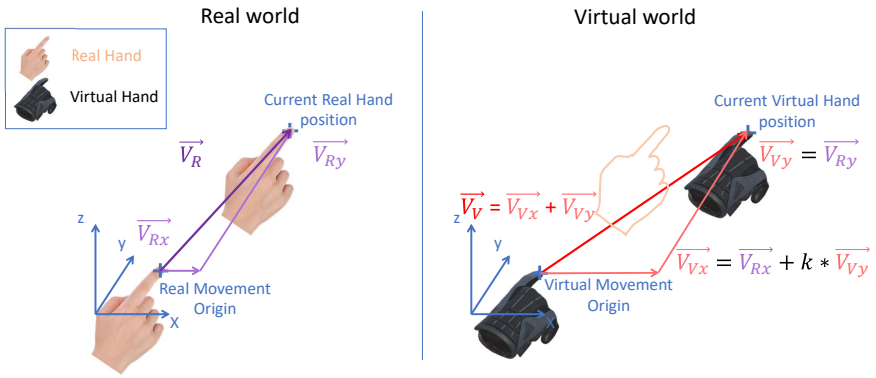

Figure 2.13: Illustration of the technique of hand redirection by a progressive shift of the virtual hand with respect to the real hand during movement. Here, the virtual hand has not the same gain in every direction with respect to the real hand. The difference between $\vec{V_{Vx}}$ and $\vec{V_{Rx}}$ increases proportionally to the vector $\vec{V_{Vy}}$ assuring a gradually increasing shift between the two hands. Note that the shift can be implemented in several different ways and that a difference in the hand's orientation should also be considered.

The same technique is also used to ensure the compliance criterion. Cheng et al. [2017] propose a passive haptic interface with multiple surfaces of different orientations. They use the *Body Warping* [Azmandian et al., 2016] technique to redirect the user's hand to the haptic surface that is most consistent with the virtual object that the user wishes to explore (see Figure 2.14). In a similar fashion to the work proposed to improve the degree of undetectable rotation for walking redirection [Sun et al., 2018, Sra et al., 2018], recent work [Zenner et al., 2021] proposes to use change blindness and blink suppression to increase the rate of undetectable shift between the virtual and real hand.

Note that the use of redirection techniques is not exclusive to passive haptics. They have also been used to improve active haptic interfaces: Abtahi and Follmer [2018] propose to combine different manipulations of C/D ratio, including redirection techniques to improve shape-display interfaces composed of a matrix of actuated pins. Redirection has also been used to overcome the displacement delay of intermittent contact haptic interfaces [Gonzalez et al., 2020].

Figure 2.14: Illustration of hand redirection for the application proposed by Cheng et al. [2017]. We observe on the left (a) their proposed passive haptic interaction interface. It is composed of several surfaces of different orientations. When users want to interact with a virtual object, their intentions are predicted by gaze analysis. They then redirect the user's hand to the surface, offering the best compliance with the virtual object. The interface (a) offers a haptic interaction compatible with different virtual scenes like the one presented in (b) and (c).

2.3 *Conclusion*

In this chapter, we presented an overview of the main illusions involving vision and serving as promising interaction techniques in VR. They are used to overcome certain limitations of VR and aim at improving the user's experience. These illusions are multisensory. They have in common a shift, voluntarily introduced, between the visual stimulus and the stimulus characterizing the same physical event but intended for another modality. In most cases, this shift should be imperceptible to preserve the realism of the VR scene. Indeed a too-important shift will be detected by the user. It results in a decrease in the realism of the VR experience: the opposite of the expected effect. In case of an undetected shift, it disrupts the user's perceptions and movements. The implementation of these techniques requires an understanding of the consequences of this disruption. To investigate these issues, we choose to focus on illusions where the virtual hand is gradually shifted from the real hand during motion. These illusions have the advantage of combining a dynamic shift between visual and proprioceptive information and a disruption of the sensorimotor loop.

In the following chapters, we focus on hand redirection to study the mechanisms that lead to the detection of an illusion and the tools to measure the boundary of illusions.

3

Definition and Measures of Illusion Detection

A class of illusions called *beyond real illusions* [Abtahi, 2021] regroups illusions where users are fully aware that an illusion is implemented and accept this manipulation. In contrast, we discuss in this thesis illusions whose detection would disturb the user experience. Thus, to better understand the detection threshold, we propose to explore how this detection impacts the VR experience and define criteria that are affected by the implementation of illusions. We can then understand the mechanisms that lead to the detection of illusions.

Therefore, in the first section, we select criteria that define a successful VR experience, more specifically, the central notion of Presence and one of its major components: the sense of Embodiment. In the second section, we present the mechanisms that lead to a successful illusion. We define why the illusion can break and negatively impact Presence and Embodiment. In the last section, we review the different methods to measure Presence and Embodiment and discuss how these

methods are transposed to measure an illusion's effectiveness and detect when it breaks.

3.1 Criteria of Evaluation

3.1.1 Immersion and Presence

Immersion and Presence are two measures of users' experience in VE. We define and compare these notions in this section.

Immersion

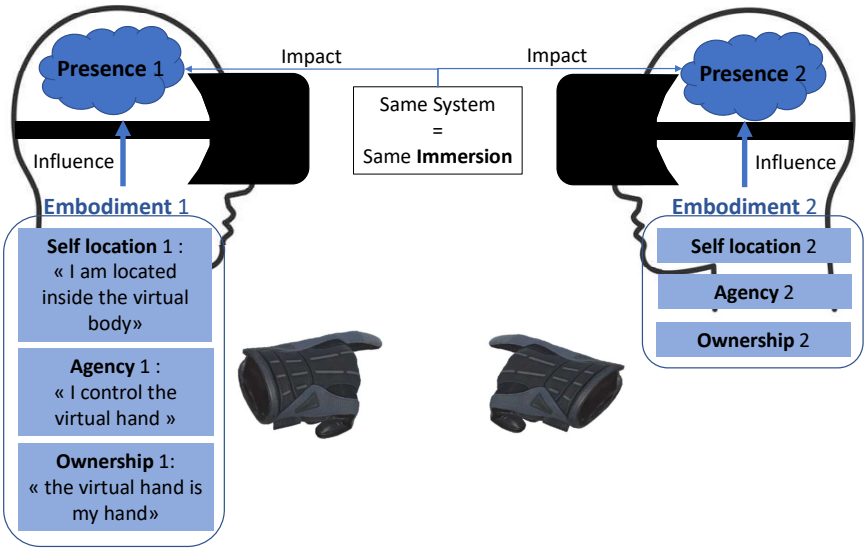

Figure 3.1: Representation of two users in VR with the same system. The two users have the same Immersion. However, their level of Presence can be different. In particular, they can have a different level of Embodiment toward the virtual body (here represented by a virtual hand). Three main properties lead to a sense of Embodiment (SoE): the Sense of Agency (SoA), the Sense of Self Location, and the Sense of Ownership (SoO).

Immersion refers to the system's technical capability to deliver a convincing environment in which the participant can interact [Sanchez-Vives and Slater, 2005]. The degree of Immersion depends on the system and can be evaluated independently of user experience. It depends on factors such as the number of modalities the system stimulates, the quality of rendering of each sensory modality, and the fluidity of users' motion tracking. Following the definition of Slater and Wilbur [1997], a system is more immersive if it is superior in at least one of the characteristics that define the realism of a virtual environment. Slater [2009] extends this definition. They characterize immersive systems by the sensory-motor contingencies that they can provide. For example, when users rotate their heads, the field of view in virtual should change accordingly. Likewise, users, when reaching to touch an object, should physically encounter the object (haptic interaction) at the end of the

movement. Thus a system A is at a higher level of Immersion if the sensory-motor contingencies available with B are a subset of the ones available with A. These considerations are important but do not reflect users' experiences in the VE. To address this, we need another marker: the Presence in the Virtual Environment.

Presence

The concept of Presence in the context of VR is the topic of numerous studies [Skarbez et al., 2017], and its definition is subject to debate. The notion of Presence in a Virtual Environment can be traced to James Gibson's work [Gibson, 2014] via Steuer [1992]. The Gibsonian idea is that: "Presence is a subjective feeling generated by our perception of the real world as mediated by our sensory organs and the mental processes governing and integrating them". In other words, Presence was first defined as the sense of being here in an environment; for Gibson, it could be the real environment. This concept was called telePresence [Minsky, 1980, IJsselsteijn et al., 2000] to define the phenomenon in which a human operator develops a sense of being physically present in a remote location through system's interaction. In the context of VR, it is the sense of being in the Virtual Environment instead of the real world. This definition of Presence can be qualified as "passive". The user observes the aesthetic realism of the VE and feels located in this VE; it is: "the subjective experience of being in one place or environment, even when one is physically situated in another" [Witmer and Singer, 1998].

The definition of Presence was extended to consider the active exploration of the VE. In 2001, Biocca [2001] defined Presence as "the phenomenal state by which an individual feels located and active in an environment". Thus Flach and Holden [1998] proposed that more than the realism of the VE, the most important characteristic of a VE is the quality of provided interaction. Presence can then be seen as the correspondence between the perception/action coupling in the VE and the one learned in the real world [Zahorik and Jenison, 1998, Slater, 2003]. Slater [2009] regroups the concept of feeling located and the coherence of the perception/action loop in the VE under the term **Place Illusion**, which he describes as: "the strong illusion of being in a place despite the sure knowledge that you are not there". With this definition, Presence is either in place (the illusion is working) or broken.

At this point, one can wonder what the difference between Presence and Immersion is (see Figure 3.1). Indeed, we characterize Immersion as the ability of a system to provide sensory-motor contingencies. Thus, it seems that by measuring the Immersion of a system, it is possible to predict the feeling of Presence of users,

according to the definition of [Zahorik and Jenison, 1998, Slater, 2003, 2009]. Let's see two examples to differentiate Immersion and Presence here: Imagine two users, one slowly walking in a VE and another actively exploring and touching all the virtual objects. The VE provides the same Immersion for both. However, the second user is more likely to experiment a break in sensory-motor contingencies that decreases the feeling of Presence in the VE: the two users are likely to have two different feelings of Presence. Imagine a second case where a professional tennis player and a beginner play a tennis game in a VE. The professional tennis player is more likely to notice a sensory-motor problem from a fine-tuned gesture learning. Thus, *Immersion* refers to the technical capability of the system, and *Presence* refers to users' personal experience with the system.

To complete his view on Presence, Slater [2009] proposes a second illusion, the *Plausibility illusion* (PSi). While the *Place Illusion*(Pi) refers to how the VE is perceived: "I sense that I'm here", **Plausibility illusion** is about what is perceived: it is the conviction that events are real even though you know they are not real. This illusion is strongly related to an event in the VE over which you have no direct control but that you caused. For example, if we wave at a virtual avatar in front of us and the virtual avatar waves back in a VE, the PSi is reinforced. Thus Plausibility is not strongly related to the realism of stimuli provided by the system but more to the coherence and the likeliness of the event that occurred.

If Presence is seen as an illusion, it leads to the idea that Presence is either on or off if the illusion is either in place or broken. It is the opinion of Lombard and Ditton [1997] that defines Presence as binary. However, several authors contradict this idea [Spagnolli and Gamberini, 2004, Schubert, 2009] and assume that Presence is a more continuous function. In other words, we can experience different levels of Presence.

One easy way to assess that you are in a real physical environment is to look down on your body and see it. You can move your arm and acknowledge the coherence between your movement's intention, the movement you see, and the movement you perceive with proprioceptive feedback. The body is a powerful vector of Presence in an environment, and particularly a virtual avatar of your real body is a central factor for Presence in a VE [Slater, 2009]. The Sense of Embodiment towards a virtual avatar is a combination of PI and PSi, where the coherence of events and how events are perceived are equally important.

3.1.2 Embodiment

Similar to Presence, there are several ways of defining the sense of Embodiment (SoE). Here we follow the definition proposed by Kilteni et al. [2012] based on previous partial definitions of De Vignemont [2011] and Blanke and Metzinger [2009]: "SoE toward a body B is the sense that emerges when B's properties are processed as if they were the properties of one's own biological body".

Based on the literature, three main properties define our biological body and lead to SoE (see Figure 3.1). First, we feel located inside our bodies. For example, in a video game, if you control a character from a third-person point of view, you do not feel located inside the character's body. This feeling of not being located inside our body can also be experienced in out-of-body experiences [Blanke and Mohr, 2005], where a person experiences the world from a location outside the body. On the other hand, in everyday life, one has the feeling to control their body from the inside, that one's body and self are in the same position. This feeling of our self being located inside the body is called **Sense of Self-Location**. Self-location should not be confused with PI. In virtual reality, the sense of self-location would be the feeling of being located inside a virtual body. It is then an extension of PI because the virtual avatar is necessarily in the virtual environment. Although it is an important component of Embodiment, we do not detail this term further because it is less relevant in our study of illusion. The two other parameter are **the sense of Agency** (SoA), and **the sense of body Ownership** (SoO).

Sense of Agency

The sense of Agency is typically defined as the experience of controlling one's own actions and, through them, changes in the external environment [Grünbaum and Christensen, 2020]. The SoA has been widely studied in the field of cognitive neuroscience mainly because trouble in SoA is strongly related to illnesses such as schizophrenia [Frith, 2015]. In the context of HCI, in addition to the implication for the Embodiment of a virtual avatar, it can inform on how users feel in control when interacting with technology [Limerick et al., 2014].

A distinction can be made between two different SoA: a bodily SoA and an external SoA [Grünbaum and Christensen, 2020]. To understand the difference, let's cite an example from Haggard [2017]: In the dark, if one reaches for a switch to turn on the light, they first expect to touch the switch and then that the light turns on. The feeling of control over the arm during the successful trajectory towards the switch is a *bodily SoA*. The feeling of control over the change in the external environment when the light turns on is *external SoA*. Let's discuss the mechanisms

that could lead to bodily and external SoA.

The mechanism that is frequently cited as the best explanation of bodily SoA is the so-called **comparator model** [Frith, 1987] (see Figure 3.2). According to this model, the SoA occurs when the prediction of the sensory consequence of an action matches the actual sensory feedback at the end of the action [Haggard, 2005]. When the brain creates a motor signal, it also generates a copy of this motor command called "efferent copy" [Von Holst and Mittelstaedt, 1950]. The sensory perception is then predicted based on this efferent copy [Miall and Wolpert, 1996, Wolpert and Ghahramani, 2000]. When the predicted and actual perceptions match, a strong SoA is experienced [Frith et al., 2000].

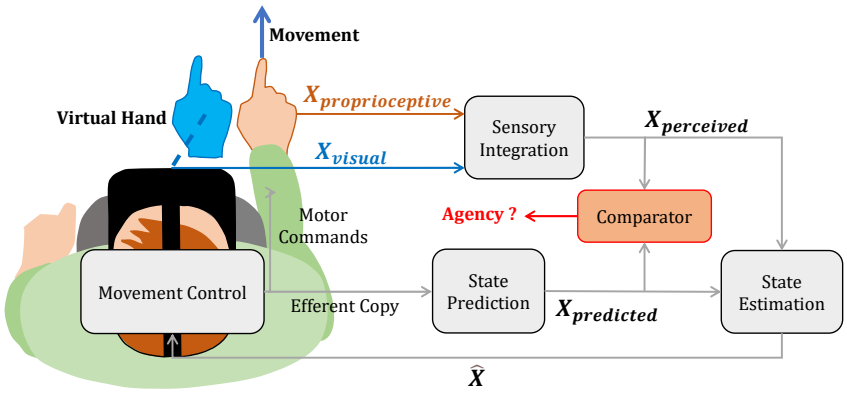

Figure 3.2: Diagram of the comparator model [Frith, 1987]. An efferent copy is emitted with the emission of a motor command. A prediction of the sensory consequence of an action calculated based on the efferent copy is compared to the actual sensory feedback. If the two information are significantly close, a strong sense of Agency is experienced. In our case, the visual sensory information is perturbed by the implementation of the illusion.

The comparator model can explain why we experience Agency over a virtual avatar. Slater et al. [2010] show that users feel the Agency over a virtual avatar matching real movement. The pertinence of the comparator model is reinforced by the fact that the user representation [Seinfeld et al., 2021] does not have to be realistic. Even if the arm of the user is represented by a sphere in VR, the SoA over the sphere is possible if it mimics arm movement [Zopf et al., 2018].

The external SoA, on the other hand, is not well explained by the comparator model [Grünbaum and Christensen, 2020], but seems more related to prior knowledge of the intended goal of the action [Limerick et al., 2014]. In our past example, let us imagine it is a halogen lamp. The light turns on several seconds after pressing the switch. The external consequence (light on) is thus temporarily separated from the arm's movement, and the event occurs through an intermediate tool: the switch. However, one still feels to be the cause of the event. Thus, low-level sensory feedback or motor factors does not seem to be linked to a strong SoA here. This assumption is comforted by the fact that one can experience SoA over action that one did not cause [Synofzik et al., 2008]. For example, a user

can feel a SoA over a virtual walking body while seated while only allowed head movement [Kokkinara et al., 2016]. Wegner et al. [2004] also shows that a user can feel a SoA over the movement of the arm of another person if the movement is coherent with the movement they could have made and if they hear instructions prior the movement, describing the seen action .

Sense of Body Ownership

The literature suggests making a difference between the feeling of being the master of your movement, "I control my arm", which is the SoA, and the feeling of Body Ownership, "I sense that it's my arm " [Gallagher, 2000]. Body Ownership refers to one's self-attribution of a body [Gallagher, 2000, Tsakiris et al., 2006]. It has a possessive nature, implying that the body is the source of the experienced sensations. The SoO seems to have its origin in a combined bottom-up and top-down approach [Tsakiris and Haggard, 2005, Tsakiris, 2010]:

Bottom-up approach Here we refer to the idea that perceptions coming from different modalities strongly influence the SoO. As in the rubber hand illusion (RHI) (subsection 2.1.2), a congruent visuo-haptic simulation is sufficient to induce the SoO [Botvinick and Cohen, 1998]. Also a visuo-proprioceptive congruency can achieve this goal too [Sanchez-Vives et al., 2010], although the resulting SoO is weaker than the one induced by visuo-tactile congruence [Dummer et al., 2009]. This approach is particularly interesting in VR, where users can experience Ownership over a virtual avatar that mimics their movement [Maselli and Slater, 2013]. Moreover, Ownership over the virtual body can be enhanced by other sensory congruences. For example, adding a haptic confirmation when a user touches a virtual object reinforces Ownership over the virtual hand [Slater et al., 2009].

We notice here some similarities between the mechanisms leading to SoO and SoA. Indeed in a voluntary action (for example, reaching for a target), SoO is experienced by the synchronous visuo-proprioceptive stimulation, and SoA is experienced with the coherence between perception and motor action. The question that arises is whether the two feelings influence each other [Braun et al., 2018]. Despite some results denying a reciprocal influence of SoO and SoA [Walsh et al., 2011], there is ample evidence that they strengthen each other [Dummer et al., 2009, Kalckert and Ehrsson, 2012, Braun et al., 2014].

Top-down approach According to the neurocognitive model of SoO [Tsakiris, 2010], the SoO results from the comparison of sensory information and prior knowledge of our body state. To consider a body as our body anatomical/textural, spatial

and postural constraints have to be fulfilled [Braun et al., 2018] (see Table 3.1). The anatomical and textural constraints impose that the artificial body must be realistic; for example, it cannot be an artificial hand or a wooden block [Haans et al., 2008, Tsakiris and Haggard, 2005, Tsakiris, 2010], or cannot have white skin if the user has black skin [Lira et al., 2017]. The spatial constraints impose that the artificial body must be spatially close to the real body. For example, in the RHI, the greater the distance between the real and rubber hand, the weaker is the SoO [Lloyd, 2007, Preston, 2013, Kalckert and Ehrsson, 2014]. Finally, the postural constraints impose that the artificial body limbs must be anatomically aligned with the real ones. If the rubber hand is in a different orientation from the real hand, the RHI diminishes. [Tsakiris and Haggard, 2005, Braun et al., 2014].

Table 3.1: List of Constraints that must be respected for a SoO toward an artificial limb to arise.

Factors	*Constraints on the artificial limb*
Anatomical	Body-shaped object [Haans et al., 2008]
Textural	Natural skin texture [Haans et al., 2008] match the user skin color [Lira et al., 2017]
Spatial	Horizontally close to the real limb [Lloyd, 2007, Preston, 2013, Kalckert and Ehrsson, 2014] Vertically close to the real limb [Kalckert and Ehrsson, 2014]
Postural	Anatomically aligned with the real limb [Tsakiris and Haggard, 2005, Braun et al., 2014]

We saw several factors (*Immersion, Presence, Embodiment*) characterizing the possibilities offered by a VE to make users believe that what is happening is realist. We saw in the first chapter that it was possible to create illusions in VR by manipulating the C/D ratio between users' real movements and their virtual avatar's. If the illusion "works", we can assume that the manipulation has only a limited impact on users' Embodiment (perturbation of the SoO or SoA) or, in a more global way, on the realism of the virtual experience and thus in the feeling of Presence in the VE.

To understand how illusions can affect these criteria, let's first understand what mechanisms are responsible for the emergence of illusions.

3.2 Impact of Illusions on Presence

Several mechanisms participate in the emergence of an illusion from the manipulation of visual stimuli [Gonzalez-Franco and Lanier, 2017]. Understanding these

mechanisms can help us understand how an illusion stops working as well. It can also inform us on what criterion of Presence breaks because of the sensory-motor perturbation induced by the illusion. In this section, we first explicit the mechanisms that lead to the emergence of an illusion. Then, with the help of these mechanisms, we analyze the impact of amplitude of illusion on the criteria presented in the first section.

3.2.1 Model of Illusions in VR

The illusions we study in VR are based on a voluntary mismatch between information from different modalities. The illusion results from the attempt of the brain to solve this mismatch. To do so, it combines two mechanisms: bottom-up, and top-down [Gonzalez-Franco and Lanier, 2017].

Bottom Up Sensory Processing

Perception is the organization, identification, and interpretation of information about events in the environment coming from our sensory modalities. Various sensory organs continuously provide our brains with uncertain information about our environment. For example, we often struggle to perfectly localize the origin of a sound: the auditory modality provides noisy information on the origin of the source. In most cases, the brain combines all the information it has about a physical event: perception is multi-sensory [Stein and Meredith, 1993]. The brain aggregates these differently encoded, noisy information on different temporalities to form a robust and unique representation of the environment. Thus, a **bottom-up sensory processing** informs us about our surroundings and the state of our bodies. As we have seen in the subsection 3.1.2 this bottom-up sensory processing is a key aspect of the SoO and SoA.

In the chapter 6, we will see in more detail that the brain can combine the different sensory information in a statistically optimal fashion [Ernst and Bülthoff, 2004]. With this process, it solves the possible discrepancy between the sensory information. Let's note that the more information are congruent, the more the brain is likely to trust the final combined perception. The "spatiotemporal rule" holds that stimuli presented in spatiotemporal proximity have a higher probability of being combined to form a perception of a physical event [Meredith, 2002]. In our brain, the responses of multi-sensory neurons are increased in case of spatiotemporal congruence and decreased otherwise [Wallace et al., 1993]. For example, a congruent seen and proprioceptively perceived movement favors the SoE toward the virtual avatar and, thus, Presence in the VE. However, if the presented information is too

Multi-sensory neurons: neurons integrating data coming from different modalities

ambiguous or asynchronous, the brain can reject the data from this modality. We saw, for example, in the subsection 2.2.2 that a user sitting in the real world while moving in VR can experience cyber-sickness [Rebenitsch and Owen, 2016]. One of the main causes of cyber-sickness seems to be the non-congruent visual and vestibular sensory information [Akiduki et al., 2003].

Visuo-haptic illusions in VR are based on the mismatch between vision and haptic perception. The brain can solve this issue without a break in Presence or Embodiment. Indeed, the multi-sensory system can enhance or depress the role of each unimodal stimulus exerting influence in a specific situation [Stein and Stanford, 2008]. On several occasions, because of the predominant role of vision (attention, exploration), more weight is given to the visual information in case of incongruence between different sensory modalities. This phenomenon is called *visual capture* [Rock and Victor, 1964]. For example, in the RHI, a discrepancy is introduced between the hand's seen and proprioceptively felt position. Visual capture is one explanation of how the brain solves this discrepancy [Pavani et al., 2000, Folegatti et al., 2009, Ponzo et al., 2018]. In this case, the validity of the visual information is reinforced by the visuo-tactile stimulation of the virtual hand.

Top-down manipulation of afferent feedback

We have seen in the subsubsection 3.1.2 that bodily SoA arises when the prediction of the sensory consequences of action matches the actual sensory feedback at the end of the action [Haggard, 2005]. Thus a good matching between user real and virtual movements facilitates this sensory-motor coherence and reinforces SoA and, therefore, Embodiment. Also, sensory-motor coherences can be at the origin of the RHI [Sanchez-Vives et al., 2010]. However, several C/D ratio-based illusions are a dynamic manipulation of visual information and, thus, a perturbation of the sensory-motor loop. With hand redirection, for example, the visual position of the hand is gradually shifted from the real position. Thus, the perception of the hand coming from a combination of visual and proprioceptive information can be different from the predicted position of the hand based on the efferent copy of the motor command. This incoherence could lead to a break in the SoA.

In this type of illusion, a strong top-down manipulation seems to occur [Gonzalez-Franco and Lanier, 2017]. The brain can correct sensory information if it's too different from a predicted state [Haggard and Chambon, 2012]: "I have a prediction ergo this is my final state". For example, with hand redirection, the brain can correct the proprioceptive information to match the visual information about the hand position. The brain can also choose to ignore the drift between the predicted

position and the actual position of the hand.

Illusions does not always work. Sometimes, when the mismatch between information is too important, the illusion breaks. We will see in the next subsection that, at least for the C/D ratio manipulation-based illusions, this break is mainly a break in Embodiment and especially a diminution of the SoO and SoA.

3.2.2 Detection of the illusion

The brain can reject an illusion if it notices that something is wrong. Following the definition of Spagnolli and Gamberini [2004], Schubert [2009], Presence can be seen as a continuous feeling, and therefore one can experience several levels of Presence. Following this idea, a defective illusion does not necessarily suppress the feeling of Presence, but can disturb it to a greater or lesser extent. In the case of visuo-haptic illusions, the main risk in implementing the illusion is to decrease the SoE toward the virtual avatar. More precisely, the illusion can affect the SoO and the SoA.

Decrease in the Sense of Ownership

We have seen that several factors (see Table 3.1) can modify the level of SoO induced by the rubber hand illusion. Let us remember that it is weaker if it is induced with a visuo-proprioceptive congruent stimulation compared to visuo-tactile congruent stimulation [Dummer et al., 2009], but the SoO is stronger if both stimuli are used [Kokkinara and Slater, 2014]. The SoO can also be decreased if anatomical, textural, spatial, and postural constraints are not respected [Braun et al., 2018]. The existence of the postural and spatial constraints proves that it exists a limit beyond which the discrepancy introduced between the proprioceptive and visual information is too important and decreases the SoO. In all the C/D ratio manipulation-based illusions, we can assume that there is also a limit in the discrepancy introduced between the different sensory information. In our study of hand redirection, a moment can occur where the virtual hand (visual feedback) is too far from the real hand (proprioceptive feedback). The discrepancy is too big for the brain to disregard information from one modality during the bottom-up sensory processing. For the hand redirection illusion, this could lead to lower Ownership over an avatar hand. A weak SoO leads to a weak SoE and reduce the feeling of Presence inside the VE.

Decrease on the Sense of Agency

In subsubsection 3.1.2, we've discussed the distinction between two SoA: bodily SoA and external SoA. The mechanism that seems to cause bodily SoA is the

comparator model [Frith, 1987]. During the movement, an error monitoring loop compares the actual perceived state of the body with the predicted sensory consequence of our action, created using an internal (efferent) copy of our motor commands. Let's consider the phenomenon of visual capture. The brain gives more weight to visual information; therefore, the multi-sensory perception of our body state is discordant with the predicted state. The discrepancy between the body's predicted and actual perceived state may become so large that users notice it. If the error is too important, a specific potential is generated in the brain similar to the one of a semantic or conceptual violation [Padrao et al., 2016]. This error-generated potential is different from the one generated for small errors caused by motor and sensory perception noises [Padrao et al., 2016]. The brain considers that the error in the avatar movement is not self-generated and that it violates body movement semantics.

The external SoA can help users feel a SoA toward a virtual avatar without a good similarity between users' real and virtual movements. Indeed, with visuo-haptic illusion, the final goal of the action can be achieved, even if the visual information about the state of the body during the action is disturbed. Thus, users can still feel control over their actions and changes in the external environment. Moreover, Delahaye et al. [2022] showed that users are less likely to detect a perturbation of the movement of their virtual avatar if this perturbation helps them achieve the goal of an action. For example, with hand redirection, it's possible to maintain a SoA, even if the virtual hand is significantly shifted from the real hand. To achieve this goal, we need to add a haptic confirmation at the end of the movement when the virtual hand touches a virtual target. Thus, similarly to the SoO, users would be able to experience different levels of SoA.

We have seen that a successful illusion does not decrease the feeling of Presence of users. Thus, to study visuo-haptic illusion and especially the detection of illusion, we need ways to measure Presence, Embodiment, SoA, and SoO, i.e., markers that could indicate if the illusion has broken or it is working.

We will review in the next section the different ways of measuring these different criteria. We then compare these measures to the methods to study visuo-haptic illusion detection.

3.3 Evaluation of Illusion Detection

3.3.1 Measures of Presence and Embodiment

Presence measures can be divided into subjective and objective measures [Souza et al., 2021]. Measures of SoE are a subpart of Presence measures and can be classified in the same subjective and objective manners. We detail here the different methods employed in the literature to measure Presence, especially those focused on measuring Agency and Ownership toward a virtual avatar.

Subjective Measures

The vast majority of subjective measures methods use questionnaires with questions with rating scales, such as the **Likert scale** . Let's look, for example, at one of the most widely applied questionnaires, the one of Slater et al. [1994]. It's based on questions around the idea of *"being there"* with a 7-point Likert scale. One question is, for example : *rate your sense of being there: "In the computer-generated world I had a sense of being there" from 1: not at all to 7: very much*. The questionnaire of [Witmer and Singer, 1998] is another largely used questionnaire. It aims to evaluate the level of control users have over events that happened on the VE. The Presence score is the sum of ratings of the 7-point Likert scale rating question. Note that the notions of control over what happens in an EV are close to SoA and SoE. Several questionnaires have indeed been proposed to measure Embodiment. Recently, Gonzalez-Franco and Peck [2018] proposed a standardized questionnaire of 25 questions that regroup the main idea of the past two decades of questionnaires about Embodiment. They separate their questions into six groups representing the main criteria investigated in the past questionnaires: body Ownership, Agency, and motor control, tactile sensations, location of the body, external appearance, and response to external stimuli. For example, one of the questions regarding body Ownership is: "I felt as if the virtual hand was my hand", and one regarding Agency and motor control is: "It felt like I could control the virtual hand as if it was my own hand".

A **Likert scale** is a psychometric tool for measuring an attitude in individuals. It consists of one or more statements (statements or items) for which the respondent expresses a degree of agreement or disagreement. For example, a 5-point Likert Scale would propose these response: strongly disagree, disagree, neither agree nor disagree, agree, strongly agree

The main advantage of subjective measures is that they are easy to implement, and data are easily interpreted. However, subjective methods do not inform on the evolution of Presence over the duration of the experiment. They also do not allow real-time measurement of Presence or Embodiment. Moreover, participants have their own interpretations of questions, and it is difficult to ensure that the same answer reflects the same feeling [Hale and Stanney, 2014]. To illustrate this Slater [2004] compares Presence to a made up concept call "colorfulness". They conduct

an experiment where participants are asked to evaluate their level of this invented state of mind. By this mean, they emphasize that the concept of Presence is too abstract to be studied by questionnaires.

Objective Measures

Several objective methods have been implemented to avoid the constraints of subjective measures. The idea is that the feeling of Presence or SoE can produce behavioral or physiological responses that can be measured. For example, users on the edge of a virtual precipice in a VE is more careful in their movements and can experience sudden sweating. The more the SoE or feeling of Presence is strong, the more the behavioral or physiological responses should be similar to the ones in a real environment.

Behavioral measures A notable example of behavioral measures to evaluate Ownership over a rubber hand is the response to threats (for example a stabbing [Sanchez-Vives et al., 2010]) the rubber hand. If the SoO toward the rubber hand is strong, users react quickly to prevent the rubber hand from being at risk. Concerning SoA, it can be evaluated with sensory attenuation Blakemore et al. [1998], however the most widely used implicit SoA measure is *intentional binding* [Moore and Obhi, 2012]. Intentional binding refers to the perceived contracted time between a voluntary action and the expected consequence of this action. For example, if a flash is produced 1 second after pushing a button, the voluntary push of a button results in a perceived time between the push and the flash smaller than 1 second. This time interval is only underestimated if the action is voluntary [Haggard et al., 2002] and not passively conducted [Wohlschläger et al., 2003], i.e., when users have the SoA over their actions.

Compared to physiological measures, behavioral measures have several disadvantages. Indeed, it is complicated to ensure that the experimental condition caused a behavior. Moreover, a behavioral measure may not be transposed to a different environment [Riva et al., 2003].

Physiological measures In contrast to behavioral measures, physiological measures are transposable between different VE, quantitative, and obtained continuously throughout the experiment. To evaluate users' reaction to different stimuli, it's possible, for example, to measure: the electrical activity of the heart with an electrode placed on the skin [Riva et al., 2003], the change in the electrical conductance of the skin [Meehan et al., 2002], the movement of the eyes and the dilation of the pupils [Laarni et al., 2003], and the electrical activity produced by muscles [Ravaja et al.,

2006]. Although these measures are promising, it is challenging to directly link one physiological response to a specific feeling of Ownership of Agency. Moreover, many uncontrolled variables may influence the measures [Hale and Stanney, 2014].

Neurophysiological measures

More recently, different neurophysiological techniques (i.e., based on the evaluation of nervous system function) have been proposed and used to study Presence and Embodiment in a VE, such as Functional magnetic resonance imaging (**fMRI**) and Electroencephalography (**EEG**). We now list the main studies investigating the loss of Agency or Ownership using neurophysiological techniques.

fMRI measures brain activity by detecting changes associated with blood flow. This technique relies on the fact that cerebral blood flow and neuronal activation are coupled. When an area of the brain is in use, blood flow in that region also increases.

fMRI Nahab et al. [2011] identifies the brain area involved in mismatch during finger movements, and also identified other areas that seem to process this mismatch. Padrao et al. [2016] also used fMRI to identify brain responses to an Agency violation. They record the brain activity of participants embodied in a virtual body while performing an error-prone fast reaction time task. They identified two very different Event-related potential (**ERP**) signatures for self-generated error (error due to motor or sensory noises) and false errors (error due to an external perturbation of participants' movements). The false error, if too important, should lead to a break in SoA. They thus possibly identified and measured the brain response related to an Agency violation.

EEG is a method to record an electrogram of the electrical activity on the scalp that has been shown to represent the macroscopic activity of the surface layer of the brain underneath. It's a non-invasive technique.

Using fMRI requires a complex and expensive device that is not transportable. That's why instead, it can be interesting to use EEG. Jeunet et al. [2018] used EEG in a VR experiment aiming at investigating a novel approach to characterize the SoA. They identified possible neurophysiological markers of the SoA. They argue that further investigations are needed to determine if that marker could be used to perform real-time measures of the SoA. Similarly, in a VE, Alchalabi et al. [2019] used EEG to measure the Embodiment of a virtual avatar when walking. Participants were walking in the VE, and visual feedback of their avatar movements were either congruent or incongruent with their real walking movements. In the case of incongruent movement, they identified a strong and long Event-related synchronization (**ERS**) in the central-frontal area of the brain. They hypothesize that this response is due to a break in Agency. Very recently, [Casula et al., 2022] studied how the SoO over a virtual hand is generated at a neural level. They used EEG to record participants' brain activity when embodying a virtual hand. Their result suggests that the Ownership of the virtual hand is associated with a drop in the brain region responsible for hand control.

ERP is the measured brain response that directly results from a specific sensory, cognitive, or motor event. More formally, it is any stereotyped electrophysiological response to a stimulus.

Event-related synchronization (ERS) is a relative power increase of electroencephalogram in a specific frequency band during physical motor execution and mental motor imagery.

Although these measures are promising, it is still difficult to associate a drop

in SoA or SoO with an objective brain response. In the case of hand redirection illusion, the eventual break in Agency or Ownership can happen at any time along the movement and is thus difficult to time precisely. This can make identifying a brain activation linked to this illusion detection problematic.

In the next section, we review the different measures of visuo-haptic illusions detection, and we put them in perspective with the criteria, the mechanisms, and the measures we presented.

3.3.2 Detection of C/D ratio based illusion

Subjective Measures

Presence and Embodiment are used as criteria to evaluate the effectiveness of C/D ratio-based illusion. Several researchers that proposed a new illusion based on C/D ratio manipulation were interested in the detection of the illusion. Most of the studies about visuo-haptic illusion ask participants to answer a Presence questionnaire after being subjected to the illusion. If participants maintain a feeling of Presence in the VE when the illusion is implemented, then it has proven efficient.

Several authors that implemented illusions aimed to evaluate the maximum amplitude beyond which participants notice it or judge it uncomfortable [Kasahara et al., 2017, Rietzler et al., 2018, Cheng et al., 2017, Burns et al., 2006, Abtahi and Follmer, 2018]. Similarly to the subjective measure to evaluate Presence, the most straightforward way to evaluate the impact of illusion is to use questionnaires. Thus, after being presented with various degrees of mismatch, participants are then asked simple questions such as: "was there an illusion ?" or "could you tolerate this illusion for a certain amount of time ?". The amplitude is then fixed as the biggest degree of mismatch acceptable by all participants. However, answers to questions are difficult to quantify. Some work [Abtahi and Follmer, 2018, Cheng et al., 2017] tried to add Likert scales to their question for better quantification.

These subjective measures are relevant for the design of illusions that maintain an acceptable level of Presence in a VE. However, results depend on participant subjectivity. It is challenging to consistently detect a decrease in Embodiment. Moreover, these studies do not provide a lower bound detection threshold (DT), i.e., a value of illusion amplitude that guarantees a non-detection of the illusion for a great majority of users.

Modified Subjective Measures

Studies that aimed to rigorously quantify lower bound DTs mainly focus on calculating *just noticeable differences* (JND) of conflict between the two modalities. In those studies, participants participate in a two-alternative forced-choice experiment (2AFC). Their task is sometimes to evaluate in which direction their visual feedback was manipulated [Steinicke et al., 2009]. For example, in the case of hand redirection illusion, the virtual hand of the participants is shifted either to the left or the right of the real hand. In the 2AFC experiment, participants must choose between two options "my virtual hand is on the right or on the left of my real hand". The task can also be to answer "yes" or "no" if they detect a modification of their visual movements [Gonzalez and Follmer, 2019, Ogawa et al., 2020]. Such methodologies were used in the redirected walking literature, especially by Steinicke et al. [2009] to evaluate DTs for various redirected walking techniques. It was extended in other studies. For a review, see [Grechkin et al., 2016]. This methodology was adapted for visuo-proprioceptive mismatch by Lee et al. [2015] and more recently by Zenner and Krüger [2019]. A detailed description of the experimental design can be found in chapter 4.

Although this measure is still subjective, the nature of the task (2AFC) limits participants. The processing of the data is also straightforward. The measured DT can be qualified as lower bound DTs because participants are aware that an illusion is implemented and are focusing on the manipulated stimulus. Moreover, DTs are calculated to work for every user, though those thresholds should vary between participants.

Overview of Calculated Detection Threshold

Detection Threshold for RHI and Redirected Walking The strength of the RHI and the resulting SoO over the artificial hand (rubber or virtual) can decrease if the real and artificial hand are more than 27 cm apart [Lloyd, 2007] (note that other works suggest that a distance of 45 cm can be tolerated without impact on SoO [Zopf et al., 2010]). This suggests that we can disregard a significant visuo-proprioceptive mismatch in certain conditions. Concerning redirected walking, Steinicke et al. [2009] showed using the 2AFC-based measures presented in the previous section that users can believe that they are walking in a straight line while being redirected on a circular arc with a radius greater than 22 m. This suggests that we can tolerate a constant gain between real head rotation (perceived with the vestibular modality) and the visually observed virtual head rotation. These results are useful for comparison with calculated hand redirection DT.

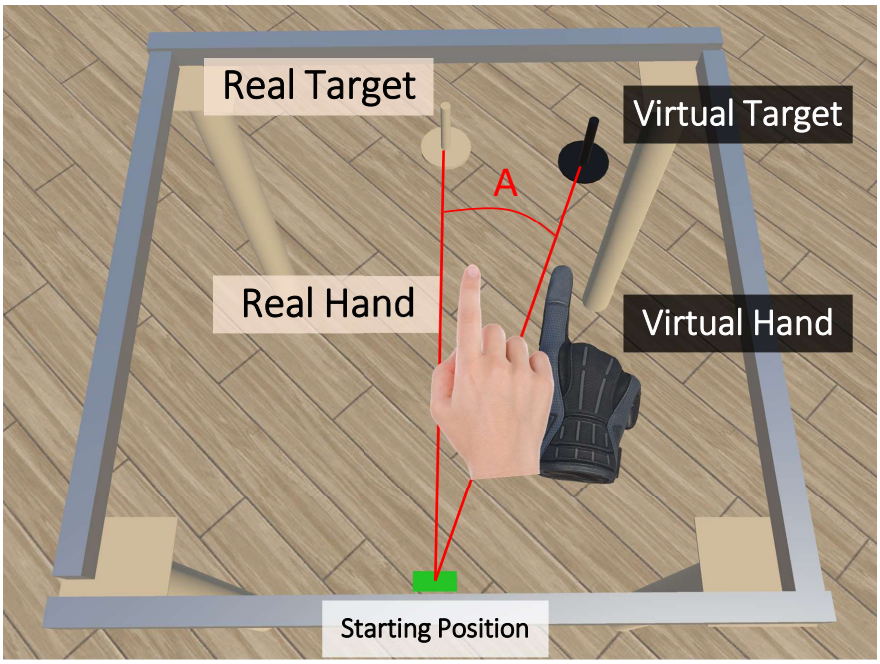

Figure 3.3: Definition of the parameter of hand redirection. The real hand and the virtual hand are in the same position at the beginning of the movement on the starting position. The amplitude of redirection A can be represented as the angle between the real target, the starting position, and the virtual target. During the movement, the two hands are separated gradually. The rate of this shift is linked to A. Indeed a bigger A means a bigger rate so that the virtual hand can reach the virtual target when the real hand touches the physical target.

Definition of Hand Redirection parameters To better understand the different studies about hand redirection DT, we need to discuss which parameters are bounded by this threshold. As we have already seen in subsubsection 2.2.4, hand redirection is based on a progressive shift of the virtual hand with respect to the real hand while moving towards a target. One important parameter is the amplitude of redirection A (seeFigure 4.1). It is defined by the angle between the starting position of the movement and the two targets (real and virtual). The distance between the two targets thus determines A. The amplitude of redirection also influences the progressive shift rate between the real and virtual hands. In the Figure 4.1, the plan of redirection is horizontal. Note that it can also be vertical. The virtual hand is, in this case, shifted downwards or upwards from the real hand. The detection threshold of hand redirection illusion can be defined as the maximum amplitude of possible redirection without a user noticing the illusion.

Hand Redirection Detection Threshold For hand redirection, tolerated amplitudes of illusion measured with questionnaires were significantly larger than calculated lower bound DT. Indeed, Cheng et al. [2017] found that a θ of 40° can be considered tolerable by more than 50% of the participants. Abtahi and Follmer [2018] found that they can impose up to a 49.5° angle between a virtual and a real hand trajectory without participants saying that they detect the illusion (see Figure 3.4). Abtahi and

Follmer [2018] have also studied the detection threshold for scaled movement and showed that a scaling of 1.9 between real and virtual movement can be accepted.

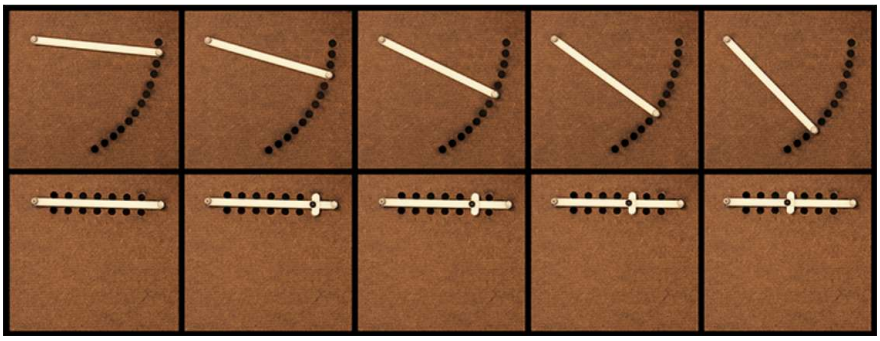

Figure 3.4: Experimental setup of Abtahi and Follmer [2018]. Top: a real bar was more or less rotated compared to a virtual one. They show that this bar can be rotated up to 49.5° without users noticing that the orientation of the two bars (real and virtual) are different. Bottom: a real bar was more or less scaled compared to a virtual bar. They show that a scaling of 1.9 between the real and virtual bar can be implemented without the user noticing it.

We list from here the DTs for hand redirection evaluated in the literature. We have voluntarily rounded the values for better readability, and we chose to convert the values of this threshold in an angle of redirection, although some of these values were expressed in distances (cm) of shift between the real and virtual hands by the authors. Two recent studies aimed to precisely measure the detection threshold for hand redirection, one to investigate the impact of bimanual hand redirection [Gonzalez and Follmer, 2019] (i.e., when both hands are redirected) and the other to study the impact of avatar appearance [Ogawa et al., 2020]. They used a 2AFC protocol where participants had to judge if "yes" or "no" the movement of the virtual hand was their movement for Ogawa et al. [2020] and if "yes" or "no" they perceived an offset between their physical and virtual hands for Gonzalez and Follmer [2019]. Ogawa et al. [2020] found a DT for horizontal redirection on the left at approximately 11° (virtual hand shifted on the left of the real hand) and on the right at approximately 14° (virtual hand shifted on the right of the real hand). They also found that a non-realistic hand avatar was decreasing the threshold. Gonzalez and Follmer [2019] found a DT for vertical redirection of approximately 16° for a downward redirection and 18° for an upward redirection. Their results also suggest that bimanual retargeting can be more noticeable to users when the hands are redirected in different directions as opposed to the same direction.

The type of questions proposed in the 2AFC experiments of the two presented articles [Gonzalez and Follmer, 2019, Ogawa et al., 2020] are still affected by participants' subjectivity. Zenner and Krüger [2019] proposed a 2AFC protocol based on the one of Steinicke et al. [2009], where the question is to judge the position of the virtual hand compared to the real hand (left or right). They had different conditions where users were more or less distracted (audio, visual, vibration, and dual-task distraction). They investigate the threshold for horizontal, vertical, and

scale redirection. They found that for horizontal redirection without distraction, the DT is approximately 4° for left and right redirection, for vertical redirection, the DT is approximately 4.5° for up and down, and for scaled movement, the DTs are a gain of 1.07 for increased movement and 0.88 for decreased movements. We see that these DTs are sensibly smaller than the ones obtained with more subjective questions. It's not surprising because, with this protocol, participants focus on the hand's position, and in a situation of doubt, they are requested to answer a direction (left or right). Therefore, the DT found by Zenner and Krüger [2019] can really be considered a lower bound DT.

Study	**Measure**	**perception investigated**	**DT left - right**	**DT up - down**	**DT scale up - down**
Cheng et al. [2017]	questionnaire	tolerance to illusion	40°	40°	-
Abtahi and Follmer [2018]	questionnaire	detection of the illusion	49.5°	-	1.9
Zenner and Krüger [2019]	2AFC experiment	virtual and real hand relative position	4.38° - 3.81°	4.48° - 4.40°	1.07 - 0.88
Gonzalez and Follmer [2019]	2AFC experiment	offset between the real and virtual hand	-	18° - 16°	-
Ogawa et al. [2020]	2AFC experiment	the virtual hand movement is my movement	11° - 14°	-	-

Table 3.2: Summary of hand redirection detection threshold

3.4 Conclusion

A successful illusion preserves or increases the level of Presence in a VE. More precisely, in the case of C/D ratio manipulation-based illusions, it should preserve the SoE over the virtual body. The SoE is preserved despite a mismatch between the information provided by the different sensory modalities. This is due to a combination of bottom-up and top-down mechanisms, where the brain solves the mismatch between perceptions and the incoherence of the sensory-motor loop. However, the mismatch can be too important, and the illusion can decrease the level of two components of SoE: the SoA and the SoO. This situation leads to the detection of illusion.

Consequently, several approaches have been proposed to quantify Presence and Embodiment, to evaluate the effectiveness of an illusion. Subjective measures such as questionnaires and 2AFC experiments have been adapted to evaluate the effectiveness of visuo-haptic illusions and, notably, the estimation of lower bound

DT. However, it is challenging to link the DT calculated with a decrease in Presence. There is a lack of explanation of why the illusion breaks down and if it is a loss of Agency or Ownership. Moreover, depending on the experimental device and the chosen measure, the DT measured can vary substantially for a similar illusion.

Therefore we aim in this thesis to explain and predict the impact of illusion on Presence and Embodiment. We argue that the mechanism leading to the detection of illusion can help us achieve this goal.

4

Study of Task Factors: Impact of Hand trajectory on Illusion Detection

In the previous chapter, we discussed the different measures of the effectiveness of illusions, especially hand redirection illusions. These measures are useful to establish lower bounds detection thresholds of illusions. We aim in the following chapters to provide new ways of studying visuo-haptic illusions and especially how to predict and enlarge detection thresholds. Especially previous studies mainly focus on one factor. We propose to consider three classes of factors: the factors related to the Task, the System, and the User. Based on these factors, we aim to provide models and methods for VR designers to study the detection of illusion.

In the two following chapters, we use hand redirection illusion as a case study. Similar to Azmandian et al. [2016], we use hand redirection for haptic retargeting. We redirect the hand toward a physical cylindrical target similar in shape to the

virtual one (see Figure 4.1). We adapt methods from the HCI literature to measure detection thresholds and implement hand redirection illusion. We saw that several levels of detection of illusion are possible. Here, we work with lower bounds detection thresholds. If A (the amplitude of redirection, see Figure 4.1) is inferior to this threshold, users should not notice the illusion.

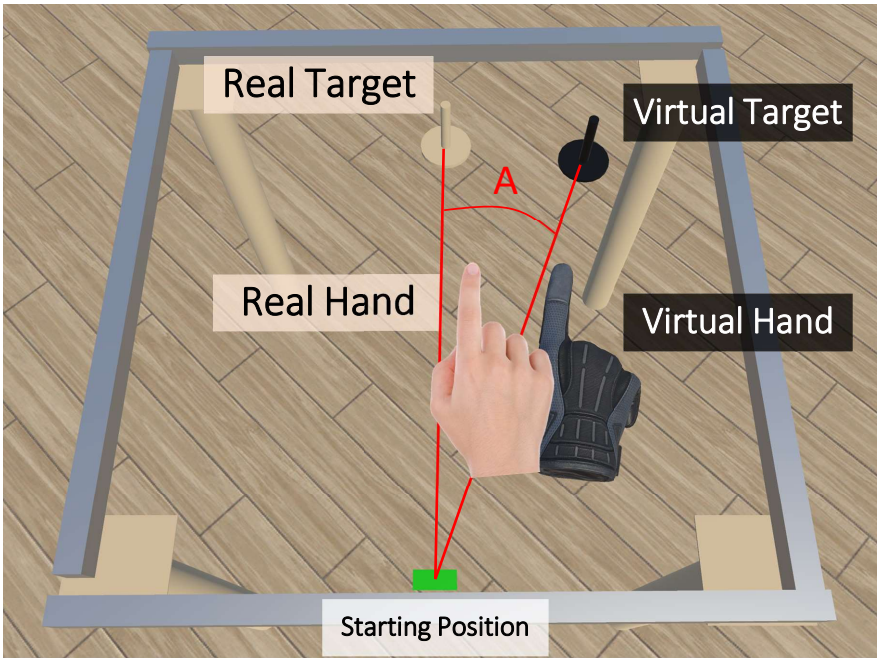

Figure 4.1: Definition of the parameter of hand redirection. The real hand and the virtual hand are in the same position at the beginning of the movement on the starting position. The amplitude of redirection A can be represented as the angle between the real target, the starting position, and the virtual target. During the movement, the two hands will be shifted gradually. The rate of this shift is linked to A. Indeed a bigger A means a bigger rate so that the virtual hand can reach the virtual target when the real hand touches the physical target.

In this chapter, we focus on the task factors. We address RQ2 :"What task **factors** to consider and how they influence illusion detection?" (see Figure 4.2). We propose to investigate in more detail the influence of the most common task factor: the amplitude of redirection. Indeed, most studies on hand illusion detection aim to find the maximum amplitude of redirection possible without detecting the illusion. However, it does not explain the precise influence of the amplitude of redirection on illusion detection. Here, we present a model that links the real hand trajectory under hand redirection to the amplitude of redirection. We use this model to study the hand trajectory's influence on the illusion's detection.

4.1 Motivations and Approach

Hand redirection illusions are based on manipulating the visual information about users' hand positions, resulting in a new hand trajectory. This modified trajectory is an easily observable consequence of the disturbances induced on the sensory-motor

loop by the implementation of hand redirection. A naive hypothesis is that the bigger the redirection amplitude, the bigger the trajectory perturbation.

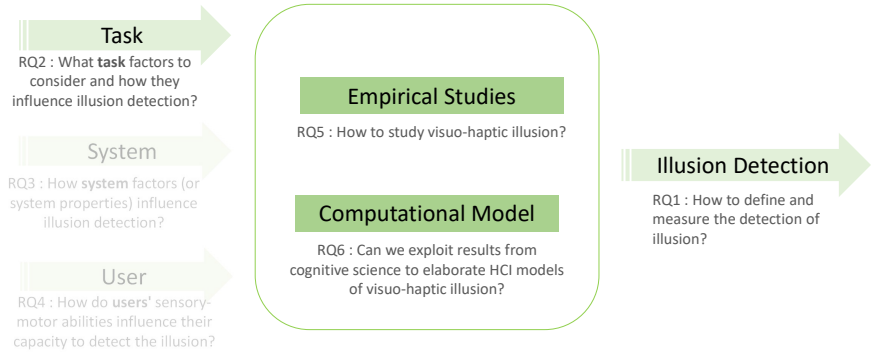

Figure 4.2: Reminder of our approach. We focus in this chapter on the factors related to the task.

Previous works were interested in the effect of redirection on hand velocity and trajectory.Gonzalez et al. [2019] looked at tangential velocities and noted that the minimum jerk model [Flash and Hogan, 1985] , which does not hold for large amplitudes of redirection. They did not, however, analyze the evolution of hand trajectory. The correction of the hand trajectory under redirection has been *qualitatively* mentioned by Azmandian et al. [2016]. They observed the general shape of the trajectory and pointed out that it sometimes exhibits a kink towards the end. However, it remains unclear how hand trajectory is affected by redirection and if there is a relation between the hand trajectory and the detection of the illusion.

The Minimum-Jerk model is a well-established model of multijoint arm movement. It suggests that humans minimize the derivative of their hand acceleration when executing reaching movements. For goal-directed reach, this results in a symmetric, bell-shaped hand speed profile [Gonzalez et al., 2019]

In this chapter, we propose a trajectory model linking the amplitude of redirection and the shape of the real hand trajectory. Based on the comparator model detailed in the theoretical approach of chapter 3, a decrease in SoA can be experienced if hand redirection leads to a too strong perturbation of the sensory-motor loop during the reaching movement. A too-strongly curved trajectory instead of a

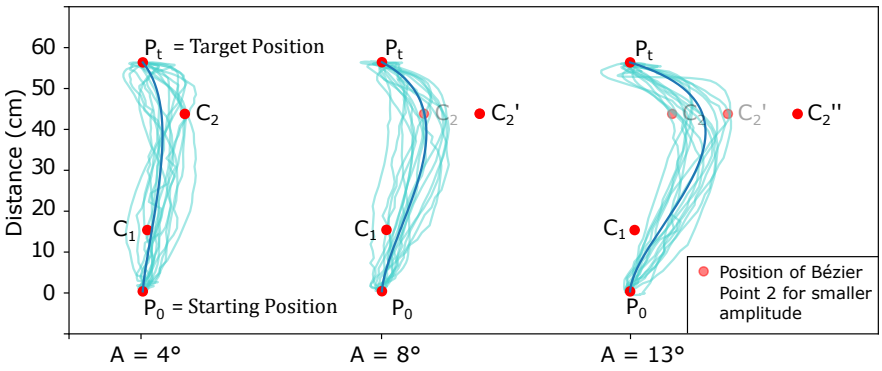

Figure 4.3: Visualisation of all the trajectories for three different amplitudes of redirection and the same participant. We display the Bezier curve resulting from the model M_b. All the control points are fixed except C_2, which have a linear relation with the amplitude.

straight trajectory to reach for a target is evidence of a sensory-motor loop perturbation. Therefore we hypothesize that the detection of the illusion stems from users observing the distortion of their movement. The detection of the illusion can then be predicted from a geometric description of the hand trajectory.

4.1.1 Scope of the Model

The interaction is performed on a plane surface: a table. The user is seated in front of the table, a common position for desktop scale interaction. The target's position and the starting position of the user's hand are known. The target's position can be moved, but the distance between the target and the starting position is fixed. We do not know if our model can be transposed to other distances; however, the distance chosen corresponds to an arm's length and can be seen as a base distance to explore other configurations.

4.1.2 Intermediate Research Questions

We investigate the relationship between the trajectory (T) of the hand movement, the amplitude of redirection (A), and the Detection Threshold (A_{DT}). We propose two intermediate research question :

- **IRQ1**: *What is the influence of the amplitude of redirection on hand trajectory*? ($A \rightarrow T$)
- **IRQ2**: *Does the detection threshold depend on the features of the trajectory*? ($T \rightarrow A_{DT}$). In particular, we aim to study whether the probability of detecting the illusion is better explained by the trajectory deformation under redirection $(A+T)$ instead of A alone.

4.1.3 Problem Formulation

Hand trajectory. Let $T = P_0, P_1, ...P_n$ the trajectory of the hand movement where p_0 is the starting point and $P_n = P_t$ the position of the target (t). We assume it exists a function f such as:

$$T = f(u, P_t, P_0, A) \tag{4.1}$$

where T is the trajectory produced by the participant u, when reaching the target t at the location P_t, from the position P_0, with an amplitude of redirection A. We aim to determine the function f to answer the first research question (**IRQ1**).

Model of Gesture Trajectory. We choose to model hand trajectory as a Bézier curve. A Bézier curve is a polynomial parametric curve and is defined as :

$$B(l) = \sum_{i=0}^{k} \binom{k}{i} (1-l)^{k-i} l^i C_i \tag{4.2}$$

where k is the degree of the Bezier curve and $C_0, ..., C_k$ the control points.
This parametric model is widely used in mechanical design and computer graphics and has also been used to model hand trajectories [Faraway et al., 2007]. This formulation has several advantages. First, it considerably reduces the complexity of the description of a trajectory as the number of control points is small compared to the number of points of the trajectory $k << n$. Moreover, the description is smooth, continuous, and invariant to the user speed and sampling rate. Finally, the position of the control points provides a convenient and geometrical interpretation of the trajectory (see figure 4.4. In particular, the first and last control points are the start and end points of the trajectory, so these are fixed in our modeling.

$$C_0 = P_0; C_K = P_t \tag{4.3}$$

Figure 4.7 shows the impact of moving the control point C_2 (while keeping the three other controls fixed) on the Bézier curve.

number of control points A choice must be made regarding the degree k of the Bézier curve, i.e., the number of control points. A higher k better describes a given trajectory, but it increases the complexity of the model and reduces its interpretability. Moreover, it is important to use the same k for different trajectories to compare them. Based on pilot studies, we found that cubic Bézier curves with 4 control points ($k = 4$) were sufficient to describe, compare, and explain the different trajectories well.

Based on the equations 4.1 and 4.3, we can then reformulate our problem as estimating the function g such as (see 4.4):

$$C_{1x}, C_{1y}, C_{2x}, C_{2y} = g(u, P_t, P_0, A) \tag{4.4}$$

where C_{ix} and C_{iy} are the x and y coordinates of the control point C_i. To achieve this, we conducted a user experiment to collect data and identify the model parameters (see section 4.2). Validation of the model will allow us to predict the trajectory for a given user u, under any redirection A.

Figure 4.7 shows the impact of moving the control point C_2 (while keeping the

three other controls fixed) on the Bézier curve.

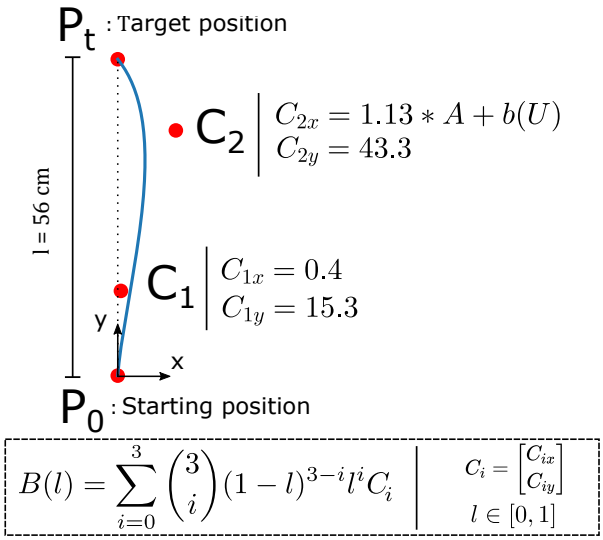

Figure 4.4: Model Overview. Our hand trajectory model is a Bézier Curve. The resulting trajectory $B(l)$ is defined by 4 control points: P_0, C_1, C_2 and P_t. We show that the redirection can be accounted for by only adjusting the x coordinate of point C_2. This adjustment depends on the redirection amplitude A and a user-dependent factor $b(U)$.

Detection Threshold Based on the literature [Zenner and Krüger, 2019, Steinicke et al., 2009], the population model predicting the probability P of detecting the illusion given the amplitude of redirection (A) is a psychometric function:

$$P(A) = \frac{1}{1 + \exp -\frac{A - PSE_G}{\sigma}} \tag{4.5}$$

where PSE_G is the global point of subjective equality, i.e. the amplitude such as $P(PSE_G) = 50\%$. It can be seen as the amplitude where the participants estimate that no redirection is applied and is usually different than 0. σ is the spread (inverse slope). A_{LT} and A_{RT} are two other specific values such as $P(A_{LT}) = 25\%$ and $P(A_{RT}) = 75\%$. The detection threshold A_{DT} is then defined as:

$$A_{DT} = A_{RT} - A_{LT} \tag{4.6}$$

The smaller σ, the steeper the slope of the psychometric curve is and, in our case, the smaller A_{DT} is. The same methodology can be applied to the whole population (population model) or each individual (individual model).

So, the second intermediate research question (**IRQ2**) has the objective to estimate PSE_G and σ as a function of the trajectory T:

$$P(A, T) = \frac{1}{1 + \exp -\frac{A - PSE_G(T)}{\sigma(T)}} \tag{4.7}$$

4.2 Data Collection

To investigate our research question, we first need hand trajectories for different redirection amplitudes (IRQ1). Secondly, we need to measure detection thresholds for hand redirection (IRQ2). We choose an experimental protocol using modified objective measures inspired by past studies [Steinicke et al., 2009, Zenner and Krüger, 2019] to measure detection thresholds. Thus in our user experiment, participants perform a pointing task in VR while experiencing hand redirection illusions. The first objective is to investigate the probability of detecting the illusion depending on the amplitude of redirection. We also investigate hand trajectory to refine, calibrate and test our model.

4.2.1 Participants

10 participants (8 male and 2 female, between 25 and 30 years old) took part in the study. 2 participants were left-handed, 8 were right-handed. 4 participants wore glasses, and one wore contact lenses. They did not report any other visual impairment or neuromuscular disorder. All the participants except 2 had experienced a VR headset before, but all less than three times. None were familiar with VR.

4.2.2 Apparatus

Physical setup. Participants were seated in front of a standard table and with a fixed position seat. They wore an HTC Vive head-mounted-display (HMD), white-noise headphones, and a right-hand glove with a cluster of optical markers on the index finger. Both positions and orientations of the HMD and the glove were tracked by a motion capture system (Optitrack), providing submillimeter precision. We thus saved the 3D positions of the real hand and projected them on a horizontal plane. We used a sampling rate of 0.03s, resulting in around 40 points per trajectory.

On the table was a haptic marker for "starting position", a joystick placed on the left of the starting position, and 6 cylindrical targets located along a semi-circular arc illustrated Figure 5.5-left. Participants touched only the 4 central targets. The targets at the two extremities of the arc were just used as lures. These targets are located at a 30 cm distance from the starting position. The 30 cm distance was chosen to be easily reachable by participants while seated on the chair. The angular distance between targets is 15°. It is large enough to avoid accidental physical collisions and to study the influence of target orientation on hand trajectory and illusion detection.

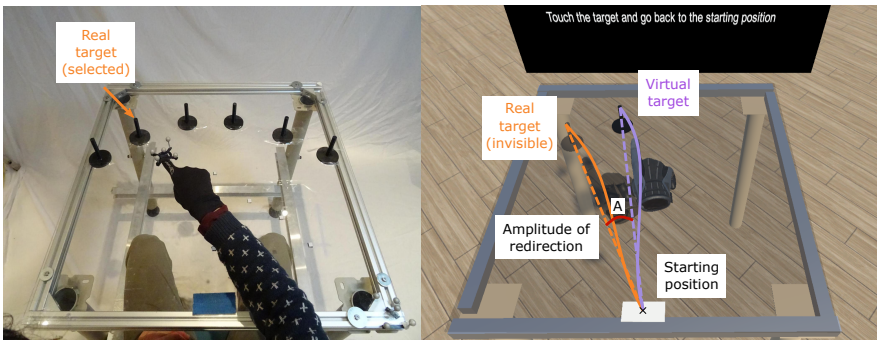

Figure 4.5: Left: The experimental table with 6 physical targets. Right: The virtual scene as seen by participants during the experiment. The phantom of the real hand (left) is displayed for illustration purposes but was not visible during the experiment. The dashed lines represent the straightest reach toward the target for the real hand (orange) and the virtual hand (purple). The curved lines represent the actual trajectory of the two hands.

Virtual scene. The virtual scene is illustrated on Fig. 5.5-right. It mimics the real setup. It is implemented with the *Unity3D* game engine and shows the table, the starting position, one virtual target, and an avatar of the participant's right hand. The virtual target has the same color and shape as the real one.

Hand redirection implementation. The virtual target's position was computed from the position of the chosen real target and the amplitude of redirection (see Figure 5.5). The shift between the virtual and the real hands was implemented such as it increases linearly during the reaching motion, and the real hand reaches the real target simultaneously as the virtual hand reaches the virtual target. As such, users touch a real object, providing a *haptic confirmation*. Participants compensate for the shift while reaching the target, resulting in a curved trajectory (see Figure 5.5). Note that in our implementation, the hand is considered a single point, the forefinger tip.

4.2.3 Experimental Design

Stimulus and Task. The experiment is a *two-alternative forced choice* (2AFC): Once the participants' right arm is in the starting position, the trial starts, and the virtual target is displayed. The participants are asked to touch the target with their right hand and then return to the starting position (we made this choice to minimize task difference among participants, thus, we restrain even left-handed participants from using their right arm). The participants are asked to move naturally toward the target as we do not know the effect of speed on illusion detection. If the participants are too fast or too slow, the experimenter asks them to slow down or to accelerate. After returning to the starting position, they move the joystick in the corresponding direction with their left hand to indicate whether their real hand was positioned on the left or the right of its virtual avatar. No feedback is provided.

Conditions. In this experiment, we controlled two factors. The primary factor is AMPLITUDE of redirection with 15 levels from $-13°$ to $13°$ ($-13°$, $-10°$, $-8°$, $-6°$, $-5°$, $-4°$, $-2°$, $0°$, $2°$, $4°$, $5°$, $6°$, $8°$, $10°$, $13°$). The second factor is TARGET Orientation from $-22.5°$ to $22.5°$ (step of $15°$).

Procedure. The participants were first instructed about the experiment's goal and the task to perform. In particular, the concept of hand redirection was explained in these terms: "*A virtual hand that follows the position of your hand is displayed in the VE. During the reaching task, an offset will be gradually introduced between this virtual hand and your real hand. The virtual hand will be located either on the left or the right of your real hand*."

Participants put on gloves, HMD, and headphones. They then performed a training phase. It consists of 2 blocks of 10 trials where they experience hand redirection with an amplitude of either $-13°$ or $+13°$ (corresponding to the highest amplitudes in the main experiment). During the training phase, participants received feedback at the end of the trial regarding the direction (left or right) of the redirection. They were also informed about the trial time as they had to calibrate their speed, so the trial time was between 1s and 2s. Finally, during the first block, the position of the *real* hand was displayed in the virtual scene in addition to the hand avatar to understand the concept of hand redirection.

design. We used a within-subject design. Each participant completed 4 blocks. In each block, the participants tested the 60 combinations of AMPLITUDE and TARGET in a randomized order. In summary, the experimental design is : 10 participants $\times$ 4 blocks $\times$ 15 AMPLITUDES $\times$ 4 TARGETS $=$ 2400 trials.

Dependent variables. The two dependent variables are CHOICE (left or right) and Hand TRAJECTORY, i.e., the sequence of points to reach the target.

4.3 Analysis 1: Trajectory and Amplitude of Redirection

In this section, we analyze how the amplitude of redirection influences the position of the two control points C_1 and C_2. We first describe our empirical findings. We then refine our model and compare four model variants.

4.3.1 Empirical Results

Method We first removed 60 (2.5%) outliers trajectories. We calculated the distance (MSE) between a given trajectory and the mean trajectory for each amplitude

of redirection. Each trajectory with an MSE larger than a threshold was plotted to confirm its wrong shape. For the resulting 2340 trajectories, we estimated the four parameters C_{1x}, C_{1y}, C_{2x}, C_{2y} of the Bézier curve that minimize the Dynamic Time Warping (DTW) distance [Sakoe and Chiba, 1978, Velichko and Zagoruyko, 1970]. DTW is appropriate as it is independent of the user speed. We use the python package DTAIDistance for calculating the DTW distance and the function "minimize" of the "scipy.optimize" package with the Nelder-Mead algorithm for the optimization method. The resolution of the Bézier curve is 250 points per trajectory.

result. The Figure 4.6 shows the mean value of the four parameters with 95% confidence Interval (CI) as a function of the amplitude of redirection. We were expecting that the four parameters vary with the amplitude, but the results show that three parameters can be approximated by a constant: $C_{1x} = 0.35cm$ $(ci = [-0.0, 0.8])$, $C_{1y} = 15.3cm$ $(ci = [15.2, 15.4])$, $C_{2y} = 43.4cm$ $(ci = [42.6, 44.2])$. However, C_{2x} linearly increases with the amplitude ($R^2 = 0.99$, $MSE = 1.9$).

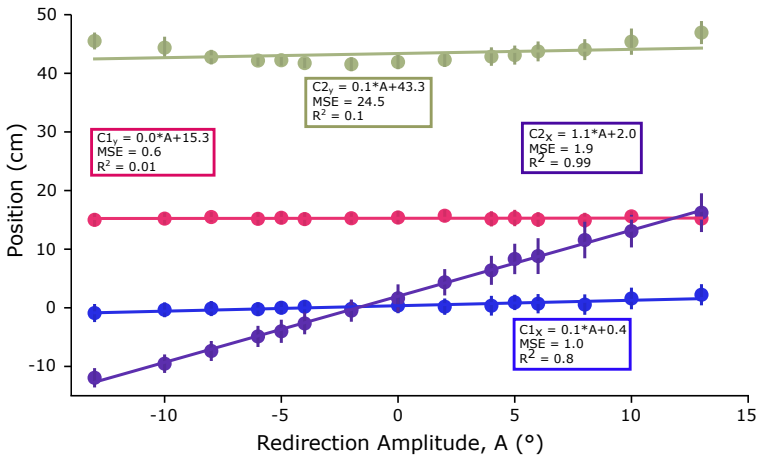

Figure 4.6: The value of the four parameters C_{1x}, C_{1y}, C_{2x}, C_{2y} as a function of the amplitude of redirection. Error bars show 95% confidence interval.

Discussion. We learned three things. First, as C_1 is fixed and aligned with $\overrightarrow{P_0P_T}$, it confirms that the initial direction of the user's movement is towards the virtual target. Second, as only one parameter varies, these results suggest that using a Cubic Bézier curve model is appropriate. Third, a simple and elegant linear relationship exists between C_{2x} and the amplitude of redirection. We can thus revisit our model, reduce its complexity and improve its explainability.

4.3.2 Refining and Evaluating the Model

Based on our findings, we revisit our model (equations 4.3 and 4.4) and propose four model variants summarized in Table 4.1. Three parameters (C_{1x}, C_{1y}, C_{2y}) are fixed. We introduce two novel parameters a and b to approximate the x coordinate of C_2:

$$C_{2x} = aA + b \tag{4.8}$$

where A is the amplitude of redirection, a is the slope, i.e., the sensitivity to the amplitude, and b, the intercept, reflects the natural human bias at doing curved trajectories even when no hand redirection is applied [Wolpert et al., 1994]. To study whether these two parameters are the same for all participants (population parameter) or participant-dependent (individual parameter), we defined four model variants (Table 4.1) reflecting the four configurations.

Model	**Fixed parameters**	**Population parameters**	**Individual parameters**	**k**	**DTW**	**-LL**	**BIC**
M	C_{1x} C_{1y}, C_{2x}	a, b	-	2	670	501	1012
M_b	C_{1x} C_{1y}, C_{2x}	**a**	**b**	**11**	**576**	**401**	**857**
M_a	C_{1x} C_{1y}, C_{2x}	b	a	11	661	457	969
$M_{a,b}$	C_{1x} C_{1y}, C_{2x}	-	a, b	20	559	396	896

Table 4.1: Comparisons of four model variants in terms of fixed and free (population and individual) parameters, number of free parameters (k), distance (DTW), likelihood, and BIC. The model with b as a user-dependent parameter has the lowest BIC score.

4.3.3 Model Comparison

We compare the capacity of the model variants to accurately predict the trajectories of each class C_A^u where A is the amplitude of redirection and u a user (participant). To achieve this, we first define $d(A,u,m)$ the average DTW distance between the predicted trajectory $T_{pred}(A,u,m)$ and all observed trajectories $T_{obs}^0(A,u)...T_{obs}^N(A,u)$ of the class C_A^u for a given model m:

$$d(A,u,m) = \frac{1}{N}\sum_{i=0}^{N} DTW\left(\, T_{pred}(A,u,m),\, T_{obs}^i(A,u)\,\right) \tag{4.9}$$

We can then use a Boltzmann soft-max function to transform the distance $d(A,u,m)$ into probability $P(C_A^u \,|\, A,u,m)$:

$$P(C_A^u|A,u,m) = \frac{e^{-\beta\, d(A,u,m)}}{\sum_a e^{-\beta\, d(A,u,m)}} \tag{4.10}$$

where the parameter β indicates how much the probability distribution is concentrated around the positions of the smallest distance. We chose $\beta = 1$.

Model Likelihood.

Based on the equation 4.10, we now compare the result of the models' fitness function. In Bayesian terms, we compare the likelihood of the data given the model, that is, the maximum probability $P(C_A^u)$ that the model chooses the correct class of trajectories C_A^u. Formally, we estimate:

$$LL(m) = \sum_{A,u} \log P(C_A^u | A, u, m, \theta_m^p) \tag{4.11}$$

where θ_m^u is the set of parameters of the model m for the participant u.

BIC score.

In the process of model selection, it is common to include a penalty term for model complexity, i.e., for the number of parameters [Raftery, 1995]. The Bayesian Information Criterion (BIC score) is commonly used. It is estimated as $BIC = -2LL + k \times log(N)$ where LL is the likelihood (equation 4.11), k, the number of parameters (i.e. individual parameters + population parameters), and $N = 150$ ($10\,participants \times 15\,amplitudes$), the number of points to predict.

Result.

The Table 4.1 indicates that the model $M_{a,b}$ better fits the data. It is unsurprising as it has many more parameters than the other model variants. When penalizing for the number of parameters, the BIC score suggests that M_b better explains the data. This result indicates that a is not sensitive to the user id. In contrast, model prediction benefits each user's estimation of b.

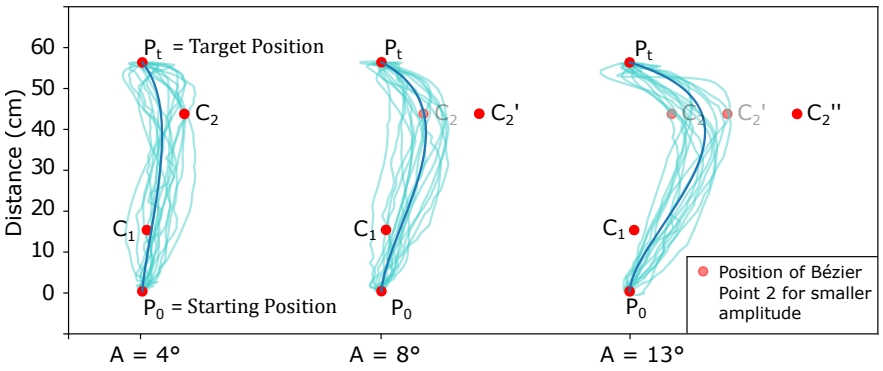

Figure 4.7: Visualisation of all the trajectories for three different amplitudes of redirection and the same participant. We display the Bezier curve resulting from the model M_b. All the control points are fixed except C_2, which have a linear relation with the amplitude.

4.3.4 Discussion

IRQ1: *What is the influence of the amplitude of redirection on hand trajectory*? Our analysis showed a clear impact of the amplitude of redirection on hand trajectory. More precisely, we learned that 1) if we model hand trajectory as a simple cubic Bézier curve, the amplitude of redirection **only affects** the x coordinate of a single control point (C_2). This makes the model highly interpretable (Figure 4.7). Moreover, 2) this x coordinate increases linearly with the amplitude of the redirection; 3) the slope is independent of the participant, i.e., increasing the amplitude by 1° moves C_{2x} of 1.13cm on the right; 4) the intercept is user dependent (mean = 2.1 cm, std = 3.9). This result is in line with [Wolpert et al., 1994] indicating that humans perform curved trajectories (due to visual perceptual distortion) even when no redirection is applied. The degree and direction of curvature depend on the participant.

Interestingly, the calibration of the model is easy to perform. Indeed, the individual parameter b is the intercept, i.e. it is the value of C_{2x} when $A = 0$ (equation 4.8). It is thus possible to estimate b for each participant **without** experiencing hand redirection. b can be estimated by simply performing a reaching task without illusion.

4.4 Analysis 2: Detection threshold

In this section, we study the second research question IRQ2: *Does the detection threshold depend on the features of the trajectory*?. We first evaluate the probability of detecting the illusion as a function of the amplitude of redirection and then as a function of the deformation of the hand trajectory.

4.4.1 Amplitude of Redirection and Detection Threshold

Figure 4.8-Left illustrates the probability $P(A)$ to detect the illusion as a function of the amplitude of redirection A (psychometric function corresponding to the equation 4.8) for the whole population. We found $PSE_G = -1.13°$, $A_{LT} = -4.52°$, $A_{RT} = 2.27°$. We compute the detection threshold A_{DT} = A_{RT} - A_{LT} = 6.79°. Our results are in the same order of magnitude than Zenner et al. study [Zenner and Krüger, 2019] ($PSE_G = -0.28°$,$R = 8.19°$). The difference can be due to the experimental setup and/or the absence of haptic confirmation at the end of the movement.

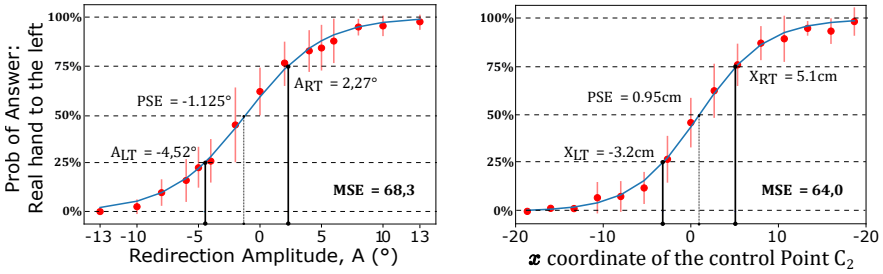

Figure 4.8: Psychometric fit of the answer of the 2AFC experiment. Left: detection according to the amplitude of redirection. Right: detection of the illusion according to the C_{2x} coordinate.

4.4.2 *Hand Trajectory and Detection Threshold*

We now investigate the link between the hand trajectory and the probability of detecting the illusion. As C_{2x} is sufficient to describe the hand trajectory, we analyze the probability to detect the illusion $P(C_2x)$ as a function of C_{2x} with the same methodology of section 6.1. We discriminated C_{2x} into 15 groups based on its magnitude. We made this choice to compare the two psychometric functions, $P(A)$ and $P(C_{2x})$ of the figure 4.8.

Figure 4.8-right shows the result of the psychometric fit for $P(C_{2x})$ ($MSE = 64.0$) which is better than the one of $P(A)$ ($MSE = 68.3$), Figure 4.8-Left. It shows that the more the hand trajectory is curved, the easier the illusion is detected. This result was expected given the linear relation between A and C_{2x} outlined in section 5. However, the fact that both the amplitude of redirection and the trajectory explain the illusion detection requires further explanations.

4.4.3 *Further Explanations*

To better understand the role of C_{2x} on illusion detection, we analyzed its magnitude as a function of the absolute amplitude of redirection ($|A|$) and whether the participants answered correctly (detection of the illusion) or not (the illusion works) to the 2AFC task. We removed extreme amplitudes 0° as there was no error and $\pm 13^\circ$ as all participants detected the illusion for these amplitudes.

Our results are illustrated Figure 4.9. A two-way ANOVA confirmed the effect of AMPLITUDE on the amplitude of C_{2x} ($F_{5,45} = 109.4$, $p < .0001$). ANOVA also revealed an effect of ANSWER (Correct vs., False) on the amplitude of C_{2x} ($F_{1,9} = 7.6$, $p < .05$). A post Tukey-test indicates that at a given amplitude, C_{2x} is larger when the illusion is detected (mean= 3.4cm) than when the illusion is not detected (mean= 7.4 cm). ANOVA does not reveal AMPLITUDE $\times$ ANSWER interaction effect.

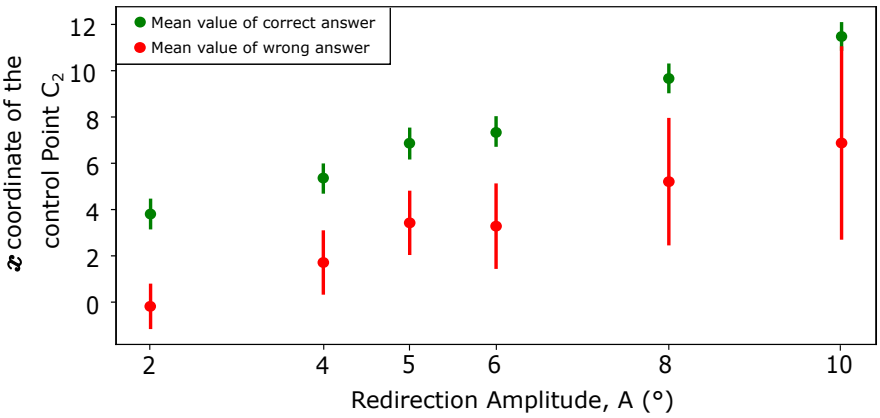

Figure 4.9: x coordinate of C_2 as a function of the redirection amplitude and whether the participants' answer is correct or false.

Discussion

The amplitude of redirection is the primary factor in explaining and predicting whether the participants will detect or not the illusion. However, given the amplitude of redirection, we demonstrate that the curvature of the hand trajectory, i.e., the magnitude of C_{2x}, refines the prediction. Indeed, participants performing low curved trajectories (i.e., small C_{2x}) are less likely to detect the illusion. The user-dependent parameter b reflects this natural tendency to perform curved trajectories (to the right ($b > 0$) or the left ($b < 0$)) under no redirection. We thus decided to study more precisely the influence of b on the detection threshold.

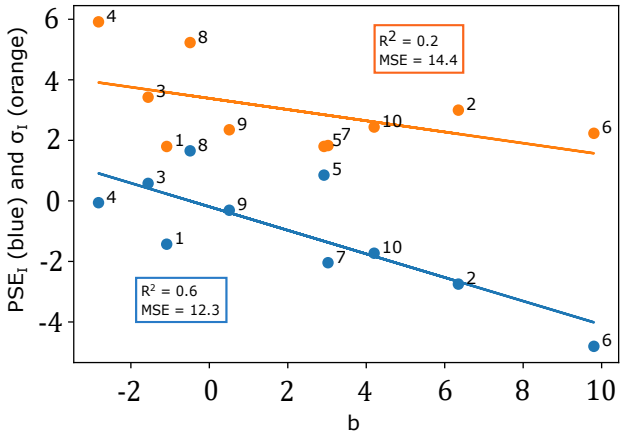

Figure 4.10: Evaluation of PSE_I (in blue) and σ_I(in orange) for each participant (1 - 10) according to parameter b.

4.4.4 User-Dependent Detection Threshold

We now evaluate the relation between the user-dependent parameter b and the probability to detect the illusion expressed in equations 4.5 and 4.7:

$$P(A,b) = \frac{1}{1+\exp -\frac{A-PSE_I(b)}{\sigma_I(b)}} \tag{4.12}$$

where PSE_I is the Point of Subjective Equality for each individual (PSE_G was the Point of Subjective Equality global, i.e., for the whole population). Figure 4.10 illustrates PSE_I and σ_I as a function of b. While no clear relationship is revealed regarding σ_I ($R^2 = 0.25$; $MSE = 14.39$), there is a weak relationship between b and PSE_I ($R^2 = 0.63$; $MSE = 12.32$):

$$PSE_I = -0.39 \times b - 0.19 \tag{4.13}$$

Thus there is a relation between the value of C_{2x} when no redirection is applied $C_{2x} = b$ and PSE_I. In other words, a user performing naturally a curved trajectory to the right ($b > 0$) will be more sensitive to redirection to the right ($PSE_I < 0$). This result is important because after estimating b, a designer can estimate PSE_I of a user and know in which direction (left or right) the user is less likely to detect the illusion. The designer can also measure b of each individual of a given population and estimate the *unique* range of amplitude of redirection that best fits this population. We illustrated this Figure 4.11. On the left, we see the range of amplitude of redirection (blue), which is not detected for each participant. The intersection is small: The vertical surface indicates the maximal ranges for which the illusion is not detected for respectively 70%, 80%, and 90% of the population. It results that only the amplitudes of redirection in [-0.7°;0.7°] are not detected for 70% of the population.

However, when b is known for each participant, it is possible to choose a unique range of amplitude of redirection and adapt it to each participant (based only on the parameter b). In other words, the designer can shift the range to the left or the right according to the participants' sensibility. For example, let us take a range of redirection of [-2°,2°] and a user performing naturally curved trajectory to the right with a value of b equal to 4. This user is more sensitive to redirection to the right, and his/her $PSE_I < 0 is \approx -2$. Therefore, the designer can choose to change the center of the range of redirection and change it to [-4°,0°]. This is illustrated in Figure 4.11-right where each amplitude range is virtually recentered based on b, offering a range of [-1.7°,1.7°] which is almost four times larger.

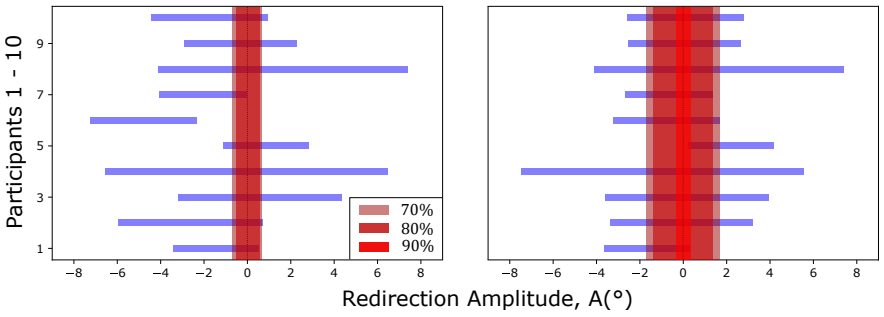

Figure 4.11: Left: The horizontal blue rectangles depict the range of redirection amplitudes for which the illusion is not detected for each participant. The vertical surfaces indicate the maximal ranges for which the illusion is not detected for respectively 70% (green), 80% (red), and 90% (yellow) of the population. The wider these ranges are, the more flexibility is offered to the designers. However, increasing the number of participants decreases this population range. Right: When taking individual differences, i.e., b, into account, we can artificially recenter their range, increasing the range of amplitudes for the whole population.

4.5 Discussion

4.5.1 Main findings

We revisit our two research questions from section 4.1.2.

IRQ1:

What is the influence of the amplitude of redirection on hand trajectory?
We have shown that a cubic Bézier curve constructed using four control points C_i, $i \in [0;3]$ approximates the hand trajectory quite faithfully. Moreover, the coordinates of 3 out of 4 control points do not depend on the redirection for a given user. The control point C_2 is the only one that is modified by the amplitude of redirection: C_{2x} linearly increases with the amplitude, such as $C_{2x}(A) = 1.13A + 1.97$ at the population level. At the individual level, further analysis revealed that the intercept is user dependent, $C_{2x}(A,u) = 1.13A + b(u)$. These results demonstrate that 1) the amplitude of redirection influences *only* a single feature of the trajectory when described with a Bézier curve; 2) the trajectory can be better approximated when considering the parameter b, which 3) can be easily estimated for each user. Indeed, b indicates the curvature of the trajectory when users do not experience an illusion.

IRQ2:

Does the detection threshold depend on the features of the trajectory?
It was well known that the detection threshold depends on the amplitude of redirection. We demonstrated that it also depends on the trajectory. In particular, we demonstrated that once the amplitude of redirection is given, users performing

trajectories with low curvature (*i.e.* smaller C_{2x}) are less likely to detect the illusion. We hypothesize that users detect the illusion through observing the distortion of their hand motion subsubsection 3.2.2. The disturbance in the sensory-motor loop will be perceived through the comparator model [Frith, 1987]. This could result in a semantic break, and a decrease in SoA [Padrao et al., 2016].

We used a psychometric function with two parameters PSE_I and σ_I to determine individual detection thresholds. Our analysis shows a relationship between PSE_I and b but not with σ_I. In other words, estimating b for each participant can increase the range of amplitudes of redirection by 258% without risking the illusion of being detected by at least 70% of our participants.

4.5.2 Implications for design

Our findings on **IRQ1** suggest a method for designers to anticipate user hand trajectory during a redirected reaching task. In particular, designers can *easily* elaborate a calibration task to estimate b and refine the trajectory model as it does not require exposing the users to the illusion ($A = 0$). This trajectory model can, for instance, be exploited advantageously to make users unwittingly circumvent obstacles or encountered-type haptic devices [Bouzbib et al., 2020, Gonzalez et al., 2020]. Our findings on **IRQ2** indicate a simple way of adapting the range of amplitude of redirection to each user. The knowledge of the parameter b allows the computation of individual PSE_I. The designer can then center the population range of amplitudes around the PSE_I to minimize the risk of detecting the illusion. Again, this only requires estimating b without exposing the user to the illusion.

Beyond a better understanding of hand redirection, the model has several implications for design. For instance, it can serve to define a light calibration task to estimate the appropriate detection threshold for each participant. It can also provide theoretical foundations to design novel interaction techniques, e.g it would be possible to dynamically adapt the amplitude of redirection to control the hand trajectory and avoid physical obstacles while maintaining the illusions.

4.5.3 Limitations

Several limitations, mainly due to the scope chosen for our model, should be noted. First, left-handed participants had to reach for targets with their right hand. This choice was made to facilitate the comparison of data between participants. Even though we interact with the environment with both hands, we favor our dominant hand for reaching tasks. Thus this could have impacted the hand trajectory and their illusion detection threshold. Moreover, the speed of the hand can have an impact

on the detection of the illusion and was not constant among participants. Then, participants were informed about the illusion at the beginning of the experiment. Thus the calculated detection threshold is likely bigger.

Furthermore, concerning the trajectory model, we assumed that 3 of the 4 coordinates of the Bézier control points are fixed. However the Figure 4.6 shows that C_{1x} and C_{2y} are slightly affected by the amplitude of redirection. The distance to the target is fixed in our task, and different distances should also be tested.

Finally, using a 2AFC experiment to determine detection thresholds is debatable. On the one hand, users can sense that something is odd in their movement without being able to pinpoint the relative position of their real and virtual hands. On the other hand, if users do not focus on the position of their hands, we would certainly find a larger range of non-detection. We hypothesize that there is not a clear breaking point of the illusion.

Despite this limitation, our work is a base on which we can build more global models of hand trajectory under illusions.

4.6 Conclusion

In this chapter, we presented a model of hand trajectory under redirection. We found that cubic Bézier curves with four control points ($k = 4$) were sufficient to well describe these trajectories. In particular, we showed that we can fix three of the four bezier points and one coordinate of the last bezier point. As a result, only one coordinate ($C2_x$) is influenced by our system's first input, the amplitude of redirection. Indeed we highlighted that it exists a linear relation between $C2_x$ and the amplitude of redirection.

We also identified a user characteristic that could impact the detection of illusion. Indeed, our results suggest that the natural curvature of a user's hand trajectory with no redirection predicts hand trajectory with redirection. Moreover, we showed that the detection of illusion stems from a too-large trajectory curvature. Thus taking two users, we can predict which user is more likely to detect a specific amplitude of redirection.

In summary, in this chapter, we addresssed RQ2 ("What task **factors** to consider and how they influence illusion detection?"), and we focused on the amplitude of redirection; however, several other task factors, such as the target distance or the absence of haptic confirmation at the end of the movement, should be considered. We also addresssed RQ5 ("How to study visuo-haptic illusion?") by showing the

relevance of studying hand trajectories to understand and predict the detection of illusions. To pursue our study, we investigate in the next chapter the system factors. Similarly to the task factors, the system factors are controlled by the creator of the VE and can explain the detection of an illusion.

5

Study of System Factors: What is the design Space of Hand Redirection Illusion

In this chapter, we focus on the system factors (see Figure 5.1). We can separate these factors between hardware and software. The hardware factors include, for instance, the HMD or the hand tracking system, and, for haptic retargeting application, [Azmandian et al., 2016], the diversity and quality of haptics probes. However, we can assume that changing the hardware is long and costly. Conversely, software factors can be almost instantly adapted for no cost. Thus we focus here on software factors that can influence illusion detection (RQ3).

In particular, we introduce and study one factor that we call **redirection function**, which is the function that determines the virtual hand's position depending on the physical hand's position. While there is theoretically an infinite number of redirection functions, previous studies rely on the same one [Azmandian et al., 2016,

Zenner and Krüger, 2019, Han et al., 2018]. Indeed, the two hands are classically shifted linearly. In this chapter, we study the design space of redirection functions on the influence on the (non-) detection of the illusion. In addition to the linear (degree=1) redirection function used in previous works, we consider second-degree polynomial functions. It gives us better control of the offset between the virtual and physical hand and, ultimately, of the hand trajectory when reaching the target. We then analyze the influence of these functions on the illusion detection threshold.

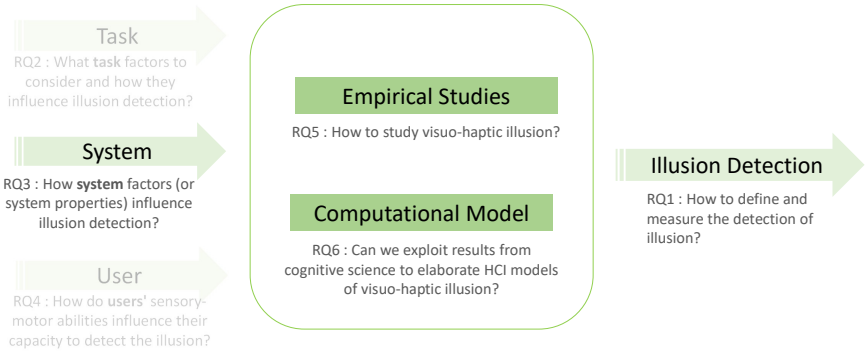

Figure 5.1: Reminder of our approach. We focus in this chapter on the factors related to the system.

5.1 Motivation

As we have seen in the chapter 3, detecting the illusion can have several interpretations. It can especially mean a decrease in SoO and/or SoA. The decrease of the SoO can come from a too big difference between the visual and proprioceptive information on the position of the hand [Braun et al., 2018]. The decrease of the SoA can come from a too big difference between the predicted and the perceived state of the hand [Padrao et al., 2016], which leads to a semantic break. It can also decrease if a consequence of the expected movement does not occur, in our case, if the user does not manage to reach the targeted object.

The manipulation of the redirection function provides a way to accentuate or limit the shift between the two hands at different movement phases. It can be hypothesized that if the distance between the two hands increases very quickly, it may favor a semantic break and, thus, a decrease in the SoA. On the other hand, reducing the shift at the end of the movement (and thus increasing it at the beginning of the movement) could favor the achievement of the goal and thus increase the SoA. If we consider only the SoO, it is also possible that the detection results from the spatial distance between the two hands. Therefore, the shift rate is less important for detecting the illusion.

Studying different redirection functions that will increase and decrease the lag rate at the beginning or the end of the movement is interesting to explore all these possibilities.

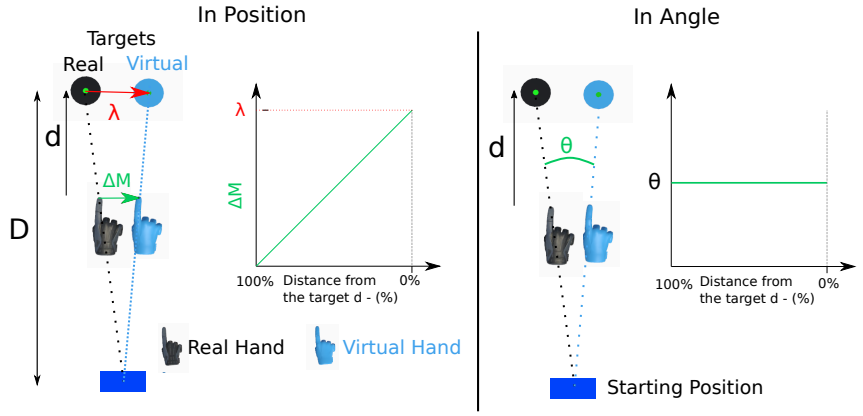

Figure 5.2: Common hand redirection techniques in VR. The virtual hand's position (blue) on the left is computed by adding a portion of vector $\vec{\lambda}$ to it according to the distance d. On the left, the virtual hand's position is computed by rotating the real hand's position around the starting position by the angle created by the targets. Both descriptions are equivalent.

5.1.1 Usual Implementation of Hand Redirection

In the implementation of hand redirection illusion of the previous chapter, the virtual hand position is set by rotating the virtual hand around the starting position using the angle formed by the real target, the starting position, and the virtual target. This implementation can be seen on the right panel of figure 5.2.

An other implementation of the hand redirection illusion is the *Interpolated Reach* [Han et al., 2018]. They define the offset between the real hand and the virtual hand $\vec{\Delta_M}$ with a linear function of the distance between the **R**eal **H**and $\vec{P_H^R}$ and the **R**eal **T**arget $\vec{P_T^R}$. The position of the **V**irtual **H**and is then equation 5.1.

$$\vec{P_V^H} = \vec{P_R^H} + \vec{\Delta_M}(\vec{P_H^R}, \vec{P_T^R}) \tag{5.1}$$

$$\vec{\Delta_M}(\vec{P_H^R}, \vec{P_T^R}) = \left(1 - \frac{||\vec{P_H^R} - \vec{P_T^R}||}{||\vec{P_O} - \vec{P_T^R}||}\right)\vec{\lambda} \tag{5.2}$$

with P_O the starting point which defines the area where the illusion is activated and $\lambda = ||\vec{P_T^V} - \vec{P_T^R}||$ the vector formed by the real and virtual targets. For ease of reading, we define the distance between the real hand and the target $d = ||\vec{P_H^R} - \vec{P_T^R}||$ and the distance between the starting point and the real target $D = ||\vec{P_O} - \vec{P_T^R}||$. Thus,

equation 5.2 becomes

$$\vec{\Delta_M}(d) = \left(1 - \frac{d}{D}\right)\vec{\lambda} \tag{5.3}$$

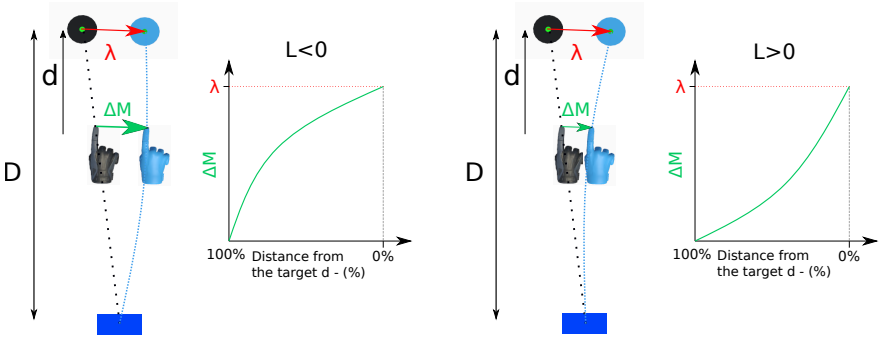

Figure 5.3: The hand redirection technique with a 2^{nd} order polynomial function. On the left, the function ($L < 0$) redirects the user faster at the start of the movement rather than at the end. On the right, the function ($L > 0$) redirects the user faster at the end of the movement rather than at the start. The offset curves (Δ_M) are the same as those figure 5.8.

Note that D and $\vec{\lambda}$ are constant, and as the real hand reaches the target, only d fluctuates. This equation is then a simple linear equation with two parameters $\{-\frac{\vec{\lambda}}{D}, \vec{\lambda}\}$. Equation 5.3 guarantees that when the real hand is on the starting position ($d = D$), the offset $\vec{\Delta_M}$ is null and when the real hand reaches the real target ($d = 0$), the offset equals $\vec{\lambda}$. In the case where the hand is further from the real target ($d > D$), the offset is set to 0. This implementation can be seen on the left panel of figure 5.2.

Both implementations are quasi equivalent. The only difference is how they handle the rotation of the hand during movement. For small redirection the difference is small.

5.2 *Generalization of the Hand Redirection Function*

Equation 5.3 is a first order polynomial: $f_1(d) = (a \times d + b)$. We generalize this equation:

$$\vec{\Delta_M}(d) = \left\{ \begin{array}{ll} f_n(d)\vec{\lambda} & \text{if } d < D \\ 0 & \text{otherwise} \end{array} \right\} \tag{5.4}$$

with $f_n(d)$ a polynomial of degree n with two constraints: $f_n(D) = 0$ and $f_n(0) = 1$. These polynomials allow to create a large variety of redirection behaviour like redirecting faster at the start or the end of the movement. The polynomial

function is then

$$f_n(d) = \sum_{i=0}^{n} \left(a_i d^i\right) \tag{5.5}$$

with a_i the i^{th} coefficient to be determined. When $n = 1$ (see equation 5.3), there is no degree of freedom, we have $a_1 = -\frac{1}{D}$ and $a_0 = 1$ because of the continuity constraints at the target and the starting position. With $n > 1$, the function has 1 or more degrees of freedom.

In this chapter, we focus on second-order polynomials and their influence on the detection threshold of the hand redirection illusion. In this case, equation 5.4 becomes

$$\vec{\Delta_M}(d) = f_2(d)\vec{\lambda} = (a_2 d^2 + a_1 d + a_0)\vec{\lambda} \tag{5.6}$$

This equation has 1 degree of freedom because there are only 2 constraints for 3 parameters. Figure 5.3 shows two examples satisfying the constraints.

In a similar manner to the previous chapter we chose to write the equation with a Bézier Curve [Faraway et al., 2007] to represent the degrees of freedom with control points that can easily be manipulated visually.

A Bézier Curve defines a polynomial of degree n from $n+1$ control points (Pc_i):

$$\vec{B(t)} = \sum_{i=0}^{n} \binom{n}{i} (1-t)^{n-i}\, t^i \vec{P_{Ci}} \tag{5.7}$$

with n the order of the polynomial, $B_x(t) = D - d$ and $B_y(t) = ||\vec{\Delta_M}||$ and t the Bézier variable varying between 0 and 1. The first (P_{C0}) and last (P_{Cn}) control points correspond respectively to the starting position and the virtual target position. The other control points allow to visually control the speed at which the redirection is applied as the user approaches the target.

In reality, because our input variable is d and not t, it is necessary to solve this two equation system by determining t according to d and then computing the offset $B_y(t)$.

In this formalism, equation 5.3 is a Bézier curve with two control points $\vec{P_{C0}} = (D,0)$ et $\vec{P_{C1}} = (0,1)$. For a second-order polynomial, equation 5.7 becomes

$$\vec{B(t)} = (1-t)^2 \vec{P_{C0}} + 2t(1-t)\vec{P_{C1}} + t^2 \vec{P_{C2}} \tag{5.8}$$

where P_{C1} is the control point representing our degree of freedom. Figure 5.4 illustrates 6 redirection functions by varying the position of the control point P_{C1}.

We define each redirection function with a variable L. For L < 0, the virtual hand is redirected away from the real hand faster than with the linear function.

And the opposite is true for L > 0. Finally, for all functions, the virtual and real hands are at the same position when the real hand is at the starting point and offset by $||\vec{\lambda}||$ when the real hand is at the targets.

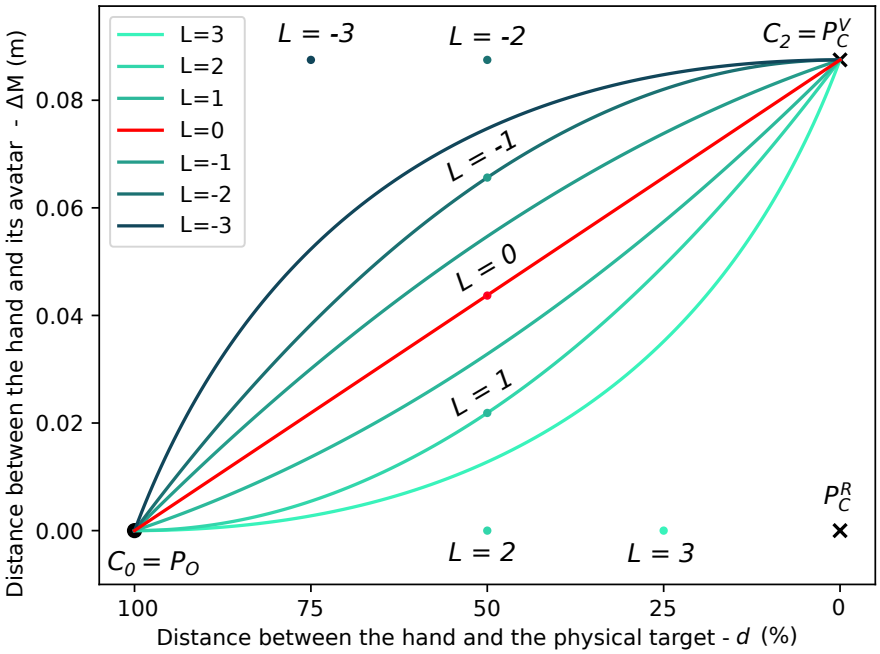

Figure 5.4: The offset between the real and its avatar Δ_M according to the distance between the real hand and the physical target d. The red curve is the standard linear redirection function $L = 0$; the six additional curves are the second-degree polynomial functions. Above the red curve $L < 0$, the redirection is applied faster at the beginning of the movement. Below the red curve $L > 0$, the redirection is applied faster at the end of the movement. In this case, the redirection is applied for an offset Δ_M of 8.75cm or 5°.

5.3 *User Study*

The aim of this user study is to evaluate the influence of non-linear redirection functions on the detection threshold of the hand redirection illusion. We focus on second-order polynomials illustrated in figure 5.4. The experimental protocol is similar to the one of the previous chapter.

5.3.1 *Participants and Apparatus*

The study was conducted with 19 participants (9 male, 10 female), aged from 20 to 29 years old (23.8 average). All participants were students volunteer from Sorbonne University. Amongst them, 2 were left-handed, 1 ambidextrous, and 15 right-handed. All participants had normal or corrected to normal eyesight (5 participants wore glasses or contact lenses). 3 of them had a regular VR experience,

11 had previous VR experience and 3 had no experience at all. No participants had musculoskeletal or proprioception disorders.

This user experiment was approved by the ethics comity of Sorbonne Université n°2020-020.

Participants were seated in front of a table wearing a VR HMD (HTC VIVE Pro) and a hand harness with a VIVE Tracker attached to it (see Figure 5.5). We choose the vive tracker for this experiment because we needed less precision about hand position than for the previous experiment. The position and orientation of the hand and finger are tracked with a precision of 1mm and 0.3°. We choose the HTC VIVE Pro because it was available and provide an appreciable confort for the participants. However our experiment protocol could be reproduced with a more accessible VR HMD.

5.3.2 Experimental Design

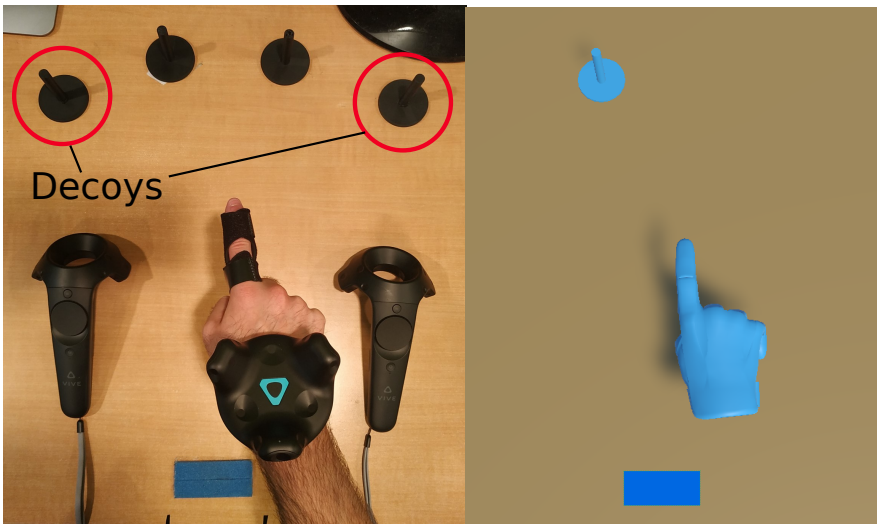

Figure 5.5: On the left, the table with 4 targets (including 2 decoys), the haptic marker and a participant's hand with the VIVE tracker. On the right, what the user sees: a single target, the hand avatar and the haptic marker.

A blue haptic marker is placed on the table as a starting position. 4 targets are arranged in an arc of a circle 56cm away from the starting point and offset by 15° from each other. We choose this distance so that all participants could reach the targets while seated. Similarly, the angular offset is set greater than the largest angle offset and small enough that participants couldn't detect it. Targets have a push-button on top for the users to press. Targets on the far right and far left are dummies and participants never interact with them. They are here to further "hide" the illusion from participants seeing the real setup before putting the HMD on.

The virtual scene illustrated in figure 5.5 is a copy of the real environment. It was created in the Unity3D editor. The hand is represented with a static hand with the index pointing forward. During a trial, only a single virtual target is shown to the user, the one they should point at.

Task and Stimulus

The experiment is a pointing task similar to the previous chapter experiment. The task starts with the user's finger on the starting position, a virtual target then appears. The participant reaches the target, presses the physical button, and goes back to the starting position. We ask that participants move naturally and avoid sudden movements and do the entire movement in 4 seconds. Then, participants have to choose if they had detected the illusion or not and if their real hand was on the left or on the right of their virtual hand. This first question is an extension of the more typical protocol.

In cases where participants make a mistake with the largest amplitude of redirection (14° et -14°), the ground becomes red to notify them. No further information were given to participants.

Conditions

We control 3 independant variables. The first variable is the FUNCTION OF REDIRECTION L with 7 values: $L = -3, -2, -1, 0, 1, 2, 3$ (see figure 5.4). Note that $L = 0$ is the linear reference function, i.e the function of redirection used in the previous chapter.

The second variable is the REDIRECTION AMPLITUDE θ. It is the angle formed by the real target, the starting position, and the virtual target. We consider 9 values: -14°, -10°, -6°, -2°, 0°, 2°, 6°, 10°, 14°, The extreme values should be easily detectable (14° and to some extent, 10°) whereas the closest values to 0° should be very hard to detect (2°). We compromised between having values covering a large enough spectrum to have easily detectable values, enough points to fit a psychometric curve on our data, and restricting the experiment time per participant (<1h).

The last variable is the PHYSICAL TARGET, Left or Right Target, introducing variability in the user's gesture. The leftmost and rightmost physical targets are not used in the experiment.

Procedure

Participants are first informed about the objective of the study and the task they need to perform. Careful attention was brought on explaining the concept of hand redirection and how to correctly answer the 2AFC: "Your virtual hand is represented in the virtual scene. During the task, an offset is added gradually between this virtual hand and your real hand. This offset shifts the virtual hand either on the left or on the right of your real hand." Participants then put the hand harness and the HMD on. Participants had time to accommodate with the illusion and the virtual scene by doing 4 training trials where their real hand was visible on top of their shifted virtual hand. The offset values were -10°, -2°, 2° et 10°. After each trial, participants were informed of the direction of redirection. They then realize the full experiment without seeing their real hand position. At the end, they fill out a demographic questionnaire.

Design

This study follows a within-subject design. Each participant did 2 repetitions of each combination of the 9 REDIRECTION AMPLITUDES, 7 REDIRECTION FUNCTIONS and 2 PHYSICAL TARGETS, i.e. 2 blocks of 126 trials. The different conditions are pseudo-randomized in each bloc. In summary, the experimental design is 18 Participants $\times$ 2 blocks $\times$ 9 REDIRECTION AMPLITUDES $\times$ 7 REDIRECTION FUNCTIONS $\times$ 2 PHYSICAL TARGETS = 4284 repetitions.

5.4 Analysis

Similarly to the previous chapter we plot the psychometric curve of the population to estimate the detection threshold of the illusion. The main aim of our analysis is to estimate if and how the *IND* is influenced by the REDIRECTION FUNCTION.

5.5 Results

5.5.1 Outliers

We removed participants from the analysis when any of the following conditions were met:

- The left or right non-detection interval *IND* for the linear redirection function ($L = 0$) is less than -14° or greater than 14°, similar to [Benda et al., 2020].
- The correct response percentage is less than 80% for the 14° and -14° angles and

for the linear redirection function ($L = 0$).

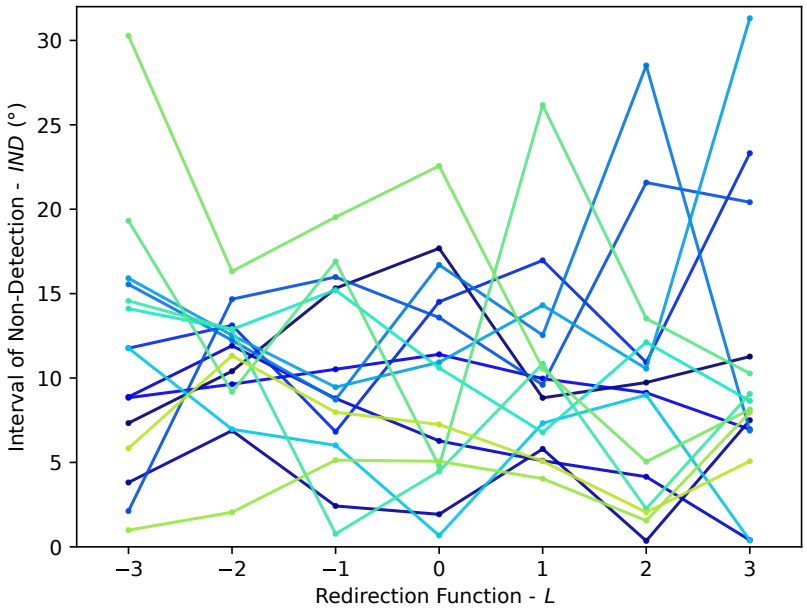

Figure 5.6: The interval of non-detection *IND* for each redirection function and for each participant.

Therefore, 3 participants were excluded for a detection interval of 15.0°, 16.2° and 28.5° and one participant for a correct response rate of 60%. The results presented here are therefore those of the 15 remaining participants. The experimental design is therefore : 15 Participants × 2 blocks × 9 REDIRECTION AMPLITUDE × 7 REDIRECTION FUNCTIONS × 2 PHYSICAL TARGETS = 4032 repetitions.

5.5.2 *Target effect*

We calculated the non-detection interval (*IND*) for each of the two physical targets and each redirection function. A Two-Way ANOVA (PHYSICAL TARGETS × REDIRECTION FUNCTIONS) on *IND* indicates no significant effect of PHYSICAL TARGETS ($F_{1,15} = 0.003, p > 0.05$), nor interaction effects ($F_{6,15} = 0.984, p > 0.05$).

5.5.3 *Redirection Function effect on Detection*

A One-Way ANOVA (REDIRECTION FUNCTION) for each REDIRECTION AMPLITUDE on the illusion detection question shows no significant effect on the detection.

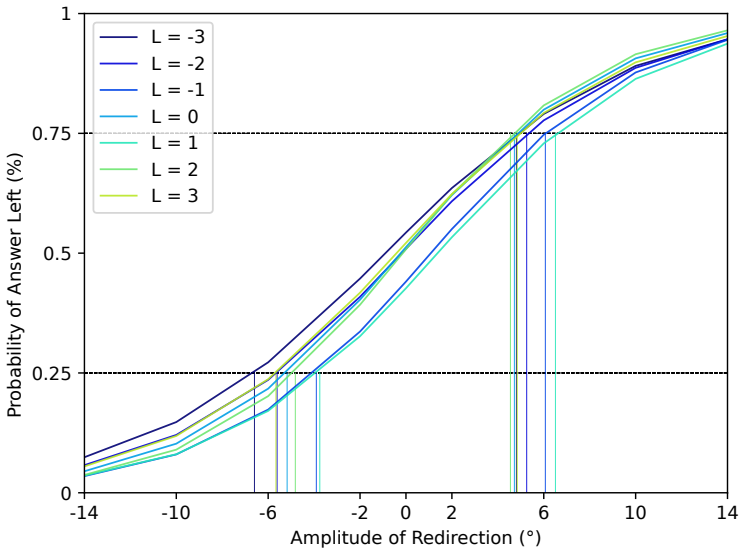

Figure 5.7: The psychometric function for each redirection function according to the angle of redirection. Vertical lines show the interval of non-detection *IND* for a redirection on the right (25%) and on the left (75%).

5.5.4 Interval of Non-Detection

Figure 5.7 shows psychometric curve for each REDIRECTION FUNCTION. The vertical bars indicate the Left and Right Intervals of Non-Detection. They vary on the left from -7.75° to -3.45° and on the right from 3.99° to 6.79°. Non-detection interval in the linear case $L = 0$ is $IND = 10.6°$.

These values are comparable to the one of the previous experiment and results of Zenner and Krüger [2019]. The distance between the source and the target is within the same magnitude and their results are very close with a $IND = 8.19°$. The results reported by [Ogawa et al., 2020] and [Benda et al., 2020] show higher *IND* (respectively $IND = 26.7°$ and $IND = 44.6°$). However, the distance between the origin and the real target is much smaller: around $20cm$ for the first one, and variable value for the second one (around $24cm \pm 7,5cm$), against $56cm$ in our study.

Figure 5.8 represents Intervals of Non-Detection according to the redirection functions L. The area around the curve represents the 95% confidence interval calculated with the 1000-sample Bootstrap technique. The curve tends to be constant, which would indicate that the detection interval appears to be invariant to the redirection function. A One-Way ANOVA of the REDIRECTION FUNCTION over the *IND* reveals no significant difference: $F_{8,15} = 0.876, p > 0.05$. An equivalence test carried out on all pairs of L REDIRECTION FUNCTION, the Two One-sided T-test (TOST), confirms the equivalence with the lower limit -3.5° and the upper

limit +3.5° ($p < 0.05$). Nevertheless, the TOST does not allow us to conclude on the equivalence of the *IND* with -2° and +2° bounds.

We therefore did not find any significant effect of the REDIRECTION FUNCTION on the detection of the illusion.

5.5.5 *Point of Subjective Equality*

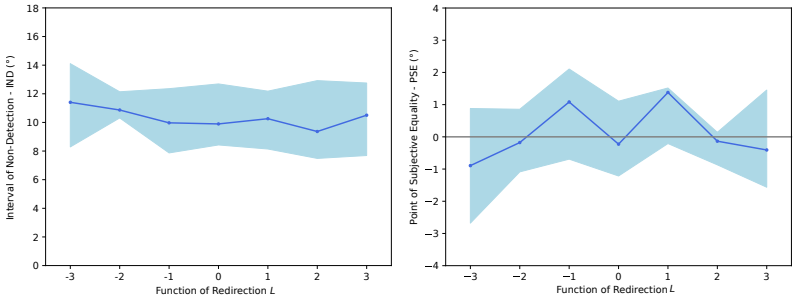

Figure 5.8: On the left, the interval of non-detection *IND* according to the redirection function. On the left, the point of subjective equality *PSE* according to the redirection function. The colored area shows the 95% confidence intervals computed with the bootstrap method.

Figure 5.8 shows the *PSE* for the different redirection functions. For the linear case $L = 0$, the *PSE* is $-0.23°$. As for *IND*, our value of *PSE* is similar to the results obtained by Zenner *et al.* [Zenner and Krüger, 2019], with a $PSE = -0.28°$.

A Two-Way ANOVA (PHYSICAL TARGETS × REDIRECTION FUNCTION) on the *PSE* indicates no significant effect of PHYSICAL TARGETS ($F_{1,15} = 3.491, p > 0.05$) nor interaction effect ($F_{6,15} = 1.895, p > 0.05$).

Table 5.1 shows a summary of our results.

5.5.6 *Participant Analysis*

Figure 5.6 shows the non-detection interval for each user (one colour per participant) depending on the redirection function. We do not observe any particular pattern such as groups of behaviors.

	IND	PSE
L=-3	11.41°	−0.89°
L=-2	10.87°	−0.18°
L=-1	9.97°	1.08°
L=0	9.89°	−0.23°
L=1	10.26°	1.38°
L=2	9.37°	−0.13°
L=3	10.51°	−0.41°

Table 5.1: Summary of our results: Interval of Non-Detection IND and Point of Subjective Equality PSE as a function of the function of redirection L.

5.6 *Hand Trajectory analysis*

Leveraging on the approach of the previous chapter, we analyze participants' hand trajectories with the help of Bezier curves. We logged the positions of the hand over time to analyze the real hand trajectory when reaching for the target as a function of the redirection function. We first removed trajectories where the hand tracking was not optimal (<5%) and then grouped trajectories for all participants by amplitude of redirection and redirection function. Here we choose 4 bezier points again.

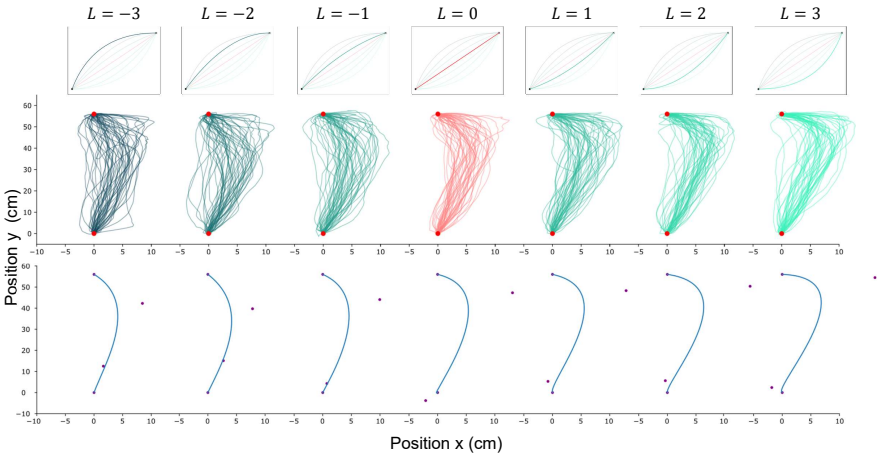

Figure 5.9: A visualization of participants' trajectories for each redirection function evaluated. These trajectories come from all trials with a redirection amplitude of 14° on both physical targets. Bottom: the mean Bezier curve (with four Bezier point) for each redirection function. We fixed three of the four Bezier point. This representation well illustrates the strong correction at the end for L>1.

Figure 5.9 illustrate all the trajectories as a function of the function of redirection for the redirection amplitude 14°. We observe that the trajectory shape is influenced by the redirection function L: a strong redirection at the beginning of the movement (L<0) generates a smooth reversed *C* shaped trajectory (Figure 5.9-Left). In contrast, a strong redirection at the end of the movement (L>0) generates a trajectory with a stronger correction at the end of the movement. (Figure 5.9-Right).

In the Figure 5.9 on the bottom, we plot the mean bezier curve for these Trajectories. We observe that the x and y positions of the 3rd Bezier point increase when L increases (see Figure 5.10). It illustrates the strong late correction for L>0. Let us note here that we had established a relation between illusion detection and trajectory curvature in the previous chapter. Considering the results of the previous section, this relation does not seem to be verified here. We develop this in the following section.

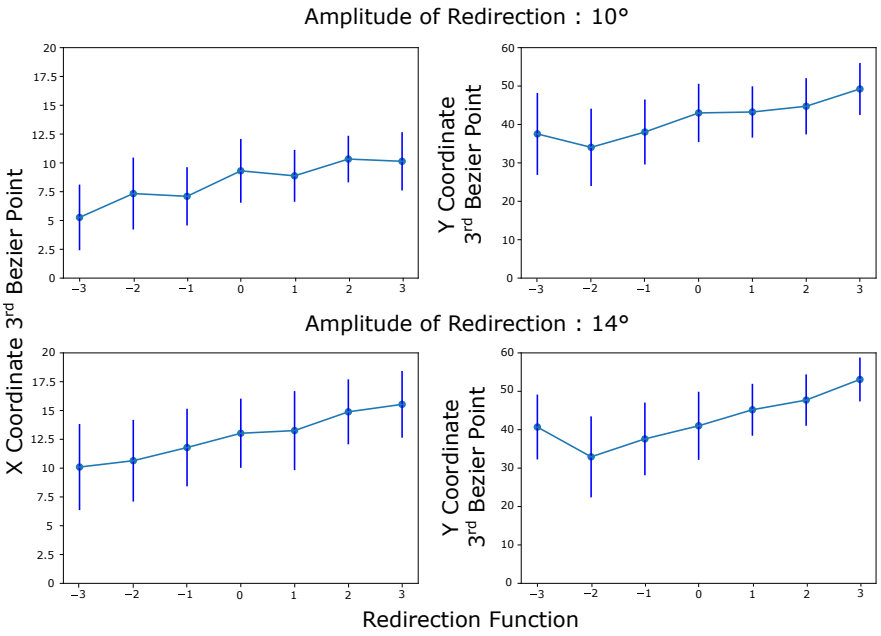

Figure 5.10: Evolution of the third Bezier point coordinates according to the redirection function. We plot the mean value of the X coordinate on the left and Y coordinate on the right for each trajectory and each participant for the two greatest positive amplitudes of redirection (10° and 14°).

5.7 *Discussion*

This chapter explores the design space of redirection functions for the hand redirection technique: we generalized the current implementation by considering polynomials of degree 2. The user study's main objective was to investigate the influence of the redirection functions on the interval of non-detection of the illusion. We considered 6 redirection functions with different dynamics (a shift at the beginning or the end of the movement). Our results show no significant effect of the redirection function on the interval of non-detection. Moreover, a Two-One Sided T-test (TOST) suggests the equivalence of the non-detection intervals for the different redirection functions.

We now discuss possible explanations for why different redirection functions do not affect the detection of the illusion. A two-component model suggests that an aimed movement is divided into two phases: first, a ballistic movement followed by a correction movement [Woodworth, 1899]. In the ballistic phase, the movement is faster as the users do not rely on vision to correct errors. Recent studies [Azmandian et al., 2016, Geslain et al., 2021] about visuo-haptic illusions show that some participants strongly adjust the trajectory of their real hand towards the target only during the final part of the movement. This observation is in line with the two-component model, suggesting that participants only noticed the offset between the predicted and actual position of the virtual hand at the end of the

ballistic movement.

By generalizing the redirection functions, we can choose whether the offset between the real and the virtual hand mainly increases during the ballistic or correction phase. Indeed, with $L < 0$, the offset is likely to increase during the ballistic phase (beginning of the movement), while $L > 0$, the offset is likely to increase during the correction phase (end of the movement). A difference regarding the detection of the illusion between $L < 0$ and $L > 0$ would suggest that users are more sensitive to the offset increase in one of the two phases. We could also make the hypothesis that in the non-linear case ($L \neq 0$), the important shift either at the beginning ($L < 0$) or at the end ($L > 0$) can favor semantic break and thus, the detection of illusion compare to the linear case ($L = 0$).

Surprisingly, our results do not show differences regardless of the value of L. One explanation could be that users are not sensitive to when the offset increases but only to the maximum offset amplitude at the end of the trial, i.e. when the users touch the physical target. This hypothesis is in line with an SoO view of illusion detection: we mainly detect the shift between visual and proprioceptive information, not the disturbance of our sensorimotor loop. Another explanation might be that the ballistic phase is much shorter than expected. Participants' movements could have been too slow due to our instructions favoring correction movements. The slow movement also favors the correct reaching of the target, even with an important shift rate at the end or beginning of the movement. Therefore, the resulting decrease in SoA does not occur. Participants could also have focused too much on their virtual hand rather than the target to answer the 2AFC choice accurately.

In future work, we plan to study possible interaction effects between movement speed and redirection function. Indeed, faster movements and potentially more contrasted redirection functions could make some phenomena more salient. Furthermore, future work should also control the effect of the distance from the real hand to the body as the visual and proprioceptive accuracy might vary in the ballistic (currently close to the body) and correction phase (far from the body). For instance, we will consider a reverse movement where the hand's starting position is away from the body, and the target is close to the body. Another possible explanation is that an effect is present but not visible due to the lack of data points. Future work should consider a larger number of participants and/or a larger number of samples per participant. The instructions might have been more difficult to interpret than expected, as some participants might have noticed the visuo-haptic mismatch but could not correctly indicate the mismatch's direction.

5.8 Implications for Design

Our results have implications for design interactions. They suggest that the designer can better control the real hand trajectory during hand redirection. For example, in a complex scene with multiple physical objects that can be accidentally hit, the designer can use an appropriate function to avoid obstacles along the real hand's path. Also, many interaction techniques involve using actuated robots to provide haptic feedback. It is conceivable to alter the hand's trajectory to avoid unwanted contact with the robot.

5.9 Conclusion

In this chapter, we investigated the design space of hand redirection illusion. We generalized the hand redirection technique by considering other redirection functions like 2^{nd} order polynomials. We empirically compared the influence of 6 of those functions with the standard linear function. Our results suggest that the redirection function does not influence the Interval of Non-Detection. We also found that the redirection function offers more flexibility to designers to control the hand trajectory.

We aimed to explain and predict illusion detection with system factors. Even if our results are surprising, we saw that the shift rate between the two hands does not seem to influence illusion detection. The results of the two last chapters are empirical. To further explore these findings, we propose to study the Users' factors in the next chapter. We found in the previous chapter that the parameter b, which represents the natural curvature of a user's hand movement, predicts the hand trajectory under redirection and the detection of the illusion. We hypothesize in the next chapter that other users' abilities can also be useful in understanding the detection of illusions.

6

Study of Users Factors

In this chapter, we consider the last class of factors – **users factors** – involved in the use of visuo-haptic illusions (see Figure 6.1). We argue that the ability of the users to estimate the positions of the physical and virtual hand has an impact on the likelihood of detecting the Hand Redirection illusion. Two modalities are involved when estimating the position of the hand: the visual modality and the proprioceptive modality.

The visual capture theory [Rock and Victor, 1964] states that we give more weight to the vision in case of incongruence between different sensory modalities. The aim of this chapter is thus to study the respective weight of the visual and proprioceptive sensibilities on the estimation of the position of the hand. We build on multi-sensory integration models from cognitive science to argue that the important parameter to attribute a weight to a modality is its sensibility. It raises one main challenge: how to measure the sensibility of a given modality?

We first motivate the necessity to measure the visual and proprioceptive user sensibilities for studying visuo-haptic illusions. We then present an experiment to

capture these two sensibilities at the individual level, i.e., for each participant. In this experiment, the difficulty is both the definition of the experimental protocol and the computational methods to analyze the data. We present our results and discuss their relevance. In the next chapter, we present some perspectives to link these user sensibilities to illusion detection.

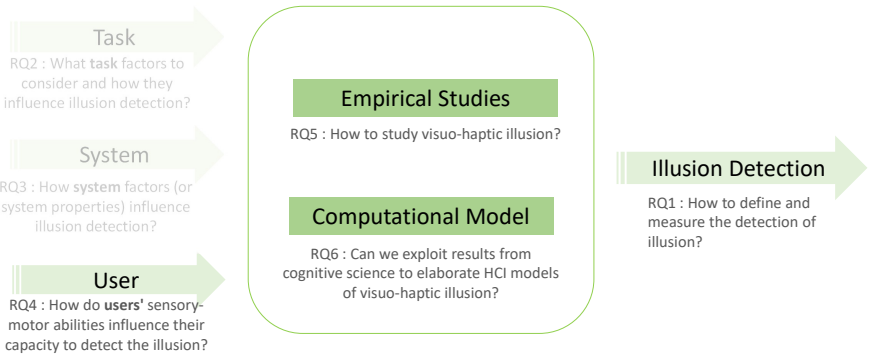

Figure 6.1: Reminder of our approach. We focus in this chapter on the factors related to the users.

6.1 *Why Users Sensory Sensibilities Are Relevant for studying Illusion Detection?*

Chapter 3 discussed two mechanisms that can lead to the detection of an illusion. The first is linked to a decrease in the sense of agency (SoA), and the second is linked to a decrease in the sense of ownership (SoO). In this section, we demonstrate the importance of estimating individual sensibilities – particularly visual and proprioceptive – to predict the break of SoA and SoO and thus predict the detection of an illusion. To achieve this, we describe some computational models linked to the decrease in SoA and SoO.

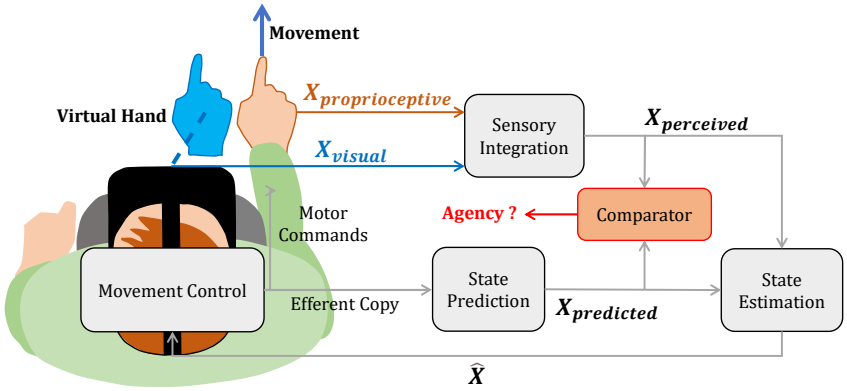

Figure 6.2: Diagram of the comparator model [Frith, 1987]. An efferent copy is emitted with the emission of a motor command. A prediction of the sensory consequence of an action calculated based on the efferent copy is compared to the actual sensory feedback. If the two information are significantly close, a strong sense of Agency is experienced. In our case, the visual sensory information is perturbed by the implementation of the illusion.

6.1.1 *Models about the Sense of Agency*

The comparator model [Frith, 1987] (see Figure 6.2) can explain a decrease of SoA. Remember that according to this model, the brain creates an efferent copy whenever a new motor command is generated. If the efferent copy matches the actual sensory perception, the movement is perceived as self-caused, and SoA arises [Braun et al., 2018]. On the opposite, if the sensory perception and the efferent copy are too different, it could lead to a semantic break [Padrao et al., 2016] and a decrease in SoA. Thus, the actual sensory perception plays an important role. In our context, the brain perception of the hand comes from an integration of discrepant information from the visual and proprioceptive modalities. To evaluate the value of this perceived position, one needs to understand how these two information are weighted to come up with a unified perception.

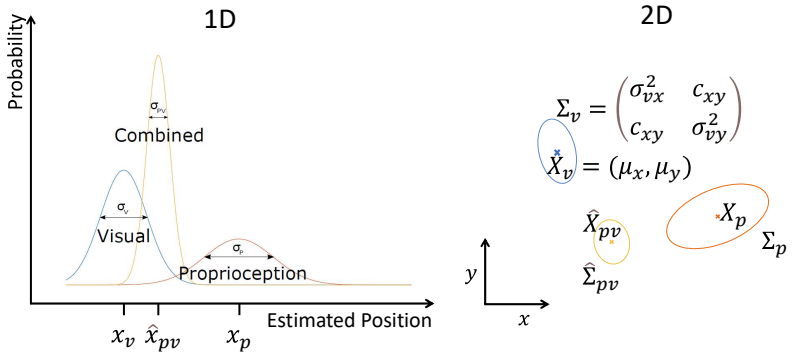

Figure 6.3: Illustration of the model of optimal multi-sensory integration. On the left, the brain combines the visual information (x_v) and the proprioceptive information (x_p) in an optimal manner. The estimated position $\hat{x_{pv}}$ is closer to x_v than x_p because the confidence in the visual information (small variance σ_v) is better than the proprioceptive one (large variance σ_p). The variance $\sigma_p v$ is smaller than either σ_v or σ_p. On the right we illustrate a similar optimal integration for 2D positioning instead of 1D. Here the confidence in a positional information is represented by confidence ellipse. These ellipses have 3 parameters, the x and y variance and the covariance, that describe the relative elongation and orientation of the ellipse.

Computational models related to the optimal multi-sensory integration can help us predict the estimation of the hand position from the integration of visual and proprioceptive information. For instance, according to the Gaussian association model, the estimation of a quantity by a combination of different modalities (e.g. vision+proprioception) depends on the confidence that the brain has in each modality. This confidence is characterized by the sensibility of the corresponding modality. Consider the estimation of the x position of an object (1D estimation) by the visual and proprioceptive modalities. The sensibility of these modalities can be mathematically represented by their corresponding variances: σ_v^2 for the **v**ision and σ_p^2 for the **p**roprioception. The final position estimation of the object by the brain $\hat{x_{pv}}$ is thus a weighted combination of the estimation made by the visual x_v and proprioceptive x_p modalities:

$$\hat{x_{pv}} = \frac{\sigma_p^2}{\sigma_v^2 + \sigma_p^2} x_v + \frac{\sigma_v^2}{\sigma_v^2 + \sigma_p^2} x_p \tag{6.1}$$

The final estimation x_{pv} is more precise than the most precise modality estimation (see Figure 6.3). Moreover, the less precise the estimation of a modality is (i.e. large variance), the less influence it has on the final estimation of the quantity. The integration is "optimal" in that sense that it minimizes the error of the estimation of the physical quantity.

The brain seems to follow this integration pattern for physical quantities such as the size of an object through vision and haptics [Ernst and Banks, 2002], the orientation of the body in space through vision and the vestibular system [Zupan et al., 2002, Fetsch et al., 2010], the shape of an object by vision and touch [Helbig and Ernst, 2007] and the localization of our limbs during a movement [Sober and Sabes, 2003, 2005, Van Beers et al., 1999, van Beers et al., 2002, van Dam and Ernst, 2013, Block and Sexton, 2020].

6.1.2 *Models about the Sense of Ownership*

Bayesian Causal inference models [Körding et al., 2007] explain the sense of ownership (SoO) in VR [Kilteni et al., 2015]. These models propose that the SoO emerges as the result of attributing all sensory information available about the body to a single common cause: the self-body [Samad et al., 2015, Schubert and Endres, 2021]. In our case the brain decides to attribute the visual (x_v) and proprioceptive (x_p) position of the hand to a common cause (C=1) or to a different cause (C=2). If the virtual hand is seen as the cause of both x_v and x_p (C=1) there is a SoO toward the virtual hand, else if the virtual hand is only the cause of x_v (C=2), no SoO occurs (see Figure 6.4).

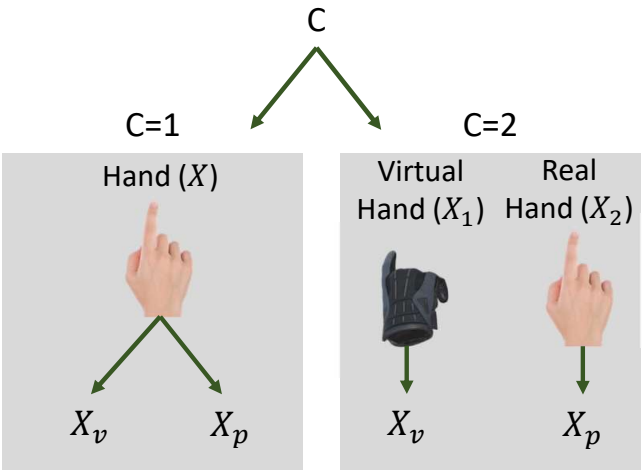

Figure 6.4: Illustration of the causal inference. Left (C=1), the brain infers that visual and proprioceptive information have the same cause: the hand. The virtual hand is considered to be also the source of the proprioceptive information (coming from the real hand), this results in a SoO toward the virtual hand. The two positional estimation x_v and x_p are integrated to one unified estimation of the hand position x. Right (C=2) the brain infers that visual information (virtual hand) and proprioceptive information (read hand) comes from independent causes: The brain perceives two different positions x_1 and x_2 and then dissociates the virtual and the real hands.

To select the most likely cause the brain infers each cause probability considering

the available information: $P(C1|X_v,X_p)$ and $P(C2|X_v,X_p)$. The Bayes's theorem is used to calculate these probabilities:

$$P(C=i|x_v,x_p) = \frac{P(x_v,x_p|C=i) \times P(C=i)}{P(x_v,x_p)} \tag{6.2}$$

where i equals 1 or 2. In this equation, $P(C=1)$ is the prior probability of a common cause and $P(C=2)$ the prior probability of a different cause. These two prior probabilities are fixed by the brain and do not depend on the sensory sensibility. The term $P(x_v,x_p)$ is constant and can be disregarded when comparing $P(C=1|x_v,x_p)$ and $P(C=2|x_v,x_p)$. Finally $P(x_v,x_p|C=1)$ and $P(x_v,x_p|C=2)$ are the likelihoods of having the positions of the hand at x_v and x_p given C=1 or C=2. These likelihoods are calculated based on users' visual and proprioceptive sensory sensibilities.

Therefore to predict both the breaks in SoA and SoO with computational models, it is necessary to first capture and measure users' visual and proprioceptive sensory sensibilities.

6.2 Measures of Sensory Sensibilities

The task we consider in this thesis is a pointing task in VR with the right hand. The specificities of this task are that 1) two modalities are involved (vision and proprioception) and 2) a pointing movement involves multiple joints (wrist, elbow, shoulder and potentially finger) and 3) we consider two quantities (the final x an y positions). Our objective is to estimate the visual sensibility S_V of the users as well as the proprioceptive sensibility of their right hand $S_{P_{RH}}$ for this task. While it is easy to estimate an overall sensibility GS_1 by measuring, for instance, the dispersion of the final hand points, it is difficult to estimate the respective contribution of each modality.

From a mathematical point of view, the problem consists of resolving a single equation with two unknowns:

$$GS1 = f(S_V, S_{P_{RH}}) \tag{6.3}$$

Both sensibilities S_V and $S_{P_{RH}}$ can be decomposed into precision *i.e. the variance of the distribution*, and accuracy *i.e. the systematic bias*.

2 main experimental protocols have been proposed in the literature to measure the sensory sensibility of modalities. However, they can not directly be applied to

our task. In this section, we briefly present these protocols and justify the choice of the experimental protocol for the study described in the following subsections.

One protocol consists of simply asking participants to perform several times the same pointing task (estimating quantities). With several repetitions, the participants form a distribution whose variance and mean can be extracted. The mean inform on the accuracy and the variance on the precision. The global sensibility of this task is thus the measure of this variance and mean. A variant of this protocol has been extensively used in health and sports to measure proprioceptive sensibility for multiple joints (e.g. the ankle [Deshpande et al., 2003] or the knee [Tsang and Hui-Chan, 2003]). It was possible because the task did not involve vision. In our context, the global proprioceptive sensibility of the right hand $S_{P_{RH}}$ also depends on the proprioceptive sensibility of multiple involved joints. While it could be informative to measure the sensibility of each joint, this approach is time-consuming, tedius and not necessary to study visuo-haptic illusion.

Another protocol [Ernst and Banks, 2002, MacNeilage et al., 2007] is based on a 2AFC experiment. The participants compare two quantities (e.g., the size of an object [Ernst and Banks, 2002]) and should estimate which one of the two quantities is smaller/larger (forced choice). The more finely a participant can discriminate the two quantities with one modality, the greater the accuracy of this modality is. This 2AFC protocol has been used in different contexts [Reuschel et al., 2010], [Matsumiya, 2019], [Henriques et al., 2014].

As it is, these protocols do not allow to distinguish the visual and proprioceptive sensibilities of each modality for a pointing task. One can consider suppressing one modality when performing the pointing task to measure the sensibility of the other modality. However, it is extremely challenging. For instance, if the visual modality is suppressed, the stimulus, the target, is not visible. It would require to carry the hand of the participant to defined positions. Beyond the difficulty (time and setup) to implement such study, it remains that the participants would perform passive movements instead of active movements. Similarly, it would also be possible to suppress the proprioceptive modality, but it would require invasive operations (anesthesia).

To solve this problem, Van Beers et al. [1998] proposed an original method on which we build on to measure users' sensibilities.

6.3 Methodology

As a reminder, our problem consists of resolving a single equation with two unknowns (see 6.3). Our general approach relies on the one of Van Beers et al. [1998]: The participants perform three different (pointing) tasks (instead of one). From each task, we can extract a general sensibility providing from a unique combination of visual sensibility S_V, proprioception sensibility of the right hand $S_{P_{RH}}$ and proprioception sensibility of the left hand $S_{P_{LH}}$ (see Figure 6.5). More precisely:

1. General sensibility task 1 GS_1 is the combination of visual sensibility S_v and the proprioceptive sensibility of the right hand $S_{P_{RH}}$: $GS1 = f(S_V, S_{P_{RH}})$
2. General sensibility task 2 GS_2 is the combination of visual sensibility S_v and the proprioceptive sensibility of the left hand $S_{P_{LH}}$: $GS2 = g(S_V, S_{P_{LH}})$
3. General sensibility task 3 GS_3 is the combination of the proprioceptive sensibility of the right hand $S_{P_{RH}}$ and the proprioceptive sensibility of the left hand $S_{P_{LH}}$: $GS3 = h(S_{P_{RH}}, S_{P_{LH}})$

In other words, we transform one equation with two unknowns (which does not have a unique solution) into a system of three equations with three unknowns which has the advantage to have a unique solution. We now detail the three pointing tasks corresponding to the three equations.

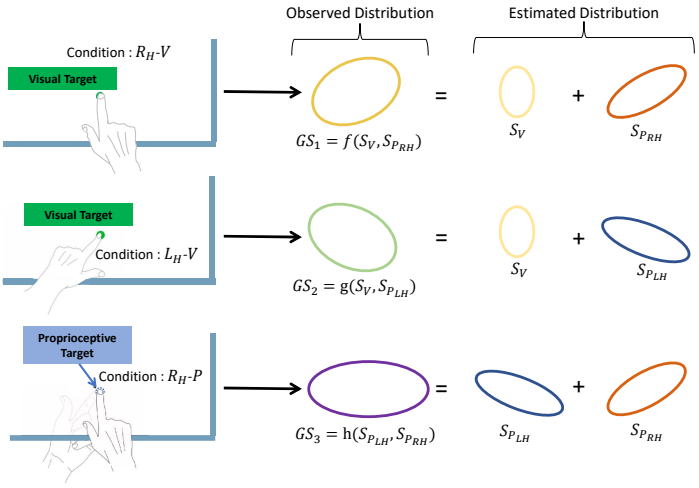

Figure 6.5: Diagram illustrating the three different pointing tasks, each corresponding to an experimental condition. In the condition $R_H - V$ and $L_H - V$ the target is visual. In the condition $R_H - P$ the target is proprioceptive (the left hand under the table). With each condition pointing to the target several times will create a distribution of points. From this distribution (here represented directly to the right of the condition diagrams) we can extract the sensibility of the modality that evaluate the target position and of the modality that evaluate the hand position. We obtain a system of three equations with three unknowns that can be solve.

6.4 Data Collection

We conducted an experiment according to the methodology detailed above.

6.4.1 *Participants and Apparatus*

The participants are the same as the study of the chapter 4. They wear an HMD HTC Vive tracked by an Optitrack system composed of 8 infrared cameras. The position and 3D orientation of the participants' index finger is also recorded with the Optitrack system, using a glove with markers.

Participants were sitting in front of a transparent Plexiglas table. 7 haptic targets are placed under the table. The locations of these targets are the same than the virtual targets that the participants can see in the HMD (see Figure 6.6). An additional haptic target indicates the starting position which is both felt and seen in the VE. A pedal is placed under the right foot of the participants and is used to validate each trial. In the virtual environment, the participants do not see their hands.

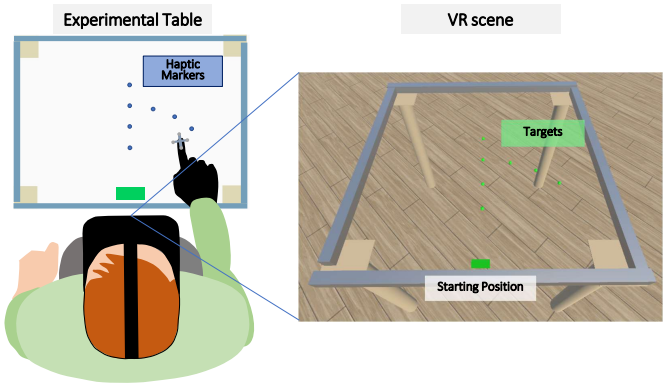

Figure 6.6: On the left : illustration of the experimental setup in the real world. The participant is seated in front of transparent table wearing the HMD and a gloves with optitrack marker (on the left or right hand in fonction of the condition). Under table 7 haptic marker are placed in the same position as the visual target displayed in VR. On the right : view of the participant in the VE. The position of the hand is never displayed in the VE. The seven target (green) are all displayed here. However during the experiment participants will see only one at a time.

6.4.2 *Task and Conditions*

The task consists of positioning the tip of their index finger as accurately as possible on one of of the seven possible targets. Depending on the conditions, participants use either their right or left hand, virtual or physical targets.

- In the first condition, participants have to match as best as possible the position of the tip of the index finger of their **right hand** with the position of a visible **visual** target in the virtual environment : Right Hand - Visual Target $R_H - V$. The visual target is represented with a green sphere of the size of a thumb (see Figure 6.6)
- In the second condition, participants had to match the position of the tip of the index finger of their **left hand** with the position of a **visual** target in the virtual environment (Left Hand - Visual Target $L_H - V$)

- In the last condition, the participants have to match as well as possible the position of the the tip of the index finger of their **right hand** on the table with the position of the index finger of their left hand placed under the table (Right Hand - Proprioceptive Target $R_H - P$). The left hand is positioned on a **physical** target. The physical targets have the same position and relative size as the visual targets, except that the thickness of the table separates them ($\sim$5mm).

Each participant performed the 3 conditions corresponding to the three tasks of the method (see Figure 6.5):

6.4.3 Procedure

We first explain the principle of the experiment to the participants and have them read and fill out a consent form. Then, they put on the HMD and glove, on their right hand for the $R_H - V$ and $R_H - P$ conditions and on their left hand for the $L_H - V$ condition. They then place their right foot on the pedal for all conditions. When they enter the VE, participants see a screen showing them their next task. They must press the foot pedal to begin the training phase. This phase is performed for each new condition.

In all conditions the participants, once the target has appeared, must place the hand wearing the glove (invisible in the VE) as best as possible on the position of this target. Once they are satisfied with the position of their hand, they must press the pedal. They must then return to the starting position to begin the next trial.

For the $R_H - V$ and $L_H - V$ conditions, the target is visual and appears as soon as the participants have reached the starting position. For the $R_H - P$ condition, the target is proprioceptive, it is the fingertip of the left hand. When participants start a new cycle (of $R_H - P$), a visual target appears. They must then place their left hand, under the table, on the haptic target corresponding to this position. They must then press the foot pedal. This causes the visual target to disappear and numerous visual targets to appear for 2 seconds. They act as a lure to make the participant forget the position of the visual target. The participant thus focuses only on the position of his left hand for the aiming task.

For the $R_H - V$ and $L_H - V$ conditions, participants perform 6 training cycles. For the $L_H - V$ condition, they perform 12 training cycles. Once the training phase is completed, the real experiment begins as soon as the participant is ready and press the pedal. Participants aim 20 times at each of the 7 targets in the same way as they did in the training phase. The number of attempts already made is displayed

on the virtual screen in front of them.

6.4.4 Design

This study follows a within-subjects design. The presentation order of the three conditions is counter-balanced between participants to avoid learning effects.

For each condition, participants perform 20 blocks. In each block (7 trials), each target is presented one time in a random order.

In summary the experimental design is: 12 participants x 3 conditions x 20 blocks x 7 targets = 5040 trials.

6.4.5 Measures

We have 3 dependent variables: The precision and the accuracy of the index finger position as well as the time to reach the target.

6.5 Analysis

6.5.1 Mathematical Formalization of Sensory Sensibility

We assume that the sensory sensibility can be represented by a confidence ellipse which contains the final positions of the index finger (see Figure 6.3). We work in this study with 95% confidence ellipses. The distribution of points to form this ellipse can be generated by a 2-D Gaussian function. A 2D Gaussian is defined by its mean $\mu = (\mu_x,\mu_y)$ representing the center of the ellipse and by its covariance matrix Σ (see Figure 6.3) representing its shape:

$$\Sigma = \begin{pmatrix} \sigma_x^2 & c_{xy} \\ c_{xy} & \sigma_y^2 \end{pmatrix} \tag{6.4}$$

The covariance matrix has three parameters. The variances σ_x^2 and σ_y^2 characterize the elongation of the ellipse in a certain direction. The covariance c_{xy} gives the orientation of the ellipse. For example in Figure 6.3 the ellipse illustrating the proprioceptive sensibility (orange) is more elongated in the x direction and therefore has a higher σ_x^2 than σ_y^2. It is the opposite for the ellipse representing the visual sensibility (blue). None of these ellipses are oriented perfectly horizontally, therefore their covariance is different from 0.

The covariance matrix Σ represents the precision of the modality. Its accuracy corresponds to the offset between the target position and the center of the ellipse: *bi* = (bi_x,bi_y). Note that in sensory integration models, the precision (i.e. covariance matrix Σ) is used to assign a weight to a modality.

6.5.2 Bimodal Data Analysis

The first step of the analysis is to put the observed data into an usable form. We have the final positions (p_x,p_y) of the left and right hand indexes (*FPI*). We have 21 (7 targets * 3 conditions) distributions for each participant. For each distribution, we calculate the 5 parameters (μ_x,μ_y,σ_x^2, σ_y^2,c_{xy}) of the 95% confidence ellipse. However, these *bimodal* confidence ellipses correspond to the combination of two sensibilities. We then need to extract each *unimodal* sensibility individually. We propose two methods of analysis.

Classical Analysis

The classical method of analysis is the one used by Van Beers et al [Van Beers et al., 1998]. For each condition, the two distributions, expressing the precision of the two modalities involved, are independent. Indeed the two modalities are measuring different physical elements. Thus the bimodal covariance matrix obtained is simply the sum of the two unimodal covariance matrices. Similarly the bias (bi) of the mean of the bimodal distribution is the sum of the biases of the unimodal distributions. For the condition $R_H - V$ for example this is expressed as follows:

$$\Sigma_{R_H-V} = \Sigma_V + \Sigma_{P_{R_H}} \tag{6.5}$$

$$bi_{R_H-V} = bi_V + bi_{P_{R_H}} \tag{6.6}$$

where Σ_{R_H-V} and bi_{R_H-V} are the covariance matrix and bias parameters of the observed bimodal distributions with the experiment, and bi_V, $bi_{P_{R_H}}$, Σ_V, $\Sigma_{P_{R_H}}$, and bi_{PM_D} are the bias and covariance matrix of the unimodal distributions representing the sensibilities of the visual (S_V) and of the right hand proprioceptive ($S_{P_{RH}}$) modalities. We can transpose the Equation 6.5 and the Equation 6.5.2 to the conditions $L_H - V$ and $R_H - P$. For each target, the 3 distributions obtained from the 3 conditions give a system of 3 equations with 3 unknowns (the unknowns being the 3 couples (bi_V, Σ_V), ($bi_{P_{R_H}}$, $\Sigma_{P_{R_H}}$), ($bi_{P_{L_H}}$, $\Sigma_{P_{L_H}}$). The Figure 6.5 illustrates the system of three equations with three unknowns. The resolution of this system

provides the 3 couples of parameters describing each unimodal distribution. In summary:

- **Input (for each participant)**:
  - 21 bimodal distributions (bi, Σ) from 7 targets and 3 conditions
- **Algorithm for each target**:
  - Selection of the 3 bimodal distributions for each target (1 per condition)
  - Construction of the equation system with the 3 bimodal distributions
  - Solving the equation system
- **Output**:
  - 7 unimodal distributions (bi, Σ) for each of the 3 modalities (visual, right and left hand proprioception)

This method directly relies on our observations and has the advantage of proposing an exact solution. However, the resolution of the equation system imposes the use of subtractions for the calculation of unimodal distributions. This can lead to parameters with impossible values such as negative variances. This problem is corrected if the results are averaged over all participants. Indeed there are more positives than negatives result which when averaged give a positive result. This method therefore provides a tool for studying modality sensibilities at the *population* level, but is not appropriate at the *individual* level.

Bayesian Analysis

To study our results at the individual level, we propose to turn the problem around. Instead of starting from the bimodal distribution and try to extract the unimodal distributions, we search the optimal unimodal parameters that will generate the observed (FPI) bimodal distribution. Indeed,

with a Bayesian inference approach [Battaglia et al., 2003], the objective is not to find the exact value of one parameter (here the covariance matrix Σ) but rather a posterior probability law on this parameter Σ. That is to say the probability distribution of the parameter value after taking into account the experimental data. A Bayesian inference approach requires a prior law of the parameters that we want to estimate. The prior law reflects the knowledge about the value of the parameter before observing the data.

To implement the Bayesian inference approach, we use the ABC (Approximate Bayesian Computation) algorithm already used in the HCI community by [Kangasrääsiö et al., 2017]. The principle of ABC is to repeatedly generate a set of unimodal

parameter values drawn from prior law. We can then calculate the bimodal gaussian law parameters and generate the bimodal points distribution. Finally, we compare the simulated distribution to the observed distribution (PFI). If the distance between the two distributions is close enough, the parameter values are accepted. We repeat this process n times. For each parameter, the accumulation of their accepted values define the parameters' probability law.

We have chosen to calculate the biases by the classical method presented in subsubsection 6.5.2 to limit the number of parameters. In summary :

- **Input for each participant:**
  - 21 bimodal distributions (bi, Σ) from 7 targets and 3 conditions
  - 3 prior laws of Σ parameters, one per modality
  - The values of the unimodal biases (bi) calculated with the classical method
- **Algorithm for each target:**

  WHILE n < 10000:

  – step 1: drawing of parameters Σ_V, Σ_{PM_D} and Σ_{PM_D} based on the chosen prior law (in total there are 3*3 = 9 parameters).

  – step 2: generation of the bimodal distributions (bi_{R_H-V}, Σ_{R_H-V}), (bi_{L_H-V}, Σ_{L_H-V}) and (bi_{R_H-P}, Σ_{R_H-P}) (see Equation 6.5 and Equation 6.5.2)

  – step 3: creation of three PFI_{sim} datasets generated following the 3 2D Gaussian laws (bi_{M_D-V}, Σ_{M_D-V}), (bi_{M_G-V}, Σ_{M_G-V}) and (bi_{R_H-P}, Σ_{R_H-P})

  – step 4: evaluation of the distance $d(PFI_{obs}, PFI_{sim})$ for the 3 conditions $R_H - V$, $L_H - V$ and $R_H - P$

  – step 5: IF $d(PFI_{obs}, PFI) < \varepsilon$ the parameters are accepted. ELSE the parameters are deleted

  END WHILE

  - final step: Draw the 9 parameters' probability laws from the accumulation of accepted parameter values

- **Output:**
  - 9 probability laws on the covariance matrices Σ for the 3 modalities (visual, proprioceptive right hand and proprioceptive left hand).

The average of these probability laws is used to compare this method with the previous classical method, which provides unique values. To apply the ABC

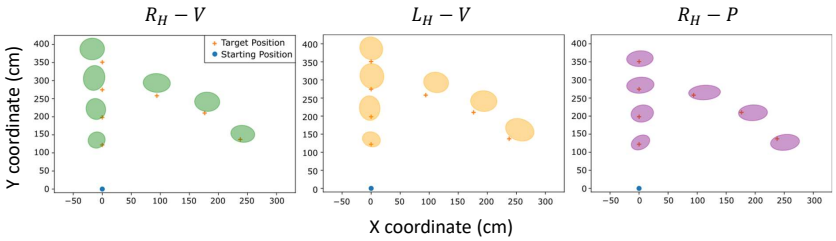

Figure 6.7: Precision and accuracy for the seven targets and the three conditions. Left: Pointing with the right hand; Center: Pointing with the left hand; Right: Proprioceptive pointing with the right hand.

algorithm we used the software package *ELFI* [Lintusaari et al., 2018]. We use a variation of the classical ABC algorithm called Sequential Monte Carlo ABC and compare the euclidean distance between the variance and the mean of the real and simulated distribution. This implementation was made under python.

6.5.3 *Frame of Reference*

The two variances σ_x^2 and σ_y^2 are expressed with respect to x and y coordinates. However, it is more interesting to express them in the frame of reference of the participant: depth and azimuth. Each covariance matrix obtained is thus now expressed along these axes.

6.6 *Results*

6.6.1 *Bimodal Data*

The Figure 6.7 illustrates the distribution (PFI) averaged over all participants for the three conditions.

Precision

We observe that the confidence ellipses of the $R_H - V$ (right hand visual target; green) and $L_H - V$(left hand visual target; orange) conditions are close to a circle and slightly more elongated in the depth direction. In contrast, the confidence

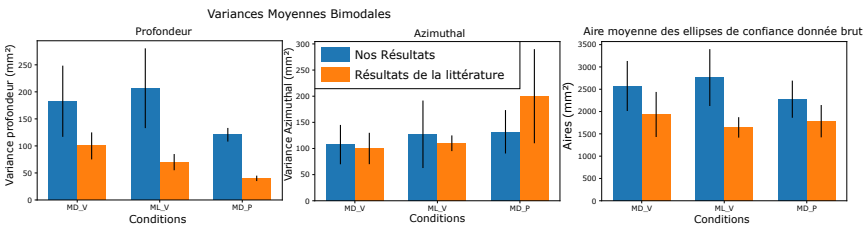

Figure 6.8: Comparison of the distribution (PFI) with the literature. left and center : display of the average variances over the participants and all the targets for each condition (azimuthal variances on the left and depth variances on the right). right : display of the average areas of the confidence ellipses

ellipses of the $R_H - P$ condition (right hand proprioceptive target; purple) are more elongated in the azimuthal direction.

The Figure 6.8 compares precision in virtual reality (our data) with the precision in a real environment (data from [Van Beers et al., 1998]). The results suggest that the precision in virtual reality are aligned with those in a real environment [Snijders et al., 2007, Van Beers et al., 1998]: proprioception is more precise with respect to depth (Figure 6.8-left) and vision is more precise with respect to azimuthal direction (Figure 6.8-center).

The Figure 6.8-right also suggests that users are more precise in a real environment than a virtual one. We observed indeed on Figure 6.8-left a large depth variance of the conditions involving vision ($R_H - V$ and $L_H - V$) which is not compensated for by the small azimuthal variances (Figure 6.8-center).

Accuracy

We observe that participants tend to overreach targets in depth especially for the conditions involving vision. There is also a lateral overreach: for the condition visual pointing with the right hand ($R_H - V$), the pointing is shifted to the left, while for the condition pointing with the left hand ($L_H - V$), it is shifted to the right. Finally, for the condition with proprioceptive target ($R_H - P$), we observe a rightward overshoot.

The data on accuracy were analyzed only qualitatively in the original article [Van Beers et al., 1998]. Therefore, we cannot make quantitative comparisons. Qualitatively, our results on accuracy in virtual reality mirror those observed in a real environment, particularly for depth overreach [Foley and Held, 1972, de Graaf et al., 1995] and lateral overreach [Crowe et al., 1987, Van Beers et al., 1998] in a task with vision. Similarly, lateral overreach for a proprioceptive task corroborates the results obtained in a real-world environment [Slinger and Horsley, 1906, Van Beers et al., 1998].

6.6.2 Unimodal Data

The Figure 6.9 illustrates the unimodal precision and accuracy for the classical analysis method. The Figure 6.10 does the same for the Bayesian Analysis. Regardless the method of analysis, we observe less precision in the depth direction for the visual modality, and in the azimuthal direction for the proprioceptive modalities. Note that the depth and azimuthal directions depend on the modality, the reference point being the middle of the eyes projected on the plane of interest for the visual

modality and the positions of the shoulders projected on the plane of interest for the proprioceptive modalities (left and right). With this convention, the shapes of the ellipses are relatively stable whatever the target, especially for the right proprioceptive modality.

Regardless the method, the areas of the ellipses are close when moving from one modality to the other, this result is different from the literature [Van Beers et al., 1998], where the visual modality has a better precision than the proprioceptive modality at least in terms of the area of the confidence ellipses. This result is discussed in the next section. We observe that one of the ellipses of the right proprioceptive modality is atrophied (see the rightmost ellipse of the central graph of the Figure 6.9). This is due to the analysis method involving subtraction and resulting in negative or almost zero variances. This impossible result is due to the imprecision of the measurement of bimodal distributions. The Bayesian Analysis avoids these negative variances. The unimodal distributions obtained with the Bayesian Analysis have smaller areas than with the classical method. The shapes and direction of the ellipses are similar in both cases.

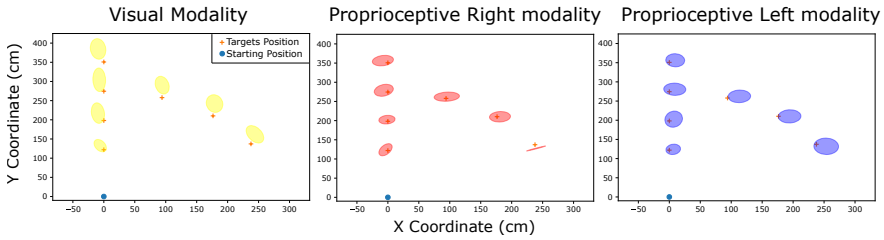

Figure 6.9: Classical Analysis [Van Beers et al., 1998] summed up on all participants

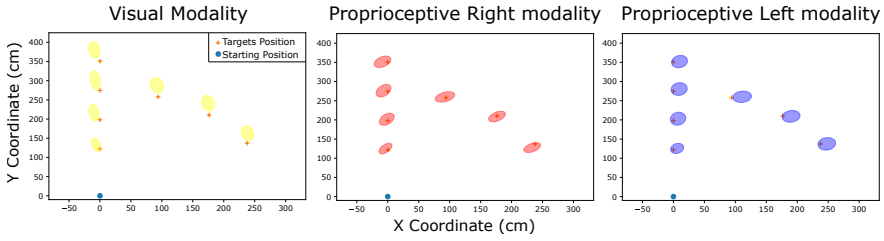

Figure 6.10: ABC treatment summed on all participants

Detailed Study of the Precision Parameters

The averaged azimuthal and depth variances and covariances by modality are shown in Figure 6.11. We can see that the azimuthal variance is more than 2 times larger on average for right proprioception and almost 2 times larger for left proprioception than the depth variance. On the other hand, the visual variance is a little lower in the azimuthal direction than in the depth direction. Above all, we obtain azimuthal

and depth variances for the visual modality that are much larger than the results of Van Beers et al. These observations are verified for both methods of analysis.

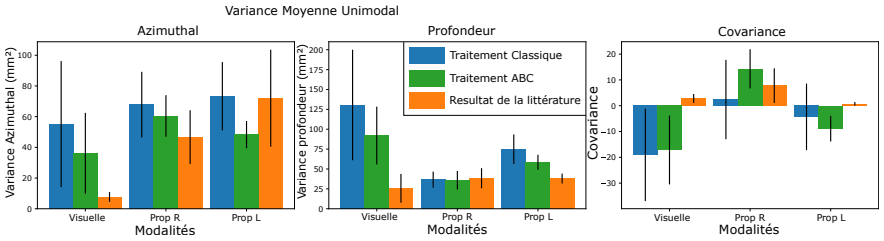

Figure 6.11: Comparison of the unimodal distributions of the two analysis methods and the literature. left and center : display of the average variances over the participants and all the targets for each modalities (azimuthal variances on the left and depth variances on the right). right : display of the average covariance over the participants and all the targets for each modalities

Evolution of Precision with Distance and Orientation

Interpreting the evolution of unimodal precision as a function of target position is difficult by looking only at the confidence ellipses in figures Figure 6.9 and Figure 6.10. We therefore display on Figure 6.12 the evolution of the mean of the areas of the confidence ellipses (and their standard deviation) as a function of the distance to the reference point of each modality (the depth r) for the two analysis methods. We note that for both analysis methods and for all modalities the areas increase with depth. Even if the classical treatment method presents important area variations, the large standard deviations prevent a clear reading of the results. This is why in the rest of this section we only present the curves obtained with the Bayesian Analysis.

On the Figure 6.13 we observe the azimuthal and depth variances as a function of r for the Bayesian analysis. We explain by these graphs the evolution of the areas of the Figure 6.12. We notice that the azimuthal variances of the proprioceptive modalities are increasing with r in contrast to their more stable depth variances. On the contrary, the visual modality is more stable in azimuth and varies strongly in depth. Thus it seems that the precision are stable in their most precise direction (depth for vision and azimuth for proprioception).

We study on the Figure 6.14 the evolution of the variances and the area of the confidence ellipses as a function of the orientation θ of the target with respect to the reference axis of each modality (perpendicular to the thorax and centered: at the middle of the body for vision, 200mm to the right or to the left for the respective proprioceptions). The azimuthal variances are increasing with θ and the depth variances are decreasing. This explains the relative stability of the area with respect to θ. Note that it is the visual modality that seems to be the most sensitive to θ.

Exploiting these evolutions can help create from little data the precision of a

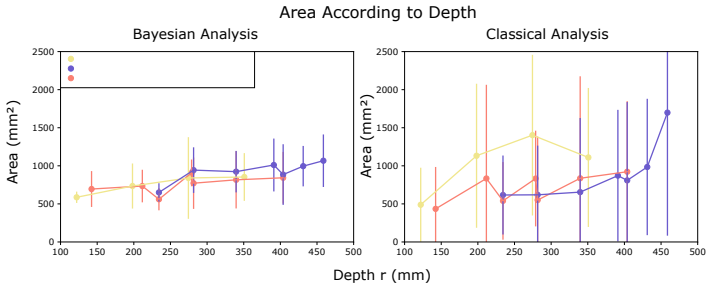

Figure 6.12: Evolution of areas according to distance for the two methods of analysis for the 3 modalities

modality and a prediction of how it will be impacted by a shift in space.

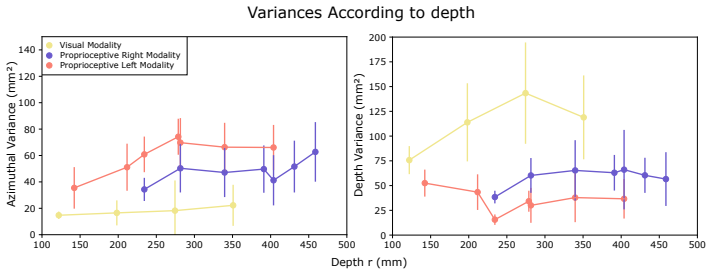

Figure 6.13: Evolution of azimuthal and depth variances for the 3 modalities according to depth r for the Bayesian analysis.

6.6.3 *Individual Level*

We have illustrated on the Figure 6.15 the mean of the confidence ellipses for each participant for the 3 modalities, and for the two treatment methods. For each participant it is reassuring to find a similar behavior for the two treatment methods. For example, if a participant has larger areas than his neighbors in the classical treatment, it is the same for the Bayesian Analysis. But the areas in the classical treatment are not a simple proportional increase of the areas in the Bayesian Analysis. Indeed, we do not observe the same ratios between the 3 modalities for the same participant for both methods. This is perhaps due to the moderating aspect of the prior law of the Bayesian Analysis. We thus observe that the inter- and intra-participant variations are more marked for the classical method with also a significant standard deviation for most of the participants and the modalities. For the Bayesian Analysis the differences between participants are smaller but the small

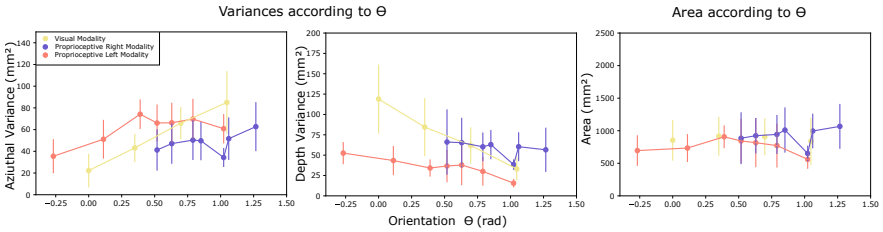

Figure 6.14: Evolution of areas and variances according to orientation for the 3 modalities for the Bayesian Analysis

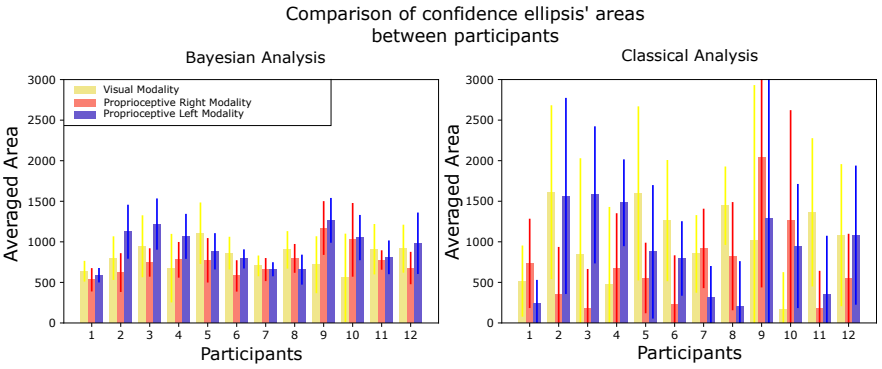

Figure 6.15: Comparison of areas of mean confidence ellipses between participants for each modality.

standard deviations make any difference more significant.

6.7 *Limitations*

Our results on visual sensory sensibilities in VR are sensibly different from the ones in the real world. One hypothesis is that the visual sensibilities will depend on the quality of visual feedback. Despite the good quality of current visual VR interfaces (HMD), the resulting VR vision is not yet similar to real-world vision. This poor visual feedback can thus explain the "bad" visual sensibilities in VR.

The experimental apparatus can also explain this result. Indeed in condition $R_H - P$, tactile information coming from the deformation of the experimental table can help participants increase their precision.

Another possibility is that participants in condition $R_H - P$ remember the position of the visual target. The addition of lures after the disappearance of the visual target may not be sufficient to forget the position of this target. In this case, the distribution (PFI) in the $R_H - P$ condition would be smaller than it should be, favoring the proprioceptive sensibilities against the visual sensibility.

6.8 *Conclusion*

The objective of this chapter was to measure users' sensory sensibilities. Our first contribution is methodological. First, we transposed an experimental protocol from cognitive psychology to HCI to capture the accuracy of visual and proprioceptive modalities. Moreover, we proposed a new Bayesian analysis method of our empirical data. We have demonstrated three advantages of this method compared to the Van Beers method [Van Beers et al., 1998]. First, it avoids outliers such as negative variances or atrophied precision. Secondly, it reduces the uncertainty

on our data, allowing us to better interpret the evolution of sensibilities in space. Finally, it allows us to estimate precision not only at the population level but also at the individual level.

Our second contribution is empirical. We collected and analyzed data from 12 participants to better understand their behavior in virtual reality. Our main results are 1) in line with known results for a real environment, the visual modality is more precise in the azimuthal direction, and the proprioceptive modality is more precise in depth; 2) visual and proprioceptive precisions obtained in VR is of the same order of magnitude contrary to results in the literature in a real environment; 3) it is possible to classify the participants according to their proprioceptive and visual sensibilities. This classification is independent of the analysis method.

These data can be used to address our research questions RQ4 and RQ6, i.e., how to predict the detection of illusion at the individual level. They are also interesting to investigate the link between these sensibilities and the users behavior in chapter 4, i.e., the natural curvature of a user's hand trajectory. This link could provide an understanding of why the illusion is detected. We discuss the perspectives of this work in the next chapter.

7

Conclusion and Perspectives

Visuo-haptic illusions are a promising tool to improve haptic interactions in Virtual Reality (VR). However, these may negatively impact immersion if users notice their use.

In this dissertation, we consider measures, factors, and methods to study visuo-haptic illusion (see Figure 7.1). This threefold approach is used to address the questions of why and how users detect visuo-haptic illusions in VR. In chapter 2, we first reviewed the different interaction techniques for visuo-haptic illusions. We presented in chapter 3 criteria and mechanisms to better define the detection of illusion and compare those criteria and mechanisms to current measures of illusion detection. Then we studied the impact of three classes of factors on illusion detection. We used hand redirection illusion as a case study. In chapter 4, we presented an empirical model that predicts the impact of a task factor – the amplitude of redirection – on hand trajectory. We also highlighted the link between the curvature of the trajectory and the detection of the illusion. In chapter 5, we explored the design space of hand redirection. This exploration suggests that the redirection function (a system property) does not impact illusion detection. Finally,

in chapter 6, we highlighted the relevance of users' sensory sensibilities as inputs for computational models predicting the probability of detecting an illusion.

In this chapter, we summarize our contributions and discuss the part of our research questions we did not cover yet. We also present the perspectives open by our work.

7.1 Contributions to Our Research Questions

We subdivided our problem of investigating the detection of visuo-haptic illusions in VR into 6 research questions (see Figure 7.1). For each of these questions, our progress and perspectives are detailed.

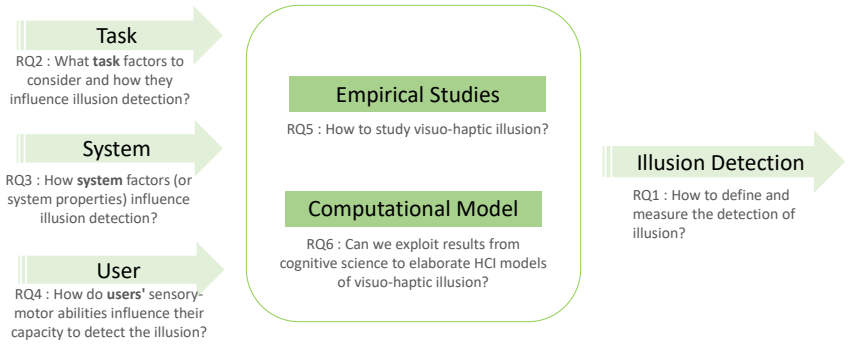

Figure 7.1: Summary of our approach and our 6 research questions.

7.1.1 RQ1: How to Define and Measure the Detection of Illusion?

Contribution

We addressed this question in chapter 3. We provided a better understanding of the term "illusion detection". We argued that the detection of C/D ratio-based illusions stems from a decrease in the Sense of Embodiment (**SoE**) and, in particular, a decrease in the Sense of Agency (**SoA**) or the Sense of Ownership (**SoO**). In particular, we identified mechanisms that could lead to the decrease of SoA and SoO. We presented subjective and objective methods to measure the level of Presence, SoE, SoA, and SoO. We compared them to existing protocols for visuo-haptic illusion detection thresholds estimation.

Perspective

The actual methods for estimating visuo-haptic illusion detection thresholds (**DT**) do not explain how the illusion is detected and what criteria of VR are impacted.

Therefore, we plan to propose new methods to measure DT and link them to a decrease in SoA or SoO.

Our most easily implementable idea is to exploit the phenomenon of *intentional bindings* (see subsubsection 3.3.1). As a reminder, it refers to the perceived contracted time between a voluntary action and the expected consequence of this action. It exists a compelling link between intentional bindings and SoA [Moore and Obhi, 2012]. Intentional Bindings could be exploited in a hand redirection experiments as an objective measures of SoA. It could have the advantage of comparing lower bound DT with DT related to a decrease in SoA.

The second promising idea is to use EEG and neurophysiological markers of SoA [Jeunet et al., 2018] and SoO [Casula et al., 2022]. The main advantage of this method is the capacity of detecting a real-time decrease in SoA or SoO. Indeed, it could be relevant to detect at which instant of the movement the detection of the illusion arise. Note that a recent study [Gehrke et al., 2019] successfully detects visuo-haptic conflicts in VR using EEG.

*7.1.2 RQ2: What **Task Factors** to Consider and How they Influence Illusion Detection?*

Contribution

In chapter 4, we studied the link between the task factor – amplitude of redirection – and the hand trajectory. First, we presented a model of hand trajectory under redirection. Thanks to this model, we highlighted a linear relationship between the shape of the trajectory and the amplitude of redirection. Moreover, we showed that the detection of illusion stems from a too-large trajectory curvature.

Perspectives

In future work, we plan to refine our model to investigate whether it significantly improves the prediction of the beginning and the end of the trajectory. The distance to the target is fixed in our task, and different distances should also be tested.

Moreover, we focused here on the task factor – amplitude of redirection – however, several other task factors should be considered. We plan, for example, to investigate the impact of a haptic confirmation at the end of the movement on the Detection Thresholds. The absence of haptic confirmation should decrease the SoA. On the other hand, a haptic confirmation can make users more willing to accept a disruption of their sensory-motor loop [Delahaye et al., 2022]

Furthermore, future work should also control the effect of the distance from the real hand to the body. For instance, we will consider a reverse movement where the hand's starting position is away from the body, and the target is close to the body. This task factor was not studied in the literature and could impact the detection of illusion. Indeed, users' visual and proprioceptive sensibilities change with the distance to the body. Therefore an important shift close to the body could be more easily detectable.

*7.1.3 RQ3: How **System** Factors or Properties Influence Illusion Detection?*

Contribution

In chapter 5, we introduced and studied the impact of one system factor – the redirection function. With this factor, we investigated the design space of hand redirection illusions. We generalized the redirection function by considering other redirection functions like 2^{nd} order polynomials. Our results suggest that the redirection function does not influence the Interval of Non-Detection. We also found that the redirection function offers more flexibility to designers to control the hand trajectory.

Perspectives

In future work, we plan to study possible interaction effects between movement speed and redirection function. Indeed, faster movements and potentially more contrasted redirection functions could make some phenomena more salient. Moreover, we showed that an effect of redirection functions on DT is present but not visible due to the lack of data points. Future work should consider a larger number of participants and/or a larger number of samples per participant. In addition, an objective measure of illusion detection (e.g., using EEG or intentional bindings) could highlight an effect not visible with the current subjective measure.

Other System factors should be considered, especially hardware factors. In chapter 6, we hypothesized that the quality of visual feedback can influence the confidence in the visual modality. Therefore, a change in hardware can impact Detection Thresholds.

*7.1.4 RQ4: How do **users'** sensory-motor abilities influence their capacity to detect the illusion?*

Contribution

In chapter 6, we motivate the relevance of studying users' visual and proprioceptive sensibilities to predict hand redirection DT. We proposed a method to measure these sensibilities in VR. We presented a new analysis method based on Bayesian inference. We noticed that visual sensibility is less important in VR than in the real world. We also described the evolution of the sensibilities in space.

In chapter 4, we identified that the natural curvature of a user-hand trajectory with no redirection can predict this user's hand trajectory with redirection. As we showed the link between the hand trajectory and illusion detection, we argued that the natural curvature of a user-hand trajectory can predict illusion detection.

Perspectives

Several other users' abilities could influence illusion detection. For example, we plan to study the impact of age, gender, experience with digital technology, and sports and artistic practices on detection illusion.

7.1.5 RQ5: How to study visuo-haptic illusion?

Contribution

In this thesis, we argue in favor of promoting methods and models to understand and predict illusion detection. We proposed to use hand trajectory to study hand redirection illusion. We proposed in chapter 4 an empirical model of hand redirection. We showed that hand trajectories provide a better understanding of how the illusion is detected. Moreover, in chapter 5, the observation of hand trajectory reveals the impact of the different redirection functions non-visible in DT. We have shown that studying illusion DT at the individual level is relevant. Identifying several users' abilities relevant to the study of illusion goes in this direction.

Perspectives

In future work, we will explore the model's generalization to other implementations of illusion. We also aim to explore if the study of trajectories is relevant for other visuo-haptic illusions and visuo-vestibular illusions, such as redirected walking.

We also want to study the impact of hand speed. Gonzalez et al. [2019] show

that a too-big amplitude of redirection significantly worsens the Minimum Jerk Model (**MJM**) fit. We plan to use the difference between the shape of hand velocity and the one predicted by the MJM to predict the detection of illusion.

7.1.6 RQ6: Can we exploit results from cognitive science to elaborate HCI models of visuo-haptic illusion?

Contribution

In chapter 3, we presented several mechanisms that could decrease SoA and SoO. We described in chapter 6 how computational models can explain the detection of illusion. We presented the Gaussian cue combination model to integrate visual and proprioceptive information. We also presented a Bayesian causal inference model to assign several sensory information to a common cause or different causes.

Perspectives

A short-term perspective is to use our participants' sensory sensibilities to predict the detection of illusion. We plan to exploit the Gaussian cue combination model to trace a hand trajectory representing the estimated hand position. We also plan to use a Bayesian causal inference model to predict the difference in DT between participants.

7.2 Common Perspectives to our 6 Research Questions

We wish to unify our findings using a hand trajectory predictive model. The interest of this model is threefold: 1) explain our empirical hand trajectory model, 2) explore the comparator model, 3) uncover a link between the natural curvature of a user hand trajectory and users' sensory sensibilities.

7.2.1 Predictive Model of Hand Trajectory

Recently Gonzalez et al. [2022] proposed a model for hand redirection by adapting a sensorimotor model for goal-directed reach from Hoff and Arbib [1993]. They propose a simplified sensorimotor control process, as illustrated in Figure 7.2. In their approach, an internal motion controller generates a control signal $u(t)$ which drives the user's movement dynamics and updates their true hand state $X = [p, v, a]^T$ with p being the position, v the velocity, and a the acceleration of the hand. This true state is then processed through the sensory system to yield an estimated state $\hat{X}$. In their approach, this estimated position of the hand is considered to be the

estimated visual state of the hand. The visual shift of the hand is incorporated as a sensory bias.

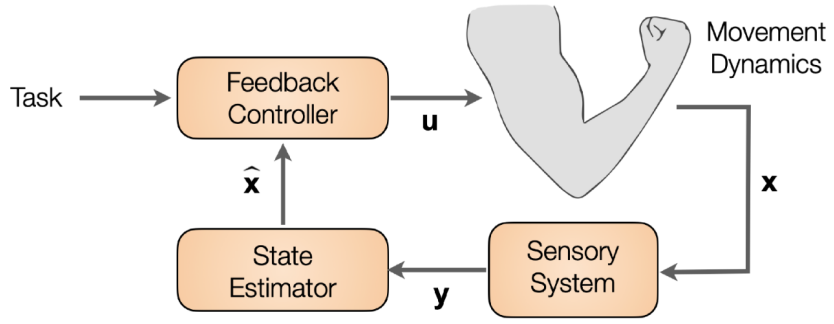

Figure 7.2: Overview of the sensorimotor control process considered by Gonzalez et al. [2022], where **u** is the motor command, **X** is the hand state, **y** is the sensory measurement, and $\hat{\mathbf{X}}$ is the estimated hand state.

Their model was effective in modeling hand trajectories with a small amplitude of redirection; however, they noticed an increase in the model error and its variance as the magnitude of redirection increases, indicating that there may still be features of redirected reaching not fully captured by their model. We plan to follow a slightly different approach by adapting a stochastic optimal feedback control model (**SOFC**) [Todorov, 2005]. The interesting aspect of SOFC is the consideration of noises in motor commands and sensory perceptions. We illustrate this other approach in Figure 7.3. Here, the estimated state is calculated based on the difference between a predicted state $X_{\text{predicted}}$ and a perceived state $X_{\text{perceived}}$. It is necessary to consider proprioceptive and visual information to evaluate the perceived state. This information is noisy and inconsistent because of the illusion implementation. Usually, proprioception is assumed to be noisier than vision.

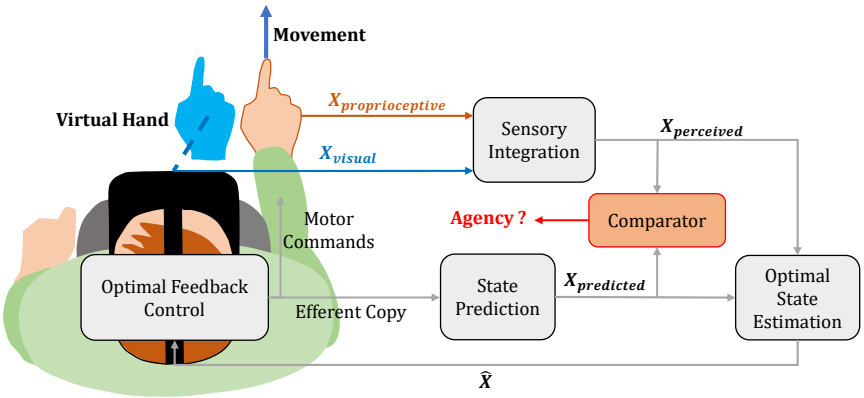

Figure 7.3: Overview of the sensorimotor control process that we plan to exploit. $X_{\text{proprioceptive}}$ and X_{visual} represent the state perceived by the visual and proprioceptive modality.

To implement the model, it's necessary to set a value for sensory noise. Usually, a significantly larger noise is assigned to proprioception compared to vision [Li

et al., 2018]. Thanks to the result of chapter 6, our originality is to be able to set relevant proprioceptive and visual noises for each participant. We hope to predict participants' hand trajectory under redirection with this model. We also want to verify our empirical trajectory model.

7.2.2 Computational Approach to Break in Agency

In Figure 7.3 we illustrate the comparator model. If $X_{\text{perceived}}$ is close to $X_{\text{predicted}}$, a strong SoA is elicited. If the difference is too important, a decrease in SoA could occur. With the planned approach, we could computationally evaluate the difference and predict a break in SoA for a specific user. The only required information would be users' visual and proprioceptive sensory sensibilities.

7.2.3 Link between Users abilities

In chapter 4, we showed that the natural curvature of a user hand trajectory with no redirection predicts hand trajectory with redirection. Moreover, we showed that the detection of illusion stems from a too-large trajectory curvature. We aim at explaining this result with the help of the SOFC. We hypothesize that with users' sensory sensibilities, we can predict the natural curvature of their hand trajectory.

7.3 Conclusion

In this thesis, we promote a new approach to study visuo-haptic illusions in VR. We believe that the use of visuo-haptic illusions is greatly beneficial to increase users' presence in VR easily. We argue that sensory-motor models are needed to understand and predict the detection of illusions at the individual level. These models are, in our opinion, important for the democratization of visuo-haptic illusions.

A

Bibliography

[1] Six flags. 2015. superman ride of steel vr.

[2] Parastoo Abtahi. From illusions to beyond-real interactions in virtual reality. In *The Adjunct Publication of the 34th Annual ACM Symposium on User Interface Software and Technology*, pages 153–157, 2021.

[3] Parastoo Abtahi and Sean Follmer. Visuo-haptic illusions for improving the perceived performance of shape displays. In *Proceedings of the 2018 CHI Conference on Human Factors in Computing Systems*, pages 1–13, 2018.

[4] Merwan Achibet, Maud Marchal, Ferran Argelaguet, and Anatole Lécuyer. The virtual mitten: A novel interaction paradigm for visuo-haptic manipulation of objects using grip force. In *2014 IEEE Symposium on 3D User Interfaces (3DUI)*, pages 59–66. IEEE, 2014.

[5] Merwan Achibet, Adrien Girard, Anthony Talvas, Maud Marchal, and Anatole Lécuyer. Elastic-arm: Human-scale passive haptic feedback for augmenting interaction and perception in virtual environments. In *2015 IEEE*

Virtual Reality (VR), pages 63–68. IEEE, 2015.

[6] Hironori Akiduki, Suetaka Nishiike, Hiroshi Watanabe, Katsunori Matsuoka, Takeshi Kubo, and Noriaki Takeda. Visual-vestibular conflict induced by virtual reality in humans. *Neuroscience letters*, 340(3):197–200, 2003.

[7] Bilal Alchalabi, Jocelyn Faubert, and David R Labbe. Eeg can be used to measure embodiment when controlling a walking self-avatar. In *2019 IEEE Conference on Virtual Reality and 3D User Interfaces (VR)*, pages 776–783. IEEE, 2019.

[8] Ferran Argelaguet, Ludovic Hoyet, Michaël Trico, and Anatole Lécuyer. The role of interaction in virtual embodiment: Effects of the virtual hand representation. In *2016 IEEE virtual reality (VR)*, pages 3–10. IEEE, 2016.

[9] Mahdi Azmandian, Mark Hancock, Hrvoje Benko, Eyal Ofek, and Andrew D Wilson. Haptic retargeting: Dynamic repurposing of passive haptics for enhanced virtual reality experiences. In *Proceedings of the 2016 chi conference on human factors in computing systems*, pages 1968–1979, 2016.

[10] Yuki Ban, Takashi Kajinami, Takuji Narumi, Tomohiro Tanikawa, and Michitaka Hirose. Modifying an identified curved surface shape using pseudo-haptic effect. In *2012 IEEE Haptics Symposium (HAPTICS)*, pages 211–216. IEEE, 2012.

[11] Yuki Ban, Takuji Narumi, Tomohiro Tanikawa, and Michitaka Hirose. Controlling perceived stiffness of pinched objects using visual feedback of hand deformation. In *2014 IEEE Haptics Symposium (HAPTICS)*, pages 557–562. IEEE, 2014.

[12] Peter W Battaglia, Robert A Jacobs, and Richard N Aslin. Bayesian integration of visual and auditory signals for spatial localization. *Josa a*, 20(7): 1391–1397, 2003.

[13] Brett Benda, Shaghayegh Esmaeili, and Eric D Ragan. Determining detection thresholds for fixed positional offsets for virtual hand remapping in virtual reality. In *2020 IEEE International Symposium on Mixed and Augmented Reality (ISMAR)*, pages 269–278. IEEE, 2020.

[14] Paul Bertelson, Jean Vroomen, Béatrice De Gelder, and Jon Driver. The ventriloquist effect does not depend on the direction of deliberate visual attention. *Perception & psychophysics*, 62(2):321–332, 2000.

[15] Frank Biocca. Inserting the presence of mind into a philosophy of presence:

A response to sheridan and mantovani and riva. *Presence*, 10(5):546–556, 2001.

[16] Sarah-J Blakemore, Daniel M Wolpert, and Chris D Frith. Central cancellation of self-produced tickle sensation. *Nature neuroscience*, 1(7):635–640, 1998.

[17] Olaf Blanke and Thomas Metzinger. Full-body illusions and minimal phenomenal selfhood. *Trends in cognitive sciences*, 13(1):7–13, 2009.

[18] Olaf Blanke and Christine Mohr. Out-of-body experience, heautoscopy, and autoscopic hallucination of neurological origin: Implications for neurocognitive mechanisms of corporeal awareness and self-consciousness. *Brain research reviews*, 50(1):184–199, 2005.

[19] Hannah J Block and Brandon M Sexton. Visuo-proprioceptive control of the hand in older adults. *bioRxiv*, 2020.

[20] L Bookstein Fred. Principal warps: Thin-plate spline and decomposition of deformations. *Transictions on pattern analysis and machine intelligence*, 11, 1992.

[21] Matthew Botvinick and Jonathan Cohen. Rubber hands 'feel'touch that eyes see. *Nature*, 391(6669):756–756, 1998.

[22] Elodie Bouzbib, Gilles Bailly, Sinan Haliyo, and Pascal Frey. Covr: A large-scale force-feedback robotic interface for non-deterministic scenarios in vr. *arXiv preprint arXiv:2009.07149*, 2020.

[23] Elodie Bouzbib, Gilles Bailly, Sinan Haliyo, and Pascal Frey. "can i touch this?": Survey of virtual reality interactions via haptic solutions: Revue de littérature des interactions en réalité virtuelle par le biais de solutions haptiques. In *32e Conférence Francophone sur l'Interaction Homme-Machine*, pages 1–16, 2021.

[24] Niclas Braun, Jeremy D Thorne, Helmut Hildebrandt, and Stefan Debener. Interplay of agency and ownership: the intentional binding and rubber hand illusion paradigm combined. *PloS one*, 9(11):e111967, 2014.

[25] Niclas Braun, Stefan Debener, Nadine Spychala, Edith Bongartz, Peter Sörös, Helge HO Müller, and Alexandra Philipsen. The senses of agency and ownership: a review. *Frontiers in psychology*, 9:535, 2018.

[26] Eric Burns, Sharif Razzaque, Abigail T Panter, Mary C Whitton, Matthew R

McCallus, and Frederick P Brooks Jr. The hand is more easily fooled than the eye: Users are more sensitive to visual interpenetration than to visual-proprioceptive discrepancy. *Presence: teleoperators & virtual environments*, 15(1):1–15, 2006.

[27] Richard Byrne, Joe Marshall, and Florian'Floyd' Mueller. Balance ninja: towards the design of digital vertigo games via galvanic vestibular stimulation. In *Proceedings of the 2016 Annual Symposium on Computer-Human Interaction in Play*, pages 159–170, 2016.

[28] Richard Byrne, Joe Marshall, and Florian Floyd Mueller. Ar fighter: Using hmds to create vertigo play experiences. In *Proceedings of the 2018 Annual Symposium on Computer-Human Interaction in Play*, pages 45–57, 2018.

[29] Géry Casiez, Daniel Vogel, Ravin Balakrishnan, and Andy Cockburn. The impact of control-display gain on user performance in pointing tasks. *Human–computer interaction*, 23(3):215–250, 2008.

[30] Elias Paolo Casula, Gaetano Tieri, Lorenzo Rocchi, Rachele Pezzetta, Michele Maiella, Enea Francesco Pavone, Salvatore Maria Aglioti, and Giacomo Koch. Feeling of ownership over an embodied avatar's hand brings about fast changes of fronto-parietal cortical dynamics. *Journal of Neuroscience*, 42(4):692–701, 2022.

[31] Michael J Cevette, Jan Stepanek, Daniela Cocco, Anna M Galea, Gaurav N Pradhan, Linsey S Wagner, Sarah R Oakley, Benn E Smith, David A Zapala, and Kenneth H Brookler. Oculo-vestibular recoupling using galvanic vestibular stimulation to mitigate simulator sickness. *Aviation, space, and environmental medicine*, 83(6):549–555, 2012.

[32] Lung-Pan Cheng, Eyal Ofek, Christian Holz, Hrvoje Benko, and Andrew D Wilson. Sparse haptic proxy: Touch feedback in virtual environments using a general passive prop. In *Proceedings of the 2017 CHI Conference on Human Factors in Computing Systems*, pages 3718–3728, 2017.

[33] Hans Colonius and Adele Diederich. Formal models and quantitative measures of multisensory integration: a selective overview. *European Journal of Neuroscience*, 51(5):1161–1178, 2020.

[34] Alan Crowe, Wim Keessen, Wim Kuus, Ronald Van Vliet, and Andre Zegeling. Proprioceptive accuracy in two dimensions. *Perceptual and motor skills*, 64(3):831–846, 1987.

[35] JB de Graaf, JFM van den Broek, H Bekkering, and AC Sittig. The visual estimation of the felt hand position is shifted towards the body midline. *Vision et adaptation*, pages 183–192, 1995.

[36] Frédérique De Vignemont. Embodiment, ownership and disownership. *Consciousness and cognition*, 20(1):82–93, 2011.

[37] Mathias Delahaye, Olaf Blanke, Ronan Boulic, and Bruno Herbelin. Avatar error in your favor: Embodied avatars can fix users' mistakes without them noticing. *bioRxiv*, 2022.

[38] Nandini Deshpande, Denise M Connelly, Elsie G Culham, and Patrick A Costigan. Reliability and validity of ankle proprioceptive measures. *Archives of physical medicine and rehabilitation*, 84(6):883–889, 2003.

[39] Huong Q Dinh, Neff Walker, Larry F Hodges, Chang Song, and Akira Kobayashi. Evaluating the importance of multi-sensory input on memory and the sense of presence in virtual environments. In *Proceedings IEEE Virtual Reality (Cat. No. 99CB36316)*, pages 222–228. IEEE, 1999.

[40] Lionel Dominjon, Anatole Lécuyer, J-M Burkhardt, Paul Richard, and Simon Richir. Influence of control/display ratio on the perception of mass of manipulated objects in virtual environments. In *IEEE Proceedings. VR 2005. Virtual Reality, 2005.*, pages 19–25. IEEE, 2005.

[41] Timothy Dummer, Alexandra Picot-Annand, Tristan Neal, and Chris Moore. Movement and the rubber hand illusion. *Perception*, 38(2):271–280, 2009.

[42] Marc O Ernst and Martin S Banks. Humans integrate visual and haptic information in a statistically optimal fashion. *Nature*, 415(6870):429–433, 2002.

[43] Marc O Ernst and Heinrich H Bülthoff. Merging the senses into a robust percept. *Trends in cognitive sciences*, 8(4):162–169, 2004.

[44] Julian J Faraway, Matthew P Reed, and Jing Wang. Modelling three-dimensional trajectories by using bézier curves with application to hand motion. *Journal of the Royal Statistical Society: Series C (Applied Statistics)*, 56(5):571–585, 2007.

[45] Christopher R Fetsch, Gregory C DeAngelis, and Dora E Angelaki. Visual–vestibular cue integration for heading perception: applications of optimal cue integration theory. *European Journal of Neuroscience*, 31(10):1721–1729, 2010.

[46] John M Flach and John G Holden. The reality of experience: Gibson's way. *Presence*, 7(1):90–95, 1998.

[47] Tamar Flash and Neville Hogan. The coordination of arm movements: an experimentally confirmed mathematical model. *Journal of neuroscience*, 5 (7):1688–1703, 1985.

[48] Alessia Folegatti, Frédérique De Vignemont, Francesco Pavani, Yves Rossetti, and Alessandro Farnè. Losing one's hand: visual-proprioceptive conflict affects touch perception. *PLoS One*, 4(9):e6920, 2009.

[49] John M Foley and Richard Held. Visually directed pointing as a function of target distance, direction, and available cues. *Perception & Psychophysics*, 12(3):263–268, 1972.

[50] Christopher D Frith. The positive and negative symptoms of schizophrenia reflect impairments in the perception and initiation of action. *Psychological medicine*, 17(3):631–648, 1987.

[51] Christopher D Frith, Sarah-Jayne Blakemore, and Daniel M Wolpert. Abnormalities in the awareness and control of action. *Philosophical Transactions of the Royal Society of London. Series B: Biological Sciences*, 355(1404): 1771–1788, 2000.

[52] Christopher Donald Frith. *The Cognitive Neuropsychology of Schizophrenia: Classic Edition*. Psychology press, 2015.

[53] Shaun Gallagher. Philosophical conceptions of the self: implications for cognitive science. *Trends in cognitive sciences*, 4(1):14–21, 2000.

[54] Lukas Gehrke, Sezen Akman, Pedro Lopes, Albert Chen, Avinash Kumar Singh, Hsiang-Ting Chen, Chin-Teng Lin, and Klaus Gramann. Detecting visuo-haptic mismatches in virtual reality using the prediction error negativity of event-related brain potentials. In *Proceedings of the 2019 CHI Conference on Human Factors in Computing Systems*, pages 1–11, 2019.

[55] Benoît Geslain, Gilles Bailly, Sinan D Haliyo, and Corentin Duboc. Visuo-haptic illusions for motor skill acquisition in virtual reality. In *Symposium on Spatial User Interaction*, pages 1–9, 2021.

[56] James J Gibson. *The ecological approach to visual perception: classic edition*. Psychology press, 2014.

[57] Eric J Gonzalez and Sean Follmer. Investigating the detection of bimanual

haptic retargeting in virtual reality. In *25th ACM Symposium on Virtual Reality Software and Technology*, pages 1–5, 2019.

[58] Eric J Gonzalez, Parastoo Abtahi, and Sean Follmer. Evaluating the minimum jerk motion model for redirected reach in virtual reality. In *The Adjunct Publication of the 32nd Annual ACM Symposium on User Interface Software and Technology*, pages 4–6, 2019.

[59] Eric J Gonzalez, Parastoo Abtahi, and Sean Follmer. Reach+ extending the reachability of encountered-type haptics devices through dynamic redirection in vr. In *Proceedings of the 33rd Annual ACM Symposium on User Interface Software and Technology*, pages 236–248, 2020.

[60] Eric J Gonzalez, Elyse DZ Chase, Pramod Kotipalli, and Sean Follmer. A model predictive control approach for reach redirection in virtual reality. In *CHI Conference on Human Factors in Computing Systems*, pages 1–15, 2022.

[61] Mar Gonzalez-Franco and Jaron Lanier. Model of illusions and virtual reality. *Frontiers in psychology*, 8:1125, 2017.

[62] Mar Gonzalez-Franco and Tabitha C Peck. Avatar embodiment. towards a standardized questionnaire. *Frontiers in Robotics and AI*, 5:74, 2018.

[63] Timofey Grechkin, Jerald Thomas, Mahdi Azmandian, Mark Bolas, and Evan Suma. Revisiting detection thresholds for redirected walking: Combining translation and curvature gains. In *Proceedings of the ACM Symposium on Applied Perception*, pages 113–120, 2016.

[64] Thor Grünbaum and Mark Schram Christensen. Measures of agency. *Neuroscience of consciousness*, 2020(1):niaa019, 2020.

[65] Antal Haans, Wijnand A IJsselsteijn, and Yvonne AW de Kort. The effect of similarities in skin texture and hand shape on perceived ownership of a fake limb. *Body Image*, 5(4):389–394, 2008.

[66] Patrick Haggard. Conscious intention and motor cognition. *Trends in cognitive sciences*, 9(6):290–295, 2005.

[67] Patrick Haggard. Sense of agency in the human brain. *Nature Reviews Neuroscience*, 18(4):196–207, 2017.

[68] Patrick Haggard and Valerian Chambon. Sense of agency. *Current biology*, 22(10):R390–R392, 2012.

[69] Patrick Haggard, Sam Clark, and Jeri Kalogeras. Voluntary action and conscious awareness. *Nature neuroscience*, 5(4):382–385, 2002.

[70] Kelly S Hale and Kay M Stanney. *Handbook of virtual environments: Design, implementation, and applications*. CRC Press, 2014.

[71] Dustin T Han, Mohamed Suhail, and Eric D Ragan. Evaluating remapped physical reach for hand interactions with passive haptics in virtual reality. *IEEE transactions on visualization and computer graphics*, 24(4):1467–1476, 2018.

[72] Haption. Virtuose™ 6D - HAPTION SA, 2019. URL https://www.haption.com/en/products-en/virtuose-6d-en.html.

[73] Hannah B Helbig and Marc O Ernst. Optimal integration of shape information from vision and touch. *Experimental brain research*, 179(4):595–606, 2007.

[74] Denise YP Henriques, Filipp Filippopulos, Andreas Straube, and Thomas Eggert. The cerebellum is not necessary for visually driven recalibration of hand proprioception. *Neuropsychologia*, 64:195–204, 2014.

[75] Bruce Hoff and Michael A Arbib. Models of trajectory formation and temporal interaction of reach and grasp. *Journal of motor behavior*, 25(3): 175–192, 1993.

[76] Ludovic Hoyet, Ferran Argelaguet, Corentin Nicole, and Anatole Lécuyer. "wow! i have six fingers!": Would you accept structural changes of your hand in vr? *Frontiers in Robotics and AI*, 3:27, 2016.

[77] Wijnand A IJsselsteijn, Huib De Ridder, Jonathan Freeman, and Steve E Avons. Presence: concept, determinants, and measurement. In *Human vision and electronic imaging V*, volume 3959, pages 520–529. SPIE, 2000.

[78] Brent Edward Insko. *Passive haptics significantly enhances virtual environments*. The University of North Carolina at Chapel Hill, 2001.

[79] Camille Jeunet, Louis Albert, Ferran Argelaguet, and Anatole Lécuyer. "do you feel in control?": towards novel approaches to characterise, manipulate and measure the sense of agency in virtual environments. *IEEE transactions on visualization and computer graphics*, 24(4):1486–1495, 2018.

[80] Andreas Kalckert and H Henrik Ehrsson. Moving a rubber hand that feels like your own: a dissociation of ownership and agency. *Frontiers in human*

neuroscience, 6:40, 2012.

[81] Andreas Kalckert and H Henrik Ehrsson. The spatial distance rule in the moving and classical rubber hand illusions. *Consciousness and cognition*, 30:118–132, 2014.

[82] Antti Kangasrääsiö, Kumaripaba Athukorala, Andrew Howes, Jukka Corander, Samuel Kaski, and Antti Oulasvirta. Inferring cognitive models from data using approximate bayesian computation. In *Proceedings of the 2017 CHI conference on human factors in computing systems*, pages 1295–1306, 2017.

[83] Shunichi Kasahara, Keina Konno, Richi Owaki, Tsubasa Nishi, Akiko Takeshita, Takayuki Ito, Shoko Kasuga, and Junichi Ushiba. Malleable embodiment: changing sense of embodiment by spatial-temporal deformation of virtual human body. In *Proceedings of the 2017 CHI Conference on Human Factors in Computing Systems*, pages 6438–6448, 2017.

[84] Konstantina Kilteni, Raphaela Groten, and Mel Slater. The sense of embodiment in virtual reality. *Presence: Teleoperators and Virtual Environments*, 21(4):373–387, 2012.

[85] Konstantina Kilteni, Jean-Marie Normand, Maria V Sanchez-Vives, and Mel Slater. Extending body space in immersive virtual reality: a very long arm illusion. *PloS one*, 7(7):e40867, 2012.

[86] Konstantina Kilteni, Antonella Maselli, Konrad P Kording, and Mel Slater. Over my fake body: body ownership illusions for studying the multisensory basis of own-body perception. *Frontiers in human neuroscience*, 9:141, 2015.

[87] Luv Kohli, Mary C Whitton, and Frederick P Brooks. Redirected touching: The effect of warping space on task performance. In *2012 IEEE Symposium on 3D User Interfaces (3DUI)*, pages 105–112. IEEE, 2012.

[88] Elena Kokkinara and Mel Slater. Measuring the effects through time of the influence of visuomotor and visuotactile synchronous stimulation on a virtual body ownership illusion. *Perception*, 43(1):43–58, 2014.

[89] Elena Kokkinara, Konstantina Kilteni, Kristopher J Blom, and Mel Slater. First person perspective of seated participants over a walking virtual body leads to illusory agency over the walking. *Scientific reports*, 6(1):1–11, 2016.

[90] Konrad P Körding, Ulrik Beierholm, Wei Ji Ma, Steven Quartz, Joshua B

Tenenbaum, and Ladan Shams. Causal inference in multisensory perception. *PLoS one*, 2(9):e943, 2007.

[91] Ashok Kumar, Ravali Gourishetti, and M Manivannan. Mechanics of pseudo-haptics with computer mouse. In *2017 IEEE International Symposium on Haptic, Audio and Visual Environments and Games (HAVE)*, pages 1–6. IEEE, 2017.

[92] J Laarni, N Ravaja, and T Saari. Using eye tracking and psychophysiological methods to study spatial presence. In *Annual International Workshop on Presence, USA, 2003*, 2003.

[93] Robert H LaMotte. Softness discrimination with a tool. *Journal of neurophysiology*, 83(4):1777–1786, 2000.

[94] Anatole Lécuyer. Simulating haptic feedback using vision: A survey of research and applications of pseudo-haptic feedback. *Presence: Teleoperators and Virtual Environments*, 18(1):39–53, 2009.

[95] Anatole Lécuyer, Sabine Coquillart, Abderrahmane Kheddar, Paul Richard, and Philippe Coiffet. Pseudo-haptic feedback: can isometric input devices simulate force feedback? In *Proceedings IEEE Virtual Reality 2000 (Cat. No. 00CB37048)*, pages 83–90. IEEE, 2000.

[96] Anatole Lécuyer, J-M Burkhardt, Sabine Coquillart, and Philippe Coiffet. " boundary of illusion": an experiment of sensory integration with a pseudo-haptic system. In *Proceedings IEEE Virtual Reality 2001*, pages 115–122. IEEE, 2001.

[97] Anatole Lécuyer, Jean-Marie Burkhardt, and Chee-Hian Tan. A study of the modification of the speed and size of the cursor for simulating pseudo-haptic bumps and holes. *ACM Transactions on Applied Perception (TAP)*, 5(3): 1–21, 2008.

[98] Yongseok Lee, Inyoung Jang, and Dongjun Lee. Enlarging just noticeable differences of visual-proprioceptive conflict in vr using haptic feedback. In *2015 IEEE World Haptics Conference (WHC)*, pages 19–24. IEEE, 2015.

[99] Zhe Li, Pietro Mazzoni, Sen Song, and Ning Qian. A single, continuously applied control policy for modeling reaching movements with and without perturbation. *Neural Computation*, 30(2):397–427, 2018.

[100] Hannah Limerick, David Coyle, and James W Moore. The experience of agency in human-computer interactions: a review. *Frontiers in human*

neuroscience, 8:643, 2014.

[101] Jarno Lintusaari, Henri Vuollekoski, Antti Kangasrääsiö, Kusti Skytén, Marko Järvenpää, Pekka Marttinen, Michael U. Gutmann, Aki Vehtari, Jukka Corander, and Samuel Kaski. Elfi: Engine for likelihood-free inference. *Journal of Machine Learning Research*, 19(16):1–7, 2018. URL http://jmlr.org/papers/v19/17-374.html.

[102] Marilia Lira, Julia H Egito, Patricia A Dall'Agnol, David M Amodio, Óscar F Gonçalves, and Paulo S Boggio. The influence of skin colour on the experience of ownership in the rubber hand illusion. *Scientific reports*, 7(1): 1–13, 2017.

[103] Donna M Lloyd. Spatial limits on referred touch to an alien limb may reflect boundaries of visuo-tactile peripersonal space surrounding the hand. *Brain and cognition*, 64(1):104–109, 2007.

[104] Matthew Lombard and Theresa Ditton. At the heart of it all: The concept of presence. *Journal of computer-mediated communication*, 3(2):JCMC321, 1997.

[105] Paul R MacNeilage, Martin S Banks, Daniel R Berger, and Heinrich H Bülthoff. A bayesian model of the disambiguation of gravitoinertial force by visual cues. *Experimental Brain Research*, 179(2):263–290, 2007.

[106] Joe Marshall, Steve Benford, Richard Byrne, and Paul Tennent. Sensory alignment in immersive entertainment. In *Proceedings of the 2019 CHI Conference on Human Factors in Computing Systems*, pages 1–13, 2019.

[107] Antonella Maselli and Mel Slater. The building blocks of the full body ownership illusion. *Frontiers in human neuroscience*, 7:83, 2013.

[108] Thomas H Massie, J Kenneth Salisbury, et al. The phantom haptic interface: A device for probing virtual objects. In *Proceedings of the ASME winter annual meeting, symposium on haptic interfaces for virtual environment and teleoperator systems*, volume 55, pages 295–300. Chicago, IL, 1994.

[109] Kazumichi Matsumiya. Separate multisensory integration processes for ownership and localization of body parts. *Scientific reports*, 9(1):1–9, 2019.

[110] Keigo Matsumoto, Takuji Narumi, Tomohiro Tanikawa, and Michitaka Hirose. Walking uphill and downhill: redirected walking in the vertical direction. In *ACM SIGGRAPH 2017 Posters*, pages 1–2. 2017.

[111] Harry McGurk and John MacDonald. Hearing lips and seeing voices. *Nature*, 264(5588):746–748, 1976.

[112] Michael Meehan, Brent Insko, Mary Whitton, and Frederick P Brooks Jr. Physiological measures of presence in stressful virtual environments. *Acm transactions on graphics (tog)*, 21(3):645–652, 2002.

[113] Miguel Melo, Guilherme Gonçalves, Pedro Monteiro, Hugo Coelho, José Vasconcelos-Raposo, and Maximino Bessa. Do multisensory stimuli benefit the virtual reality experience? a systematic review. *IEEE Transactions on Visualization and Computer Graphics*, 2020.

[114] M Alex Meredith. On the neuronal basis for multisensory convergence: a brief overview. *Cognitive brain research*, 14(1):31–40, 2002.

[115] R Chris Miall and Daniel M Wolpert. Forward models for physiological motor control. *Neural networks*, 9(8):1265–1279, 1996.

[116] Marvin Minsky. Telepresence. 1980.

[117] James W Moore and Sukhvinder S Obhi. Intentional binding and the sense of agency: a review. *Consciousness and cognition*, 21(1):546–561, 2012.

[118] Gil Morrot, Frédéric Brochet, and Denis Dubourdieu. The color of odors. *Brain and language*, 79(2):309–320, 2001.

[119] Fatta B Nahab, Prantik Kundu, Cecile Gallea, John Kakareka, Randy Pursley, Tom Pohida, Nathaniel Miletta, Jason Friedman, and Mark Hallett. The neural processes underlying self-agency. *Cerebral cortex*, 21(1):48–55, 2011.

[120] Niels Christian Nilsson, André Zenner, and Adalberto L Simeone. Propping up virtual reality with haptic proxies. *IEEE Computer Graphics and Applications*, 41(5):104–112, 2021.

[121] Nami Ogawa, Takuji Narumi, and Michitaka Hirose. Effect of avatar appearance on detection thresholds for remapped hand movements. *IEEE transactions on visualization and computer graphics*, 27(7):3182–3197, 2020.

[122] Gonçalo Padrao, Mar Gonzalez-Franco, Maria V Sanchez-Vives, Mel Slater, and Antoni Rodriguez-Fornells. Violating body movement semantics: Neural signatures of self-generated and external-generated errors. *Neuroimage*, 124: 147–156, 2016.

[123] Alexis Paljic, J-M Burkhardtt, and Sabine Coquillart. Evaluation of pseudo-haptic feedback for simulating torque: a comparison between isometric and elastic input devices. In *12th International Symposium on Haptic Interfaces for Virtual Environment and Teleoperator Systems, 2004. HAPTICS'04. Proceedings.*, pages 216–223. IEEE, 2004.

[124] Francesco Pavani, Charles Spence, and Jon Driver. Visual capture of touch: Out-of-the-body experiences with rubber gloves. *Psychological science*, 11 (5):353–359, 2000.

[125] Jérôme Perret and Emmanuel Vander Poorten. Touching virtual reality: a review of haptic gloves. In *ACTUATOR 2018; 16th International Conference on New Actuators*, pages 1–5. VDE, 2018.

[126] Sonia Ponzo, Louise P Kirsch, Aikaterini Fotopoulou, and Paul M Jenkinson. Balancing body ownership: Visual capture of proprioception and affectivity during vestibular stimulation. *Neuropsychologia*, 117:311–321, 2018.

[127] Catherine Preston. The role of distance from the body and distance from the real hand in ownership and disownership during the rubber hand illusion. *Acta psychologica*, 142(2):177–183, 2013.

[128] Parinya Punpongsanon, Daisuke Iwai, and Kosuke Sato. Softar: Visually manipulating haptic softness perception in spatial augmented reality. *IEEE transactions on visualization and computer graphics*, 21(11):1279–1288, 2015.

[129] Adrian E Raftery. Bayesian model selection in social research. *Sociological methodology*, pages 111–163, 1995.

[130] Niklas Ravaja, Timo Saari, Marko Turpeinen, Jari Laarni, Mikko Salminen, and Matias Kivikangas. Spatial presence and emotions during video game playing: Does it matter with whom you play? *Presence: Teleoperators and virtual environments*, 15(4):381–392, 2006.

[131] Sharif Razzaque. *Redirected walking*. The University of North Carolina at Chapel Hill, 2005.

[132] Lisa Rebenitsch and Charles Owen. Review on cybersickness in applications and visual displays. *Virtual Reality*, 20(2):101–125, 2016.

[133] Johanna Reuschel, Knut Drewing, Denise YP Henriques, Frank Rösler, and Katja Fiehler. Optimal integration of visual and proprioceptive movement information for the perception of trajectory geometry. *Experimental brain*

research, 201(4):853–862, 2010.

[134] Bernhard E Riecke, Aleksander Väljamäe, and Jörg Schulte-Pelkum. Moving sounds enhance the visually-induced self-motion illusion (circular vection) in virtual reality. *ACM Transactions on Applied Perception (TAP)*, 6(2):1–27, 2009.

[135] Michael Rietzler, Florian Geiselhart, Jan Gugenheimer, and Enrico Rukzio. Breaking the tracking: Enabling weight perception using perceivable tracking offsets. In *Proceedings of the 2018 CHI Conference on Human Factors in Computing Systems*, pages 1–12, 2018.

[136] Giuseppe Riva, Fabrizio Davide, and Wijnand A IJsselsteijn. *Being there: Concepts, effects and measurements of user presence in synthetic environments.* Ios Press, 2003.

[137] Irvin Rock and Jack Victor. Vision and touch: An experimentally created conflict between the two senses. *Science*, 143(3606):594–596, 1964.

[138] Hiroaki Sakoe and Seibi Chiba. Dynamic programming algorithm optimization for spoken word recognition. *IEEE transactions on acoustics, speech, and signal processing*, 26(1):43–49, 1978.

[139] Majed Samad, Albert Jin Chung, and Ladan Shams. Perception of body ownership is driven by bayesian sensory inference. *PloS one*, 10(2):e0117178, 2015.

[140] Majed Samad, Elia Gatti, Anne Hermes, Hrvoje Benko, and Cesare Parise. Pseudo-haptic weight: Changing the perceived weight of virtual objects by manipulating control-display ratio. In *Proceedings of the 2019 CHI Conference on Human Factors in Computing Systems*, pages 1–13, 2019.

[141] Maria V Sanchez-Vives and Mel Slater. From presence to consciousness through virtual reality. *Nature Reviews Neuroscience*, 6(4):332–339, 2005.

[142] Maria V Sanchez-Vives, Bernhard Spanlang, Antonio Frisoli, Massimo Bergamasco, and Mel Slater. Virtual hand illusion induced by visuomotor correlations. *PloS one*, 5(4):e10381, 2010.

[143] Ferran Argelaguet Sanz, David Antonio Gómez Jáuregui, Maud Marchal, and Anatole Lécuyer. Elastic images: Perceiving local elasticity of images through a novel pseudo-haptic deformation effect. *ACM Transactions on Applied Perception*, 10(3):17–1, 2013.

[144] Moritz Schubert and Dominik Endres. The bayesian causal inference of body ownership model: Use in vr and plausible parameter choices. In *2021 IEEE Conference on Virtual Reality and 3D User Interfaces Abstracts and Workshops (VRW)*, pages 67–70. IEEE, 2021.

[145] Thomas W Schubert. A new conception of spatial presence: Once again, with feeling. *Communication Theory*, 19(2):161–187, 2009.

[146] Sofia Seinfeld, Tiare Feuchtner, Antonella Maselli, and Jörg Müller. User representations in human-computer interaction. *Human–Computer Interaction*, 36(5-6):400–438, 2021.

[147] Ladan Shams, Yukiyasu Kamitani, and Shinsuke Shimojo. Visual illusion induced by sound. *Cognitive brain research*, 14(1):147–152, 2002.

[148] Thome Shipley. Auditory flutter-driving of visual flicker. *Science*, 145(3638): 1328–1330, 1964.

[149] Richard Skarbez, Frederick P Brooks, Jr, and Mary C Whitton. A survey of presence and related concepts. *ACM Computing Surveys (CSUR)*, 50(6): 1–39, 2017.

[150] Mel Slater. A note on presence terminology. *Presence connect*, 3(3):1–5, 2003.

[151] Mel Slater. How colorful was your day? why questionnaires cannot assess presence in virtual environments. *Presence*, 13(4):484–493, 2004.

[152] Mel Slater. Place illusion and plausibility can lead to realistic behaviour in immersive virtual environments. *Philosophical Transactions of the Royal Society B: Biological Sciences*, 364(1535):3549–3557, 2009.

[153] Mel Slater and Sylvia Wilbur. A framework for immersive virtual environments (five): Speculations on the role of presence in virtual environments. *Presence: Teleoperators & Virtual Environments*, 6(6):603–616, 1997.

[154] Mel Slater, Martin Usoh, and Anthony Steed. Depth of presence in virtual environments. *Presence: Teleoperators & Virtual Environments*, 3(2):130–144, 1994.

[155] Mel Slater, Daniel Pérez Marcos, Henrik Ehrsson, and Maria V Sanchez-Vives. Towards a digital body: the virtual arm illusion. *Frontiers in human neuroscience*, 2:6, 2008.

[156] Mel Slater, Daniel Pérez Marcos, Henrik Ehrsson, and Maria V Sanchez-

Vives. Inducing illusory ownership of a virtual body. *Frontiers in neuroscience*, page 29, 2009.

[157] Mel Slater, Bernhard Spanlang, Maria V Sanchez-Vives, and Olaf Blanke. First person experience of body transfer in virtual reality. *PloS one*, 5(5): e10564, 2010.

[158] R Townley Slinger and Victor Horsley. Upon the orientation of points in space by the muscular, arthrodial, and tactile senses of the upper limbs in normal individuals and in blind persons. *Brain*, 29(1):1–27, 1906.

[159] Hendrikus J Snijders, Nicholas P Holmes, and Charles Spence. Direction-dependent integration of vision and proprioception in reaching under the influence of the mirror illusion. *Neuropsychologia*, 45(3):496–505, 2007.

[160] Samuel J Sober and Philip N Sabes. Multisensory integration during motor planning. *Journal of Neuroscience*, 23(18):6982–6992, 2003.

[161] Samuel J Sober and Philip N Sabes. Flexible strategies for sensory integration during motor planning. *Nature neuroscience*, 8(4):490–497, 2005.

[162] Vinicius Souza, Anderson Maciel, Luciana Nedel, and Regis Kopper. Measuring presence in virtual environments: A survey. *ACM Computing Surveys (CSUR)*, 54(8):1–37, 2021.

[163] Anna Spagnolli and Luciano Gamberini. The sense of being 'there': a model for the space of presence. *EXPLORING THE SENSE OF PRESENCE*, 48, 2004.

[164] Charles Spence, Carmel A Levitan, Maya U Shankar, and Massimiliano Zampini. Does food color influence taste and flavor perception in humans? *Chemosensory Perception*, 3(1):68–84, 2010.

[165] Misha Sra, Xuhai Xu, Aske Mottelson, and Pattie Maes. Vmotion: designing a seamless walking experience in vr. In *Proceedings of the 2018 Designing Interactive Systems Conference*, pages 59–70, 2018.

[166] Barry E Stein and M Alex Meredith. *The merging of the senses.* The MIT press, 1993.

[167] Barry E Stein and Terrence R Stanford. Multisensory integration: current issues from the perspective of the single neuron. *Nature reviews neuroscience*, 9(4):255–266, 2008.

[168] BE Stein. Multisensory integration in single neurons of the midbrain. *The*

handbook of multisensory processes, 2004.

[169] Frank Steinicke, Gerd Bruder, Jason Jerald, Harald Frenz, and Markus Lappe. Estimation of detection thresholds for redirected walking techniques. *IEEE transactions on visualization and computer graphics*, 16(1):17–27, 2009.

[170] Jonathan Steuer. Defining virtual reality: Dimensions determining telepresence. *Journal of communication*, 42(4):73–93, 1992.

[171] Qi Sun, Anjul Patney, Li-Yi Wei, Omer Shapira, Jingwan Lu, Paul Asente, Suwen Zhu, Morgan McGuire, David Luebke, and Arie Kaufman. Towards virtual reality infinite walking: dynamic saccadic redirection. *ACM Transactions on Graphics (TOG)*, 37(4):1–13, 2018.

[172] Matthis Synofzik, Gottfried Vosgerau, and Albert Newen. Beyond the comparator model: a multifactorial two-step account of agency. *Consciousness and cognition*, 17(1):219–239, 2008.

[173] Paul Tennent, Joe Marshall, Brendan Walker, Patrick Brundell, and Steve Benford. The challenges of visual-kinaesthetic experience. In *Proceedings of the 2017 conference on designing interactive systems*, pages 1265–1276, 2017.

[174] Paul Tennent, Joe Marshall, Patrick Brundell, Brendan Walker, and Steve Benford. Abstract machines: Overlaying virtual worlds on physical rides. In *Proceedings of the 2019 CHI Conference on Human Factors in Computing Systems*, pages 1–12, 2019.

[175] Emanuel Todorov. Stochastic optimal control and estimation methods adapted to the noise characteristics of the sensorimotor system. *Neural computation*, 17(5):1084–1108, 2005.

[176] Manos Tsakiris. My body in the brain: a neurocognitive model of body-ownership. *Neuropsychologia*, 48(3):703–712, 2010.

[177] Manos Tsakiris and Patrick Haggard. The rubber hand illusion revisited: visuotactile integration and self-attribution. *Journal of experimental psychology: Human perception and performance*, 31(1):80, 2005.

[178] Manos Tsakiris, Gita Prabhu, and Patrick Haggard. Having a body versus moving your body: How agency structures body-ownership. *Consciousness and cognition*, 15(2):423–432, 2006.

[179] William WN Tsang and Christina WY Hui-Chan. Effects of tai chi on joint

proprioception and stability limits in elderly subjects. *Medicine & Science in Sports & Exercise*, 2003.

[180] Yusuke Ujitoko and Yuki Ban. Survey of pseudo-haptics: Haptic feedback design and application proposals. *IEEE Transactions on Haptics*, 14(4): 699–711, 2021.

[181] Yusuke Ujitoko, Yuki Ban, and Koichi Hirota. Presenting static friction sensation at stick-slip transition using pseudo-haptic effect. In *2019 IEEE World Haptics Conference (WHC)*, pages 181–186. IEEE, 2019.

[182] Martin Usoh, Kevin Arthur, Mary C Whitton, Rui Bastos, Anthony Steed, Mel Slater, and Frederick P Brooks Jr. Walking> walking-in-place> flying, in virtual environments. In *Proceedings of the 26th annual conference on Computer graphics and interactive techniques*, pages 359–364, 1999.

[183] Robert J Van Beers, Anne C Sittig, and Jan J Denier van der Gon. The precision of proprioceptive position sense. *Experimental brain research*, 122 (4):367–377, 1998.

[184] Robert J Van Beers, Anne C Sittig, and Jan J Denier van der Gon. Integration of proprioceptive and visual position-information: An experimentally supported model. *Journal of neurophysiology*, 81(3):1355–1364, 1999.

[185] Robert J van Beers, Daniel M Wolpert, and Patrick Haggard. When feeling is more important than seeing in sensorimotor adaptation. *Current biology*, 12(10):834–837, 2002.

[186] Loes CJ van Dam and Marc O Ernst. Knowing each random error of our ways, but hardly correcting for it: An instance of optimal performance. *PloS one*, 8(10), 2013.

[187] Argiro Vatakis and Charles Spence. Crossmodal binding: Evaluating the "unity assumption" using audiovisual speech stimuli. *Perception & psychophysics*, 69(5):744–756, 2007.

[188] VM Velichko and NG Zagoruyko. Automatic recognition of 200 words. *International Journal of Man-Machine Studies*, 2(3):223–234, 1970.

[189] E Von Holst and H Mittelstaedt. Das reafferenzprinzip. wechselwirkungen zwischen zentralnervensystern und peripherie. *Naturwissenschaften*, 37: 464476, 1950.

[190] Mark T Wallace, M Alex Meredith, and Barry E Stein. Converging influences

from visual, auditory, and somatosensory cortices onto output neurons of the superior colliculus. *Journal of neurophysiology*, 69(6):1797–1809, 1993.

[191] Lee D Walsh, G Lorimer Moseley, Janet L Taylor, and Simon C Gandevia. Proprioceptive signals contribute to the sense of body ownership. *The Journal of physiology*, 589(12):3009–3021, 2011.

[192] Séamas Weech, Jae Moon, and Nikolaus F Troje. Influence of bone-conducted vibration on simulator sickness in virtual reality. *PloS one*, 13(3): e0194137, 2018.

[193] Daniel M Wegner, Betsy Sparrow, and Lea Winerman. Vicarious agency: experiencing control over the movements of others. *Journal of personality and social psychology*, 86(6):838, 2004.

[194] Robert B Welch. Meaning, attention, and the "unity assumption" in the intersensory bias of spatial and temporal perceptions. In *Advances in psychology*, volume 129, pages 371–387. Elsevier, 1999.

[195] Betsy Williams, Gayathri Narasimham, Tim P McNamara, Thomas H Carr, John J Rieser, and Bobby Bodenheimer. Updating orientation in large virtual environments using scaled translational gain. In *Proceedings of the 3rd Symposium on Applied Perception in Graphics and Visualization*, pages 21–28, 2006.

[196] Preston Tunnell Wilson, William Kalescky, Ansel MacLaughlin, and Betsy Williams. Vr locomotion: walking> walking in place> arm swinging. In *Proceedings of the 15th ACM SIGGRAPH Conference on Virtual-Reality Continuum and Its Applications in Industry-Volume 1*, pages 243–249, 2016.

[197] Bob G Witmer and Michael J Singer. Measuring presence in virtual environments: A presence questionnaire. *Presence*, 7(3):225–240, 1998.

[198] Andreas Wohlschläger, Kai Engbert, and Patrick Haggard. Intentionality as a constituting condition for the own self—and other selves. *Consciousness and cognition*, 12(4):708–716, 2003.

[199] Daniel M Wolpert and Zoubin Ghahramani. Computational principles of movement neuroscience. *Nature neuroscience*, 3(11):1212–1217, 2000.

[200] Daniel M Wolpert, Zoubin Ghahramani, and Michael I Jordan. Perceptual distortion contributes to the curvature of human reaching movements. *Experimental brain research*, 98(1):153–156, 1994.

[201] RW Wood. The'haunted swing'illusion. *Psychological review*, 2(3):277, 1895.

[202] Robert Sessions Woodworth. Accuracy of voluntary movement. *The Psychological Review: Monograph Supplements*, 3(3):i, 1899.

[203] Run Yu and Doug A Bowman. Pseudo-haptic display of mass and mass distribution during object rotation in virtual reality. *IEEE transactions on visualization and computer graphics*, 26(5):2094–2103, 2020.

[204] Pavel Zahorik and Rick L Jenison. Presence as being-in-the-world. *Presence*, 7(1):78–89, 1998.

[205] André Zenner and Antonio Krüger. Estimating detection thresholds for desktop-scale hand redirection in virtual reality. In *2019 IEEE Conference on Virtual Reality and 3D User Interfaces (VR)*, pages 47–55. IEEE, 2019.

[206] André Zenner, Kora Persephone Heqitz, and Antonio Krüger. Blink-suppressed hand redirection. In *2021 IEEE Virtual Reality and 3D User Interfaces (VR)*, pages 75–84. IEEE, 2021.

[207] Regine Zopf, Greg Savage, and Mark A Williams. Crossmodal congruency measures of lateral distance effects on the rubber hand illusion. *Neuropsychologia*, 48(3):713–725, 2010.

[208] Regine Zopf, Vince Polito, and James Moore. Revisiting the link between body and agency: visual movement congruency enhances intentional binding but is not body-specific. *Scientific Reports*, 8(1):1–9, 2018.

[209] Lionel H Zupan, Daniel M Merfeld, and Christian Darlot. Using sensory weighting to model the influence of canal, otolith and visual cues on spatial orientation and eye movements. *Biological cybernetics*, 86(3):209–230, 2002.